# The International Spillover of Monetary Policy Shock: New Evidence from Nighttime Light*

Kaiji Chen † Qichao Wang‡ Juanyi Xu§ Jingbo Yao¶

18 December 2025

**Abstract**

We revisit the international spillover effects of US monetary policy using a new nighttime light (NTL) big data as a high-frequency, granular proxy for real economic activity. By merging this data with firm-level and transaction-level datasets on land auction and bond issuance by Chinese firms, we find that an unexpected U.S. monetary tightening significantly reduces its output via a novel construction channel—across cities, NTL fluctuations are primarily driven by non-built-up areas rather than city centers or suburbs, suggesting construction-related activities as a main driver for U.S. monetary policy spillovers. Furthermore, the adverse effects on NTL of land parcels purchased by real estate developers are more pronounced for highly leveraged firms, those facing tighter liquidity constraints, and those with greater reliance on foreign bond financing. We show that such a pattern of NTL response to U.S. monetary policy tightening applies to other emerging economies.

**Keywords:** Monetary Policy Spillover, Nighttime Light, Construction Channel, Financing Conditions

**JEL codes:** E44, E52, F30, F42

*We are grateful to Giacomo Candian, Zhang Chen, Sangyup Choi, Zhenyu Gao, Kaiji Robin Gong, James D. Hamilton, Rustam Jamilov, Kohei Kawaguchi, Paymon Khorrami, Nobuhiro Kiyotaki, Arvind Krishnamurthy, Byoungchan Lee, Yao Amber Li, Francesco Lippi, Yan Liu, Yang Lu, Peter Maxted, Ryungha Oh, Luigi Paciello, Benjamin Pugsley, Wei Qiao, Deyu Rao, Isabelle Roland, Harrison Shieh, Zheng (Michael) Song, Vincent Sterk, Eric Swanson, Jieran Wu, Wenbin Wu, Fan Dora Xia, Wei Xiong, Jianpo Xue, Yaoyuan Zhang, Haonan Zhou, Xiaodong Zhu, Yu Zhu, and other participants at the World Congress of ES, European ES Winter, Midwest Macro, CICF, CICM, CFRC, CES China, CES North American, IFABS, China Accounting and Finance Conference, 2nd-HKUST-Fudan-SMU Conference on International Economics, EFG, ITDGR, and seminars at PKU(NSD), UIBE, CKGSB, HKUST, University of Florida, for helpful comments and suggestions. We also thank Yi Huang and Xiaoyu Zhang for sharing the bond issuance and land transaction data, respectively.

†Emory University and ABFER. Email:kaiji.chen@emory.edu.

‡The Department of Economics at The Hong Kong University of Science and Technology. Email: qwangcq@connect.ust.hk.

§The Department of Economics at The Hong Kong University of Science and Technology. Email: jennyxu@ust.hk.

¶The Department of Economics at The Hong Kong University of Science and Technology. Email: jyaoam@connect.ust.hk.

# 1 Introduction

The cross-border spillover effects of monetary policy constitute a critical research area in both monetary and international economics, particularly regarding U.S. monetary policy as a primary determinant of global financial cycles (Miranda-Agrippino and Rey, 2020). While existing literature has extensively examined impacts on international financial markets (see Bhattarai and Neely, 2022 for a comprehensive review), empirical evidence remains limited concerning: (1) causal effects on real economic outcomes, and (2) the transmission mechanism for monetary policy international spillover.

However, these tasks face several empirical challenges using traditional macroeconomic indicators like GDP. First, their low frequency imply many confounding factors beyond monetary shocks within such long measurement windows. This extended time frame also exacerbates reverse causality concerns, as observed economic performance may shape subsequent monetary policy decisions. Second, traditional output measures suffer from measurement errors due to misreporting, statistical aggregation, or even political manipulation—a problem particularly acute in emerging markets (see Clark et al., 2020; Henderson et al., 2012; Martínez, 2022, etc. for more details). Finally, additional complications arise from cross-country inconsistencies in accounting standards and the coarse spatial granularity of available data (e.g., city-level GDP without finer subregional breakdowns).

An ideal candidate is the geospatial data of nighttime light (NTL), which has been emerging in recent economics studies, and has several advantages that suit our study. First, the data is released at a daily frequency and has been publicly available since early 2012 with an ongoing update. Second, the satellite-related measurement errors are orthogonal to economic activities (Pinkovskiy & Sala-i-Martin, 2016) and are also free of potential data manipulation (Chor & Li, 2024; Martínez, 2022). Third, the images captured by satellites at night measure the brightness of different places with a uniform lens, avoiding accounting standard differences across administrative boundaries in traditional

economic data. Fourth, spatial aggregation is also available at almost any level, enabling the evaluation of policy effects in any selected area and facilitating the identification of the transmission channel.[1]

With the NTL data and monetary shocks in hand, we study the international spillover effects of US monetary policy. In the main part, we take China, the largest emerging market, as an example, where we have detailed spatial level and micro level data to explore the channel.[2] The baseline results come from the Local Projection (henceforth "LP", Jordà, 2005) regressions of China's overall NTL on US MPs. The NTL data are from Visible Infrared Imaging Radiometer Suite (VIIRS) instruments operated by the National Aeronautics and Space Administration (NASA) with a daily frequency. The baseline MPs we use is the 30-minute high-frequency Federal Fund Rate change around FOMC announcements. We aggregate the daily series from 2012 to 2023 to weekly in the baseline to avoid unpleasant noises. Several main findings are shown as follows.

To begin with, we find that the overall NTL negatively responds to the US MPs. The response appears right after the shock, and the peak is at 7 weeks later, when the implied GDP decrease by a one-standard deviation of MPs is 1.80 percent. The impact gradually declines then and turns insignificant around 20 weeks after the shock. In addition to the aggregate response, the effects also exhibit clear spatial variation across Chinese cities. The negative impact is most pronounced in inland regions, particularly the northeast and west. In contrast, eastern coastal cities show the mildest adverse effects, with some even experiencing marginally positive outcomes.

Our results are robust to many checks such as adding year-quarter fixed effects, the subperiod analysis, alternative shocks, alternative high-frequency proxy of output, using bootstrap standard errors, adopting different specifications, applying daily frequency NTL, conducting a falsification test, and controlling more confounding variables like the US news shocks, China's monetary stance, US-China tension, and weather conditions.

[1] The GDP-NTL correlation holds when we change the unit of observation from the administrative city or county to arbitrarily chosen areas (Sherman et al., 2023).

[2] In the extension part, we also study the impacts of the US monetary policy on other economies.

We present three key pieces of evidence demonstrating that our baseline findings align with a novel construction channel through which real estate firms' financing condition play a key role of U.S. monetary policy shocks to transmit into Chinese economy: (1) Spatial Decomposition of NTL Responses: We investigate the city-level nighttime light (NTL) responses across three distinct zones—city centers, suburbs, and non-built-up areas. The results reveal that the overall decline in NTL is primarily driven by reduced activity in non-built-up areas, where construction-related operations are concentrated. Consistent with the construction channel, U.S. monetary tightening leads to a simultaneous decline in several key Chinese construction indicators, including aggregate projects under construction, construction investment, land investment, real estate investment, building sales, and land transactions.

(2) Micro-Level Validation: We then provide direct micro-level support for this channel by documenting a post-tightening reduction in NTL intensity within land parcels acquired by real estate developers. We find that the U.S. monetary tightening significantly worsens the financing conditions of real estate firms, thus harming construction-related real activities. In line with this channel, we demonstrate that the adverse effects on NTL are more pronounced for highly leveraged firms, those facing tighter liquidity constraints, and those with greater reliance on foreign bond financing. This suggests that firm financing conditions serve as a crucial transmission mechanism through which US monetary tightening affects China's real economy

(3) Cross-Sectional Heterogeneity: we find that cities more exposed to construction activities, as measured by lower urbanization rates, suffer a bigger impact in NTL after a tightening US shock. In addition, the shock has a more severe impact on cities with less developed financial systems and in cities where land transactions are more exposed to highly leveraged firms. All this lends additional cross-sectional credibility to the construction channel. This is despite the fact that the adverse effects are weaker in a city with a higher net export to GDP ratio, which partially offsets the negative effects on investment.

We provide additional evidence to shed light on the construction channel of the U.S. monetary policy spillover. First, while conventional US monetary policy shocks, such as Fed target rates, are effective, the spillover effects of its unconventional tools, like forward guidance or large-scale asset purchases, are insignificant. Third, the spillover effects of the monetary shocks from the European Central Bank and the Bank of Japan are relatively insignificant, while China's own monetary shock has significant but milder effects on the NTL. This suggests the special role of the Fed's monetary policy in affecting the global business cycle. Finally, as a check of the external validity of our findings, we show that US monetary policy has a significant negative impacts on the NTL in other economies, especially emerging market economies, while the corresponding effects on developed economies are insignificant in general.

Our work contributes to the extensive literature on monetary policy transmission, which predominantly exploit low-frequency aggregated macroeconomic data. Specifically, due to the low frequency of output data, people usually employ the VAR approach to empirically study the impact on real activities (e.g. S. Kim, 2001, Maćkowiak, 2007, Bluedorn and Bowdler, 2011, and Georgiadis, 2016; see Bhattarai and Neely, 2022 for a survey). However, this method suffers from several criticisms, such as misspecification, improper identification restriction, and instability (see Rudebusch, 1998 and Miranda-Agrippino and Ricco, 2021 for more discussion). Benefiting from a higher frequency proxy of real activities, we instead use an event-study-based approach, which is commonly used in the literature to study the responses of financial markets (e.g. Nakamura and Steinsson, 2018, Chari et al., 2021, Swanson, 2021, R. Gürkaynak et al., 2022). This method has less concern about the problem of reverse causality and omitted variables, and thus offers a sharper identification of the causal impacts of monetary policy shocks (R. S. Gürkaynak and Wright, 2013). To our knowledge, we are the first to study the effects of monetary policy on the real economy using nighttime light (NTL) as a high-frequency proxy of real activities.

Moreover, leveraging the spatial granularity of NTL (nighttime light) data, we in-

tegrate it with regional, firm-level, and transaction-specific datasets to uncover a novel transmission channel: US monetary tightening suppresses emerging market output via construction-sector linkages. Previous papers usually study the spillover impact at the country level. By contrast, the observation unit of the NTL data is as small as a square cell with about 464 meters on one side, which allows us to explore a finer heterogeneity across cities, sub-city areas, or even firms.[3]

Secondly, our paper relates to the literature on how monetary policy shapes the real estate markets (e.g. Jordà et al., 2015, Ho et al., 2018, Drechsler et al., 2022). Consistent with most of the papers in this strand, we also find that monetary tightening deteriorates the real estate market.[4] More importantly, we go a step further by demonstrating how the real estate market in emerging economies acts as the primary risk exposure through which international financial shocks impact emerging economies' real sectors. Notably, even in economies with stringent capital controls such as China, this channel also works.

Finally, our paper is also part of the emerging studies utilizing the nighttime light (NTL) data.[5] Most of these papers mainly use low-frequency and aggregate NTL data to investigate economic growth or economic development. Instead, we use the high-frequency and disaggregated NTL data to study how the business cycle fluctuates with macro shocks.[6] More generally, the cleaned dataset is also useful for other studies as a globally-available high-frequency tracker for economic activities.

[3]Besides, our approach has two other appealing advantages: (1) The data can be easily extended to other countries. Unlike traditional national accounts, such as GDP, which have different accounting standards across jurisdictions and countries, the NTL data expose all administrative units under the same measurement standard. (2) The NTL is quite objective and irrelevant to the measurement error of traditional economic indicators, originating from reasons such as statistical capacity and potential data manipulations.

[4]As we study the spillover effect, our paper is closer to Ho et al. (2018), who find that the deduction of the US policy rate since the Great Recession has led to a significant increase in China's housing market using a FAVAR model.

[5]For example, Henderson et al., 2012, Pinkovskiy and Sala-i-Martin, 2016, Bustamante-Calabria et al., 2021, Xu et al., 2021, Martínez, 2022, D. Kim, 2022, J. Kim et al., 2022, L. Jiang and Liu, 2023.

[6]Regarding this aspect, we are closer to Chor and Li (2024) who use the high-frequency NTL data to study the impact of the US-China trade war on the real economy.

# 2 Data and Measurements

To analyze the impacts of US monetary policy spillover and the corresponding mechanism, we use a series of data, including the exogenous high-frequency US monetary policy shock, nighttime light data, and other traditional measurements of real activity. Different from most of the previous literature using only aggregate data, we also take advantage of many micro-level data, such as land transaction data, bond issuance data, and firm balance sheet data, to study the policy transmission from a more granular perspective.

## 2.1 Monetary Policy Shock

The baseline monetary policy shock (MPs) used in the study is extracted from 30-minute high-frequency changes in federal fund rates around the Federal Open Market Committee (FOMC) meetings, which captures the unexpected part of interest rate changes.[7] FOMC meetings are usually held on average 8 times each year. We focus on the meetings from 2012 to 2023, as the NTL data starts from 2012. 95 scheduled FOMC meetings were held during the period, and the extracted baseline MPs (MP1) is shown in Figure A.1. In the extension part, we also use the US unconventional monetary policy shocks and the shocks in other central banks.

## 2.2 Nighttime Light

The NTL data are from NASA's Black Marble with public access dating back to 19 January 2012. We use the period until the end of 2023. The original data are in daily frequency, which is convenient for event studies to obtain a sharper identification of the policy impacts around FOMC announcements.

The NTL data are quite granular, where a pixel in the digitalized image corresponds to 15 arc seconds out of 360 degrees in both latitude and longitude, converting to 464m on the equator. These cells are small enough to identify economic activities at almost any regional level (e.g. a sub-city area or even a land of a real estate firm), which

[7]This data is from Jarociński (2024). We also use the shock of Acosta (2022) as a robustness.

greatly facilitates the identification of the causal impacts and the associated transmission mechanism.[8]

The data are captured by satellites with the VIIRS (Visible Infrared Imaging Radiometer Suite) instrument, which is the latest and the most accurate version of Suomi Polar-orbiting Partnership jointly by NASA and NOAA.[9] Unlike the previous generation of satellite images for NTL, the DMSP, the VIIRS is time consistent (Gibson et al., 2021), which supports the intertemporal comparison required in the study. It also has no top-coding problems (Bluhm & Krause, 2022), a vital issue when measuring in bright places, such as the city center. The neighboring cells are not autocorrelated (Michalopoulos & Papaioannou, 2018), which enables precisely distinguishing light sources at the cell level. We use the Black Marble VIIRS product VNP46A2, which applies the Bidirectional Reflectance Distribution Function (BRDF) on the raw satellite image. It removes distraction factors such as stray light and moonlight. It also adjusts the satellite angle, which varies daily when the satellite captures the image at the same place. Additionally, the product labels cells contaminated by cloud and snow covers, enabling our further processing to remove such noises.

We use cloud computers to process the big data at the cell level. To conduct city-level analysis, we also generate aggregated daily NTL series for 345 out of 367 cities (prefectures) in mainland China. For each of the 4,332 available days, there are 55,404,633 cells for the whole country.[10][11] The detailed process is in Appendix A.3.2.

We match the NTL with MPs data after aggregating them to weekly frequency.[12] This

[8]Once the NTL of a construction field is identified, it can be matched with the associated real estate firm using land transaction records. The granular nature of these NTL data also allows the matching of NTL to each city sector, namely the city center, the suburb and the nonbuilt-up area according to the spatial boundaries.

[9]For details of the data sources, see Appendix A.3.1. A web-based interface of the VIIRS light map is available at: https://www.lightpollutionmap.info (light pollution map).

[10]The remaining 22 cities are large in area but have relatively small populations and economic activities. The processing time on cloud computers positively correlates with the area processed. Therefore, we drop them off in the processing for budget and time considerations.

[11]When aggregating the geospatial data at the city level, the shape files of the administrative boundaries of the cities we use are derived from the official source (National Bureau of Statistics of China, henceforth NBSC) with revisions to show the updated boundaries across cities in 2022.

[12]Every week is defined as from a Sunday to the closest upcoming Saturday (included).

substantially reduces the noise while keeping the frequency sufficiently high to identify the MPs impact on the real economy. Meanwhile, as FOMC is conducted every six weeks on average, converting the daily series to weekly does not have overlapping issues. We assign each MPs value to the week of the FOMC date and interpolate the weeks with no FOMC meetings as having zero shocks. The summary statistics of the matched weekly data are in Table A.1.

## 2.3 Land Transaction Data

To verify the transmission channel in a more granular way, we employ a land transaction data, which allows us to get the land-level NTL and connect it to a specific real estate firm. This data is from Land China (www.landchina.com). We manually match each land transaction with a listed real estate firm and connect them to the associated NTL square unit according to the corresponding latitude and longitude. See Appendix A.4 for more details.

## 2.4 Bond Issuance Data

To distinguish the role of domestic and foreign borrowing in the spillover effects of US monetary policy to Chinese real estate firms, we adopt a confidential bond issuance data from Huang et al. (2024). The data match each recorded issuance with a listed real estate firm. For each issuance, we mainly use the information on total amount and the currency of debt. See Appendix A.5 for more descriptions.

## 2.5 Other Data

Apart from the data shown above, we also use the firm-level balance sheet data, regional (city/province) economic indicators, the national account records from China and other countries, financial market data, real estate and construction investment data, news shocks data, weather data, etc. For more details, please refer to Appendix A.6.

# 3 NTL and Output

In this section, we illustrate NTL is a good proxy for real output. Intuitively, NTL should positively correlates with traditional economic activity indicators, such as GDP. Figure 1 shows such associations at annual frequency and the city level.

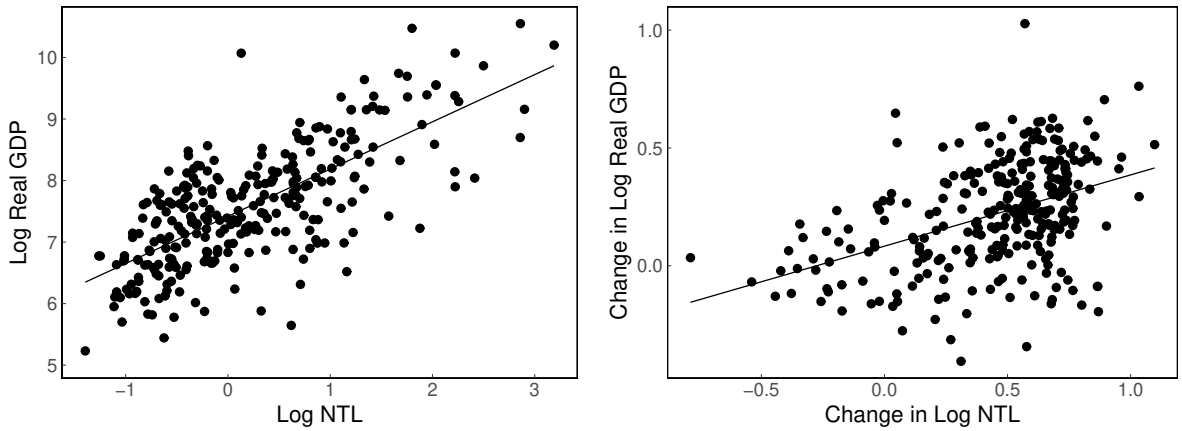


Figure 1: NTL and GDP by City

Notes: Log NTL is converted to the corresponding frequency of the national account indicators in each plot. Log NTL is the logged value of the average NTL across every day in the converted periods. For each day, NTL is the average value of all cells in each city. The left graph shows the data in 2019. The right graph shows the changes from 2012 to 2019.

Using the annual panel data with NTL and different indicators from the national accounts, we apply the following regression equation.

$$y_{i,t} = \beta_0 l_{i,t} + \gamma_i + \tau_t + u_{i,t} \tag{1}$$

Here $y$ is an output indicator (e.g., log GDP), and $l$ is the log NTL. $i$ and $t$ are identifiers for city and year, respectively. To address the endogeneity issue, we use NTL in the last year as the IV of the current NTL following J. Kim et al. (2022) and Chor and Li (2024). We also control for two-way fixed effects. When both $y$ and $l$ are in log forms, $\beta_0$ is the elasticity of output on NTL. The regression results of overall GDP and GDP by sector on NTL are in Table B.1.

The elasticity for aggregate GDP is about 0.49 (excluding Covid period), consistent with previous literature. Further looking at the elasticity by sector, the primary sector (agriculture) GDP does not correlate with NTL (Gibson et al., 2024), as agriculture activities mainly occur during the days. Both secondary (manufacturing and construction) and tertiary (service) sectors' GDP significantly and substantially correlate with NTL. Table B.2 implies the significant elasticity across periods. Therefore, the fluctuation in NTL reflects changes in economic output.

NTL partly comes from economic activities such as urbanization and trade. Table B.3 shows the significance of the two channels. First, urban expansion reflects the output in the construction sector. When the city's boundary expands from more construction, NTL in the newly built-up area increases. Figure B.1 shows the positive correlation between urbanization rate growth and NTL growth from 2012 to 2019, a period characterized by rapid urbanization in China. Second, the export-oriented manufacturing sector has night shifts, and their activities at night positively correlate with export amount (Chor & Li, 2024).[13]

Next, we run the same regression in Equation 1 at the country level using the cross-country national accounts, and the results are in Table B.4. In line with previous literature (Bickenbach et al., 2016; Henderson et al., 2012; Martínez, 2022), NTL better proxies GDP for emerging economies. Intuitively, several channels of GDP growth reflected on NTL mostly apply to emerging economies, including urbanization and night shifts in the manufacturing sector.

[13]Net export is calculated by export minus import. The unit of export and import is 10 trillion Yuan.

# 4 The Spillover Effects

## 4.1 Aggregate Impact

Following the mainstream literature (e.g. Swanson, 2021, and Jarociński, 2024), we adopt the local projection (LP, Jordà, 2005) method to study the spillover effects. Specifically, we apply the following regression equation.

$$y_{t+h} - y_{t-1} = \alpha^{(h)} + \sum_{q=1}^{Q} \phi_q^{(h)} \Delta y_{t-q} + \sum_{m=0}^{M} \beta_m^{(h)} x_{t-m} + \sum_{r=1}^{R} \gamma_r^{(h)} W_{t-r} + \tau_t + u_{t+h|t} \qquad (2)$$

where $y_t$ is log NTL in week $t$, $\Delta y_t$ is the change in log NTL in week $t$ relative to week $t-1$, $x$ is the high-frequency federal fund rate shock around the FOMC announcement.[14] We use AIC criteria to choose the lags of the dependent variable and the shocks.[15] In the extended specifications, we add controls as $W$ and time fixed effects as $\tau_t$. The key underlying assumption here is that the change of NTL is mainly affected by the US MPs in such a short window around the FOMC meetings.

Applying the equation for $h = 0, \cdots, H$, the IRF is obtained from $\{\beta_0^{(0)}, \cdots, \beta_0^{(H)}\}$. We look up to $H = 20$ for the weekly series. The IRF of the baseline LP regressions is displayed in Figure 2.

[14] We only study the effects of conventional monetary policy here. The comparison with unconventional monetary policy will be discussed later.

[15] The BIC criteria chooses the same number of lags.

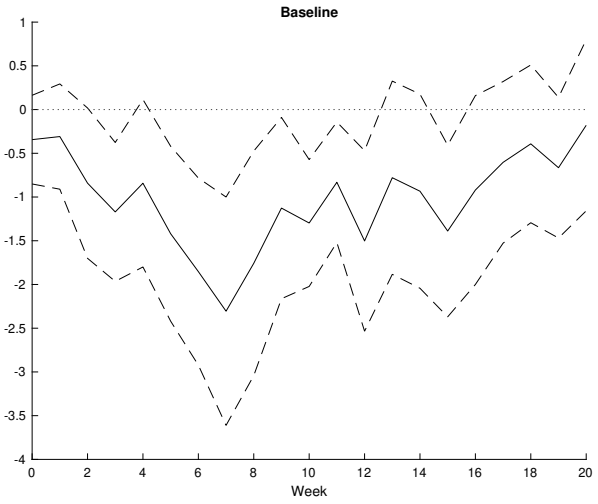


Figure 2: Local Projection of NTL on US MPs: Baseline

Notes: MPs is aggregated to the weekly frequencies consistent with the dependent variable. The number of lags of the dependent variable ($Q$) and the shock ($M$) are selected by the AIC criteria for up to 4 periods. The dashed ribbons are the 90 percent confidence intervals generated based on the Newey-West standard errors.

There are several takeaways from our baseline results: (1) Using a high-frequency specification, we confirm that the US monetary policy shocks negatively affect China's real activities, which is consistent with previous literature (e.g. S. Kim, 2001, Maćkowiak, 2007, and Bluedorn and Bowdler, 2011, etc.). (2) People tend to believe that monetary transmission, especially cross-border spillover, is lagged. Usually, the foreign real activity is assumed to be affected by US interest rate shocks by a lag of one quarter (Uribe and Yue, 2006). However, we find that the spillover effect is much quicker than people's traditional expectations. It peaks in the seventh week (about two months) after the shock and reaches half of the peak in the third week. It then gradually dies out and turns insignificant after the 20th week. (3) The magnitude of the shock on the real economy is material. A unit of the US MPs shock declines China's NTL by 2.3 log points at peak (7 weeks after the shock). Using the correlation we obtain from the NTL-GDP (0.49), the estimated decrease in GDP is around one log point after a unit shock. Since the standard deviation of the shock is 0.016 from 2012 to 2023 (our sample period), a one-standard-deviation shock would cause a peak of 1.80 percent drop in China's weekly output. Similarly, the

20-week average NTL drop is 1.02 log points, implying a one-standard-deviation shock would cause a 0.80 percent drop in China's weekly output within 20 weeks after the shock.

Our results remain robust across various validations, including adding year-quarter fixed effects, subperiod analysis, alternative shocks, alternative proxy of output, bootstrap standard errors, different model specifications, the use of daily frequency NTL, a falsification test, and additional controls for confounding factors such as US news shocks, weather conditions, and US-China tensions. See Appendix C.1 for more details.

## 4.2 Low-frequency Output Responses

Now, we compare our high-frequency results with those of low-frequency variables of output. For China's nationally aggregated time series, we look at two key indicators for real output: real GDP and Industrial Production (IP) at their highest frequency. We apply the LP method (Jordà, 2005) for quarterly GDP and monthly IP, and the impulse response functions (IRF) are in Figure 3. It was found that the spillover effects are negative overall for both series, which is consistent with our weekly and daily results. Although there is a drop in GDP in the current quarter, the responses of industrial production are relatively weak within the first 3 months. As we will explain later, the overall negative responses of NTL, especially in the current quarter, are mainly driven by construction activities in non-built-up areas rather than manufacturing activities in suburbs.

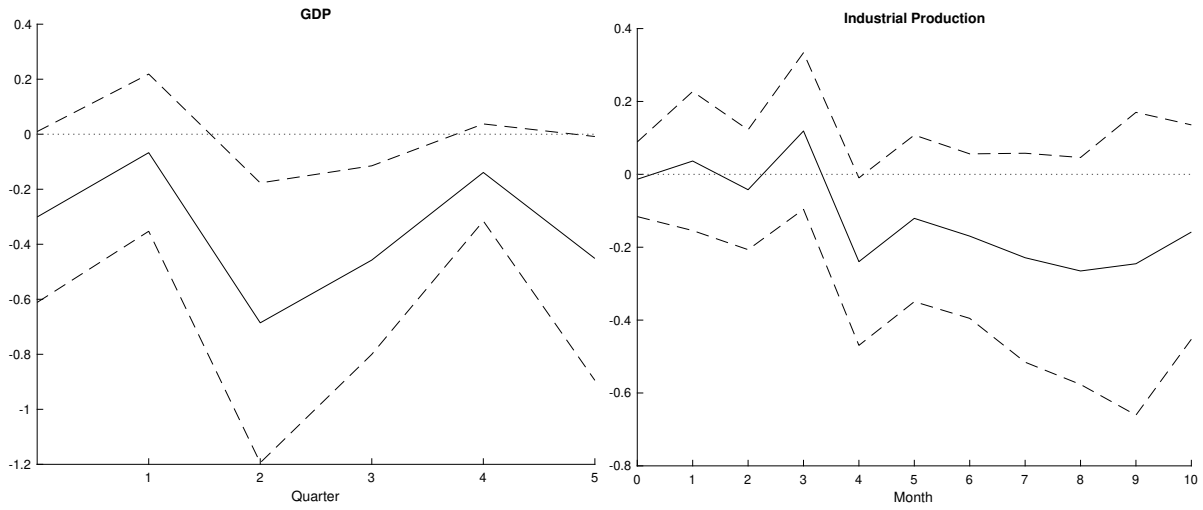


Figure 3: IRF of China's Quarterly GDP and Monthly Industrial Production on US MPs

Notes: MPs is aggregated to the frequencies consistent with the corresponding dependent variables. The number of lags of the dependent variable ($Q$) and the shock ($M$) are selected by the AIC criteria for up to 4 periods. The dashed ribbons are the 90 percent confidence intervals generated based on the Newey-West standard errors.

Then, we turn to the impacts on different parts of GDP including consumption, investment, and net export (see Figure C.15). In the current quarter ($t = 0$) consumption and net exports are barely affected (relatively insignificant), the negative responses of GDP are mainly driven by investment reduction. Later, due to a decline in investment, which may cause a rise in the unemployment rate and a drop in household income, consumption begins to shrink ($t = 2$), with the magnitude even exceeding the investment reaction. Although net export slightly increases, it cannot offset the negative impacts on investment and consumption. Recall our NTL analysis, we see that the peak of effects comes at around 7 weeks and the effects eventually die out at around 20 weeks, which suggests that the NTL variation may mainly reflect the changes of real activities on investment as consumption and export responses have a longer time lag. Apart from the official data, using the measurements from K. Chen et al. (2024) yields consistent results (Figure C.16).

## 4.3 City Level Heterogeneity

In addition to the overall response of NTL in China, the next question is what are the heterogeneous effects in different places? Previous literature usually study the spillover effects for a foreign country as a whole without exploring the heterogeneity within this country. By leveraging the advantage of the geospatial data, we further compare each city's response in China. Applying the same identification specification as Equation 2 to each city, we obtain the corresponding IRF for each place. Then, we take the average responses from the shock period to 20 weeks later.[16] The map plot of the average response by city is in Figure 4.

[16]Insignificant responses are treated as zero. For cities with significant responses of both signs along different horizons, which applies to a few cases, the average responses are also treated as zero.

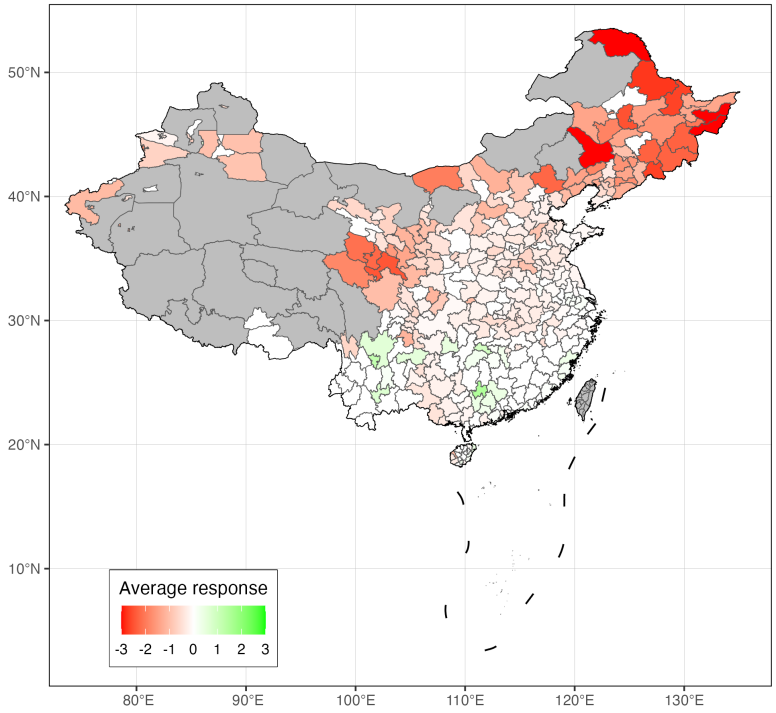


Figure 4: Average Response of NTL on US MPs by City

Notes: MPs is aggregated to the weekly frequencies consistent with the dependent variable. The number of lags of the dependent variable ($Q$) and the shock ($M$) are selected by the AIC criteria for up to 4 periods. When taking the average across the time horizon from the week the MPs is realized to 20 weeks later, insignificant values at a 90 percent confidence level are treated as zero. If the city has both significantly positive and significantly negative responses, the average response by the city is interpreted as zero. Extreme values with absolute values greater than 3 are winsorized on the map.

The spatial heterogeneity is visible across Chinese cities. The negative responses are more substantial in the hinterland, notably the northeastern and the western areas. Cities in the eastern coastal area have the least negative responses, and some even have slightly positive reactions. Therefore, the overall negative NTL response to a US tightening shock is mainly driven by the inland areas.[17][18]

[17]Like the previous section, we also add weather control variables to the identification, and the map plot is in Figure C.17. The results are qualitatively the same as the baseline. The weather data is unavailable for a considerable proportion of cities in the eastern coastal area.

[18]We also look at the heterogeneity at the province level. The map plot is in Figure C.18. The results are consistent with the city-level version, with the negative responses most substantial in the inland provinces.

# 5 Construction channel

In this section, we illustrate that our baseline finding aligns with a construction channel through four pieces of evidence: (1) We first zoom in by decomposing the aggregate NTL responses into three parts: city centers, suburbs, and non-built-up areas. It is seen that the overall negative responses of NTL are driven by the reaction in non-built-up areas that feature construction-related activities. (2) Then, from a micro perspective, we directly verify this channel by showing that the NTL in lands purchased by real estate firms declines after a tightening shock. (3) Besides, consistent with the NTL response, the aggregate projects under construction, construction investment, land investment, real estate investment, building sales, and land transactions in China all decrease after a US tightening shock. (4) In addition to these time-series evidences, we find that cities with more construction activities have a larger impact.

## 5.1 Decomposition of Different City Sectors

To look at the heterogeneous responses by different sectors, we separately apply the baseline identification on the city center, the suburbs, and the non-built-up area as of 2010. Using the satellite image-based identification by H. Jiang et al. (2022), we define the city center as the built-up area as of 1990, the suburb as the area built up in 2010 but not in 1990, and the non-built-up area as other parts.[19] We choose 2010 as the threshold year because the NTL series starts from 2012, therefore excluding potential endogeneity issues. We illustrate the city center, the suburb, and the non-built-up area for selected cities as follows.

[19]We confirm the validity of the identification after manually checking the identified centers and suburbs for major Chinese cities, including Beijing, Shanghai, Guangzhou, Shenzhen, and Hangzhou. The identification closely matches the conventional definition of centers and suburbs in these cities.

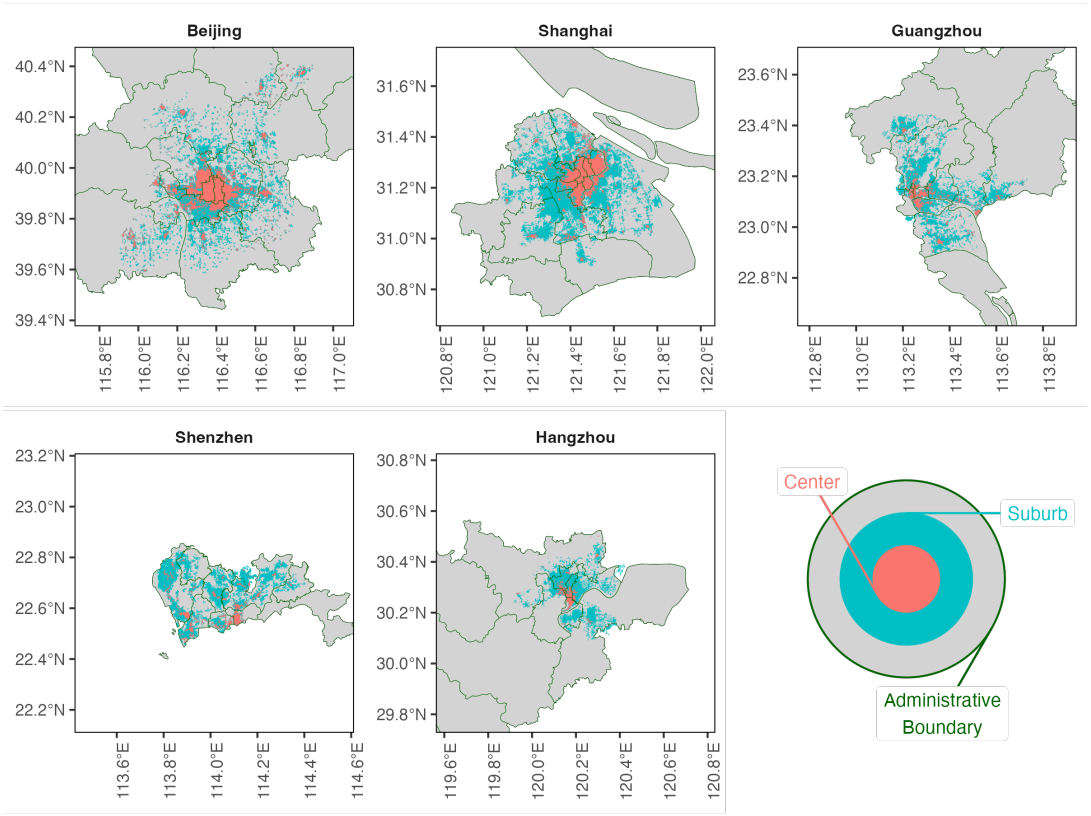


Figure 5: Built-up Areas of Selected Cities

Notes: The boundaries of the built-up areas are identified up to 2010.

The heterogeneous responses by sectors are displayed in Figure 6. It shows that the effects on non-built-up areas are quite significantly negative, driving the overall responses. The NTL in non-built-up areas mainly reflects the real activities of construction, such as the light from construction sites at night and from new buildings. These are highly sensitive to concurrent changes in the economic and financial environment. Intuitively, the US tightening could quickly worsen China's financial markets and harm people's economic outlook, and later deteriorate firms' operations[20], which would lead to a delay, slowing, or even stagnation in the construction works. During a housing market boom, real estate developers incentivize construction firms to accelerate production, enabling faster home sales and improved cash flow. This often leads to extended work hours (including night shifts) and a higher volume of completed housing units—resulting in

[20]Evidence will be provided in Section 6.

increased nighttime light emissions. Conversely, following US monetary tightening and subsequent market downturns, this dynamic reverses.

By comparison, the impacts are insignificant for the centers and suburbs, the NTL of which mainly implies service and manufacturing activities respectively. In the previous section, we display that the current quarter GDP change is mainly driven by investment. Based on the NTL responses of the different city sectors, we may further conclude that the investment reduction is more likely to be caused by construction-related activities, rather than manufacturing activities.

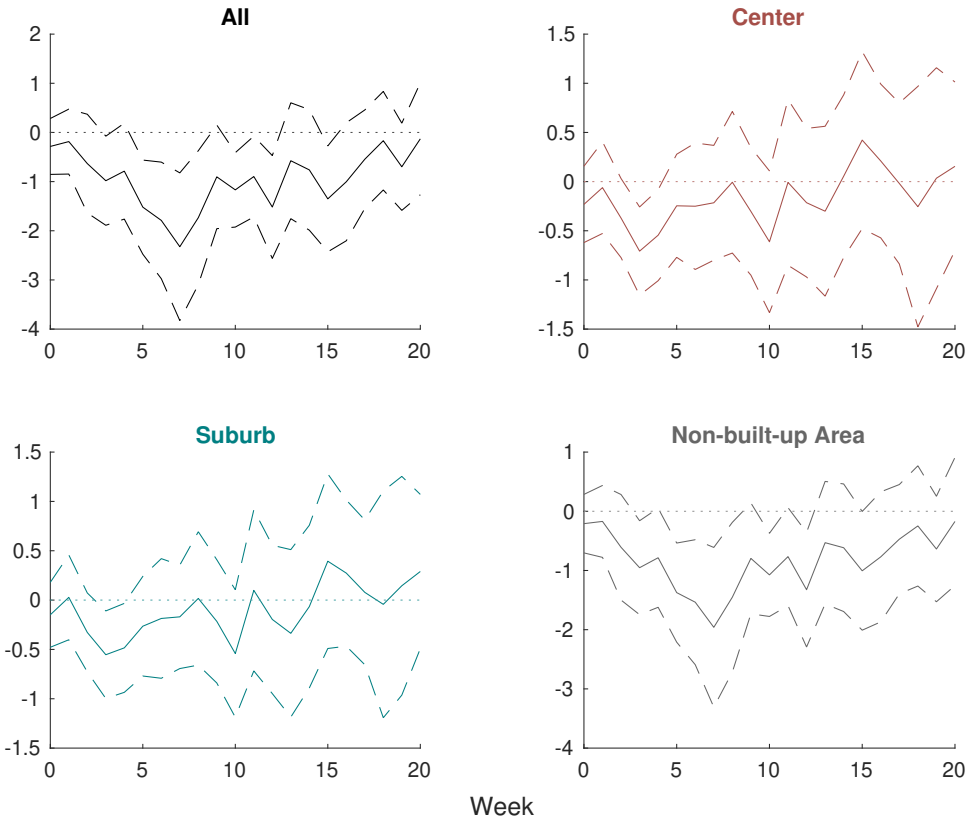


Figure 6: Local Projection of NTL on US MPs: City Areas

Notes: MPs is aggregated to the weekly frequencies consistent with the dependent variable. The number of lags of the dependent variable ($Q$) and the shock ($M$) are selected by the AIC criteria for up to 4 periods. The dashed ribbons are the 90 percent confidence intervals generated based on the Newey-West standard errors.

Robustness checks: (1) We stack the NTL of the three areas together and identify

MPs times city area dummies (MPs × Center, MPs × Suburb, and MPs × Non-built-up Area) as three separate shocks so that we can estimate the responses in different sectors simultaneously.[21] The results are similar, as shown in Figure D.1. (2) The results are consistent when we use the latest identified built-up area in the shape file, as in Figure D.2. (3) Then we look at the city-level responses across the three city areas. The results are in Figure D.3. The overall negative responses are driven by the non-built-up area for most cities, and the negative responses in the non-built-up area are mainly in inland cities.

## 5.2 Responses of NTL in Lands Purchased by Real Estate Firms

In addition to the city area decomposition, we also use the NTL of lands purchased by real estate firms to verify the construction channel directly from a more granular perspective. For each transacted land that we are able to associate with a listed firm, we geolocate the coordinate of the land by reverse geocoding the textual address.[22] Then, for each identified coordinate, we use the NTL of the cell that includes the location as the proxy for the light of the transacted land.

To directly look at the NTL changes of the transacted lands associated with real estate firms, we aggregate the NTL of all the corresponding cells and identify the response to MPs using our baseline specification. The IRF of the NTL of aggregated transacted lands is in Figure 7.

[21] The specification is $y_{i,t+h} - y_{i,t-1} = \alpha^{(h)} + \sum_{q=1}^{Q} \phi_q^{(h)} \Delta y_{i,t-q} + \sum_{m=0}^{M} \beta_{m1}^{(h)} \cdot x_{t-m} \cdot Center_i + \sum_{m=0}^{M} \beta_{m2}^{(h)} \cdot x_{t-m} \cdot Suburb_i + \sum_{m=0}^{M} \beta_{m3}^{(h)} \cdot x_{t-m} \cdot NBA_i + u_{i,t+h|t}$, where $y_{i,t}$ is the NTL of a sector (Center, Suburb, or Non-built-up ara) in time $t$, $Center$, $Suburb$, $NBA$ are three dummies of city areas. We choose $M = 0$ and $Q = 4$ for the number of lags in line with the specifications when we regress the three areas' NTL separately. We plot the IRF of $\beta_{01}$, $\beta_{02}$, and $\beta_{03}$.

[22] The API we use is Amap. For each observation, the input is the textual address, the city, and the province. The output is longitude, latitude, and the implied textual address. To exclude excessively rough results, we filter out outputs with textual addresses ending with a city or county name or being less than 16 characters.

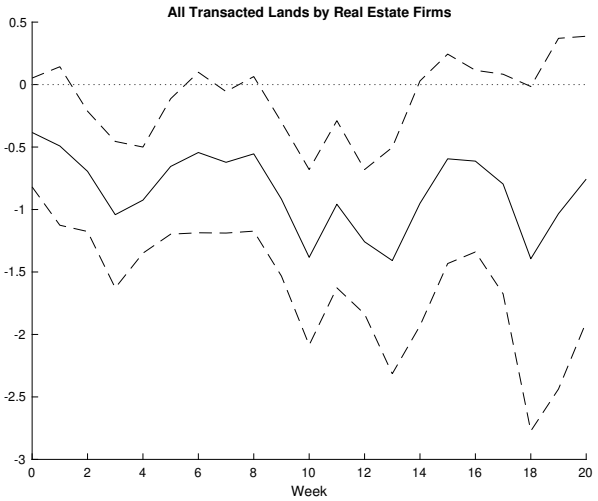


Figure 7: Response of NTL in Transacted Land on US MPs: All Transacted Lands by Real Estate Firms

Notes: MPs is aggregated to the weekly frequencies consistent with the dependent variable. The number of lags of the dependent variable ($Q$) and the shock ($M$) are selected by the AIC criteria for up to 4 periods. The dashed ribbons are the 90 percent confidence intervals generated based on the Newey-West standard errors.

The NTL in transacted lands associated with real estate firms decreases after a US tightening. The result is consistent with our baseline, implying the response by construction works as a driver for the overall NTL decrease. The NTL decrease is universal across several representative listed real estate firms (such as Greenland, Evergrand), as shown in Figure D.4.[23]

## 5.3 Responses of Construction-related Activities

Consistent with this construction channel, we also display how construction-related activities are affected using monthly market indicators.[24] The specification is similar to our baseline. In Figure 8, it is seen that after a US monetary tightening, there is a significant decrease in projects under construction in the current month and it is even more

[23]We select the six representative firms, including three listed in the stock market of Mainland China, and three listed in the stock market of Hong Kong, China, regarding their prominence in the real estate market of China.

[24]The data on market indicators are obtained from the CEIC database.

pronounced later, which directly contributes to the NTL drop in non-built-up areas.[25]

Besides, we can also observe a decline trend for construction investment, the responses of which seem to have a three-month lag. This is plausible as an investment in a building may be pre-determined so that it is free from the impact of current factors. By comparison, construction works could be quickly delayed or slowed even in the current period in facing an adverse economic or financial shock.

Also, land investment, the activities in the upstream of the construction industry, drop even more prominently and quickly.[26] Consistently, China's real estate investment and residential building investment, the activities in the downstream of the construction sector, later significantly decline too.[27] Moreover, from the transaction data, we show that both building sales and land transactions (including cases, area, and value) go down when facing a contractionary US monetary policy.

[25]Then, we look at how the NTL is associated with projects under construction. Specifically, we regress NTL changes on the number of projects under construction using the US MPs as the IV. We use lagged MPs values up to 10 months apart from the contemporary MPs in the first stage. The results are in Figure D.5. As expected, NTL increases with the number of ongoing construction projects.

[26]Land investment involves the money allocated in purchasing, holding, or developing a land.

[27]This is in line with the literature, such as Jordà et al. (2015) and Ho et al. (2018).

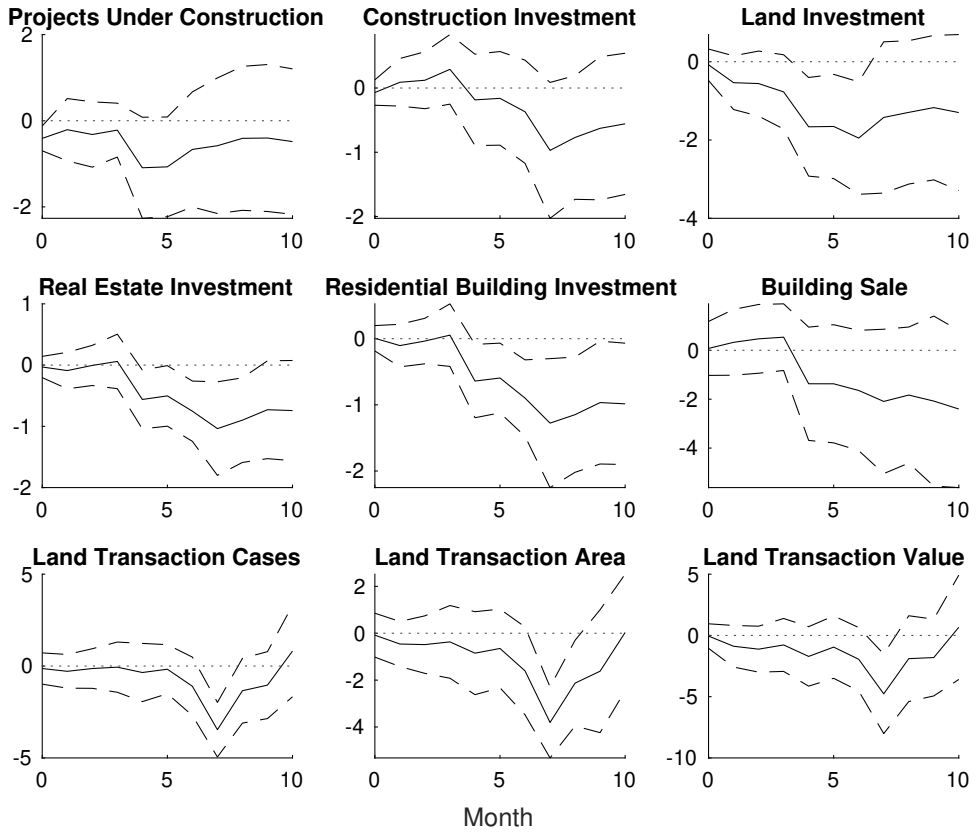


Figure 8: IRF of China's Monthly Real Estate Market Indicators on US MPs

Notes: MPs is aggregated to the monthly frequencies consistent with the dependent variable. The number of lags of the dependent variable ($Q$) and the shock ($M$) are selected by the AIC criteria for up to 4 periods. The dashed ribbons are the 90 percent confidence intervals generated based on the Newey-West standard errors.

## 5.4 Impacts are Bigger in Cities with More Construction Activities

We conjecture that if the NTL responses reflect a construction channel, cities that have more construction activities should be more affected. To verify that, we use the urbanization rate to measure the intensity of construction. For each city, the urbanization rate is defined as the percentage of the population with urban household registration over the total population. Usually, cities with lower urbanization rates should be more engaged in construction-related activities. To quantitatively associate the urbanization rate with the responses to US MPs, we identify with a city-level panel of NTL, US MPs,

and urbanization rate. The regression equation is as follows.

$$y_{i,t+h} - y_{i,t-1} = \beta_1^{(h)} s_{i,t-L} + \beta_2^{(h)} x_t s_{i,t-L} + \gamma^{(h)} W_{i,t-1} + \alpha_i^{(h)} + \tau_t^{(h)} + u_{i,t+h|t} \quad (3)$$

Here $y_{i,t}$ is log NTL in city $i$ in week $t$. $x_t$ is MPs in week $t$. $s_{i,t}$ is the urbanization rate in city $i$ in week $t$.[28] $W$ includes controls, such as weather. $\alpha$ and $\tau$ are city and week fixed effects, respectively. To exclude potential endogeneity, the urbanization rate used in the regression is lagged by $L$. We choose the length of the lag as one year in the baseline. The key coefficient estimates are $\beta_2^{(h)}$ and the IRF of each horizon $h$ is displayed in the first panel of Figure 9. We find that the coefficients of interaction terms are overall significantly positive, which indicates that a city with a lower urbanization ratio is more negatively affected by the US tightening. The results are almost similar using the urbanization rate in 2008 (see the right upper panel). What's more, the results using alternative indicators of urbanization based on land classification, such as urban area rate and urban constructed rate,[29] are in Figure 9, which are qualitatively consistent with the urbanization rate based on population compositions.[30] [31]

Consistently, we find that cities that experience higher growth in recent land transactions are also more affected by the US tightening because construction-related activities are more intensively involved in these cities. The same logic, cities with a bigger fixed asset investment to GDP ratio, and with more projects under construction, have a larger NTL decline. The results are shown in Figure D.9.

[28] In the baseline, the urbanization rate is updated on an annual basis. Therefore, the value used depends on the year in which the week $t$ is located.

[29] For each city, the urban area rate is defined as the percentage of the administrative area that is built up. The urban constructed rate is defined as the percentage of the administrative area that is used for building human facilities.

[30] Our results are robust to weather controls, which are omitted for space saving and are available upon request.

[31] The map plot of the urbanization rate and the urban area rate are in Figure D.6 and Figure D.7. The share of built-up area identified by the geospatial data is positively correlated with the urbanization rate, as shown in Figure D.8.

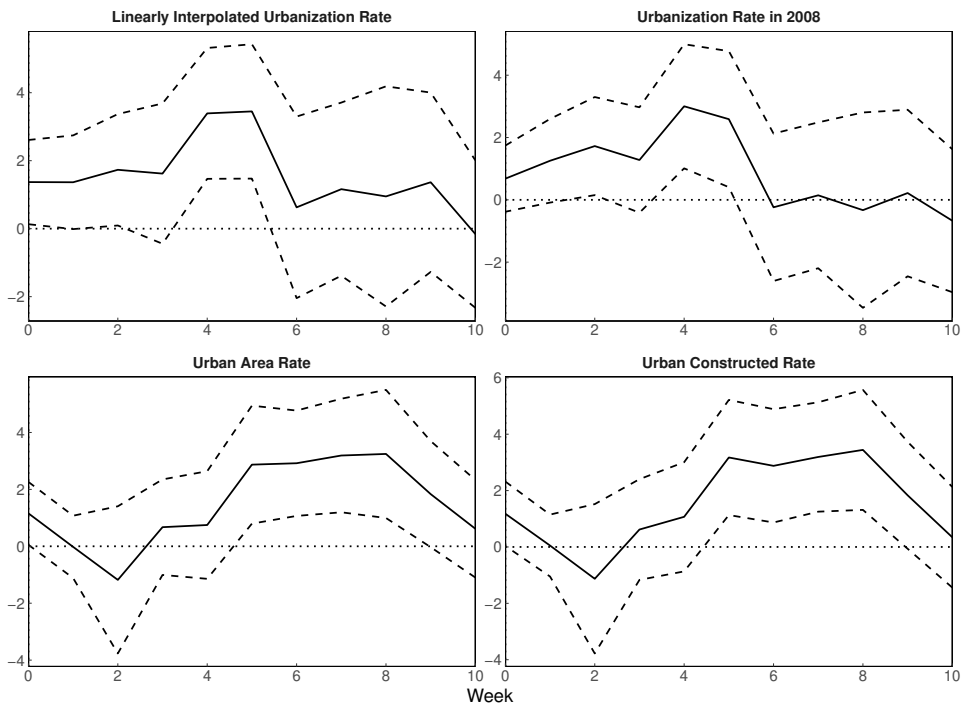


Figure 9: NTL Response to Interaction of US MPs and Urbanization, City level

Notes: The dashed ribbons are the 90 percent confidence intervals generated based on standard errors clustered to city and week.

# 6 Financing Conditions and Real Activities

Having established the construction channel's role in transmitting shocks to the real economy, we now demonstrate how real estate firms' financing conditions fundamentally shape these economic responses: (1) Consistent with the construction channel, we find negative impacts of the US tightening on firms' financing conditions, which may justify why the construction and real estate sectors are adversely affected. (2) For a firm with worse financing conditions, such as higher debt and tighter liquidity conditions, its NTL is more affected. It is worth noting that, those firms issuing foreign bonds are even more vulnerable to such shocks. (3) The impacts are more pronounced for cities with worse financing conditions.

## 6.1 Responses of Firms' Financing Conditions

Firstly, we show that the interest rates in China will increase after a US MPs tightening. This explains why there is a drop in construction activities, as construction firms and real estate firms are usually quite financially constrained.[32] The result is displayed in Figure 10. This result is robust to using other market interest rates, such as the SHIBOR rate (see Figure E.1).

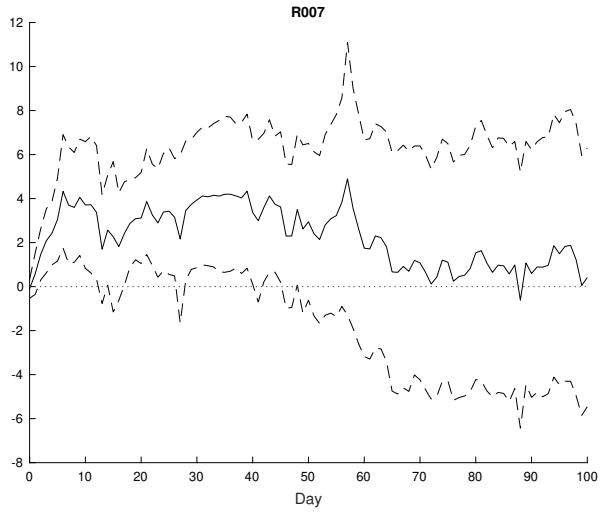


Figure 10: IRF of Interbank Bond Collateral Repo Rate on US MPs by Maturity

Notes: The number of lags of the dependent variable ($Q$) and the shock ($M$) are selected by the AIC criteria for up to 4 periods. The dashed ribbons are the 90 percent confidence intervals generated based on the Newey-West standard errors.

Secondly, the stock prices reflect the market expectation of economic performance. We use several daily Shanghai Stock Exchange (SSE) Indexes as examples and check their responses to the US MPs. These results are shown in Figure E.2. It is seen that the overall stock indexes (SSE composite, SSE 50, and SSE180) negatively respond to the US tightening, peaking at around 7 weeks after the shock, which is quite close to the impacts on nighttime light. Looking at each sector, the movements align with the overall market, with real estate stocks reacting even more negatively and quickly than the aggregate market. The aggravation in the stock market will further deteriorate the

[32]Specifically, similar to previous literature, we use the 7-day Interbank Bond Collateral Repo Rate as a proxy for China's market interest rate.

financial tightness for real estate and construction firms and hence harm their investment and other real activities.[33]

Thirdly, as suggested by the evidence of the listed firms, we find that the firm operation indicators, including revenue, profit, and trade credit (accounts receivable and accounts payable) all decline in response to US tightening and this detrimental effect is more pronounced for real estate firms (see Table E.1 and Table E.2). Moreover, for real estate firms, those get more involved in land transactions are more sensitive to such shocks. See Table E.3 for more details.

Finally, using a bond issuance data by Huang et al. (2024) (see Appendix A.5 for more descriptions), we find that the US tightening decrease the foreign bond issuance of real estate firms, especially regarding the short-term insolvency (See Table E.4).[34] Using the same identification, we do not find any significant response by domestic bond issuance, as in Table E.5.

## 6.2 Impacts are Larger for Firms with Worse Financing Conditions

If construction activities are constrained by deteriorating financing conditions, firms with weaker financial positions are likely to experience more severe impacts. We first look at whether firms with a higher debt ratio are more sensitive to the US tightening by looking at the NTL change of the firms' associated transacted lands. The identification is:

$$y_{i,t+h} - y_{i,t-1} = \alpha_i^{(h)} + \sum_{q=1}^{4} \phi_q^{(h)} \Delta y_{i,t-q} + \beta_0^{(h)} x_t + \beta_1^{(h)} x_t s_{i,t-L} + u_{i,t+h|t} \tag{4}$$

Here, $s$ is the firm $i$'s indicator. We use the operation indicators (e.g., debt ratio) in the last quarter (denoted by the lag operator $L$) to exclude potential endogeneity issues. The interaction term, $\beta_1$, captures how the operation indicator impacts the sensitivity of NTL

[33]Consistent with Ho et al. (2018), we also observe a hot money outflow, which also aggravates the overall financing conditions. See Figure E.3

[34]We scale firms' net bond standing value by the size of the firm, as represented by asset, liability, current liability, or long-term liability. The identification is: $\left(\frac{\text{Net Bond Value Standing}}{\text{Operation Indicator}}\right)_{i,t} = \beta_1 x_t + \alpha_i + \varepsilon_{i,t}$. Here, $i$ is firm, $t$ is month, and $\alpha$ is the firm FE. The point estimate to look at is $\beta_1$.

in the associated transacted lands to the US tightening. The IRF of the interaction term of MPs and the dummy of firm having debt ratio is in Figure 11.[35] The result implies firms with a higher debt ratio are more impacted by the US tightening.

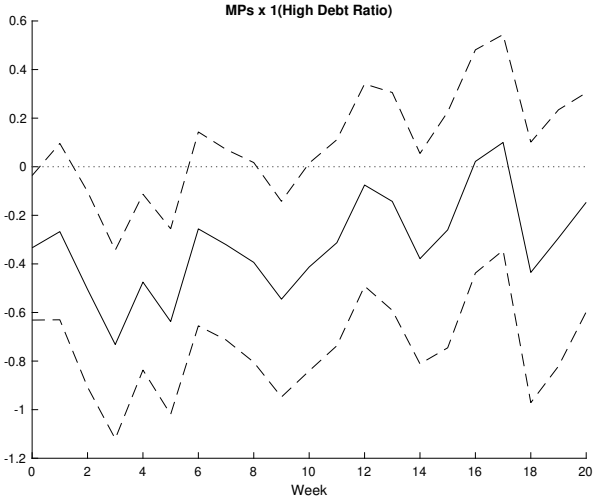


Figure 11: Response of NTL in Transacted Land on US MPs: RE Firm High-Debt-Ratio Dummy

Notes: MPs is aggregated to the weekly frequencies consistent with the dependent variable. The dashed ribbons are the 90 percent confidence intervals generated based on the Newey-West standard errors clustered to firm and week.

As a further step, we use the three red lines as measurements for the financial insolvency of real estate firms.[36] The three red line indicators include: (1) $\frac{\text{Liability}-\text{Presales Revenue}}{\text{Asset}-\text{Presales Revenue}}$, with an acceptable upper limit of 0.7. (2) $\frac{\text{Interest-bearing Liability}-\text{Cash}}{\text{Equity}}$, with an acceptable upper limit of 1. (3) $\frac{\text{Cash}}{\text{Short-term or Maturing Interest-bearing Liability}}$, with an acceptable lower limit of 1. Using the identification above, the IRFs of the interaction terms are in Figure 12. For each of the red line indicators, the result implies greater financial insolvency to generate more response to a US tightening for the real estate firms.

[35] We classify a firm as having "high debt ratio" if the firm has a debt ratio higher than the median of all firms in a given year.

[36] The three-red-line policy was introduced by the PBC, the China Banking and Insurance Regulatory Commission, and other governmental institutions in China to control the overwhelming indebtedness of real estate firms in China in order to prevent potential financial risk. It was implemented on August 20th, 2020.

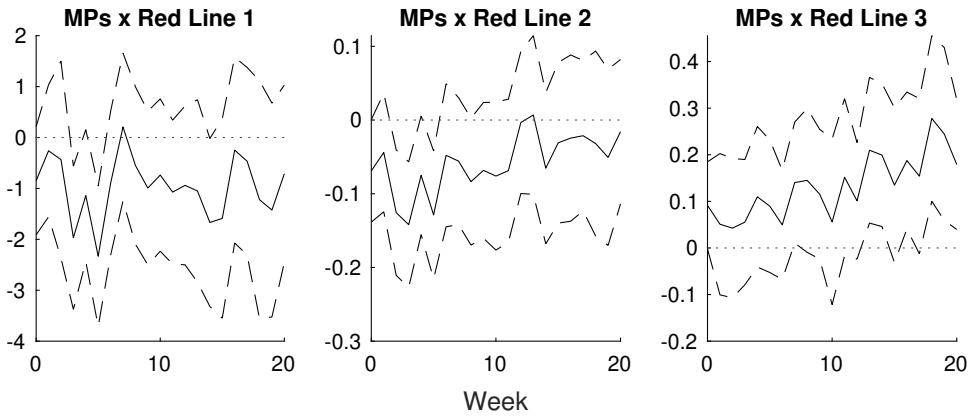


Figure 12: Response of NTL in Transacted Land on US MPs: Three Red Lines of Associated RE Firms

Notes: MPs is aggregated to the weekly frequencies consistent with the dependent variable. The dashed ribbons are the 90 percent confidence intervals generated based on the Newey-West standard errors clustered to firm and week.

When we control the domestic interest rate changes in the baseline regression, we can observe a decline in the magnitude but the negative responses are still significant, which suggests that the domestic interest rate change is not the only reason for the drop in NTL.

Since we have identified the transmission from US tightening to the foreign borrowing of real estate firms in the previous section, we further investigate whether the channel further extends to the firms' real activities proxied by NTL in the firms' associated transacted lands. We identify the impact of firms' foreign borrowing on the NTL in associated transacted lands as follows.

$$\begin{aligned} y_{i,t+h} - y_{i,t-1} =& \alpha_i^{(h)} + \sum_{q=1}^{4} \phi_q^{(h)} \Delta y_{i,t-q} + \beta_0^{(h)} x_t \\ &+ \beta_1^{(h)} x_t \frac{\text{Foreign Bond Standing}_{i,t}}{\text{Current Liability}_{i,t-L}} \\ &+ \beta_2^{(h)} x_t \frac{\text{Domestic Bond Standing}_{i,t}}{\text{Current Liability}_{i,t-L}} + u_{i,t+h|t} \end{aligned} \tag{5}$$

The key point estimate to look at is $\beta_1$, the interaction term of MPs and foreign borrowing, which captures how foreign borrowing alters real estate firms' transacted lands' NTL sensitivity to the US MPs. To compare the impact of foreign and domestic borrowings,

I also add the interaction term of MPs and domestic borrowing, $\beta_2$. The IRFs of $\beta_0$, $\beta_1$ and $\beta_2$ are in Figure 13.

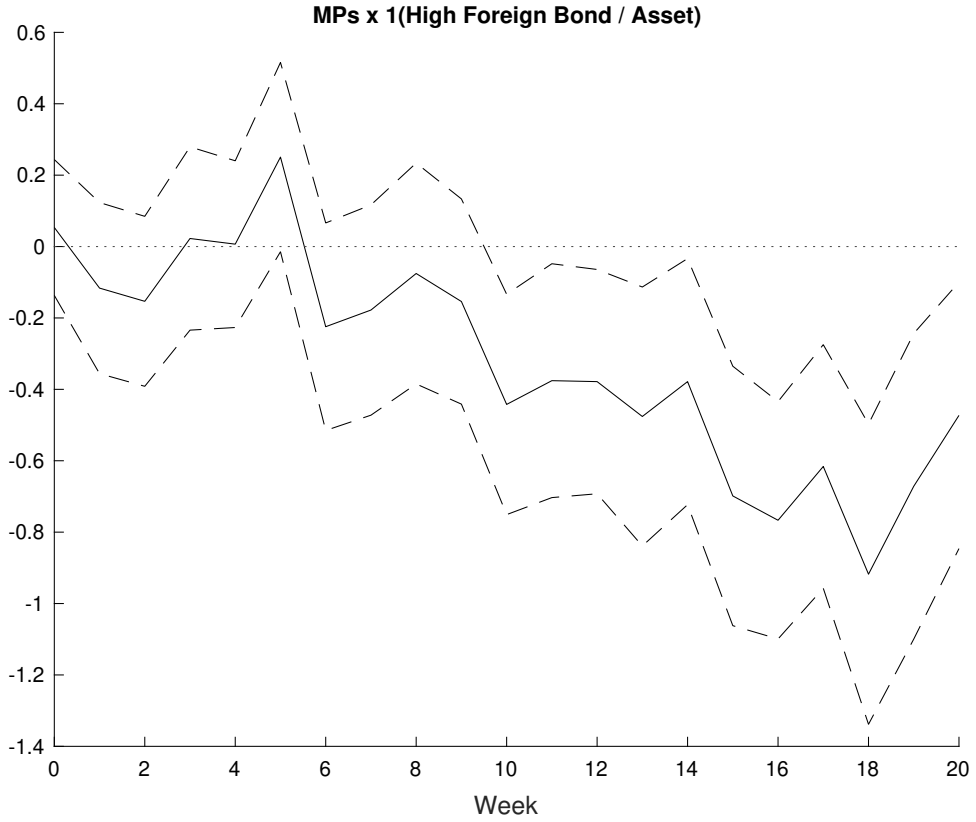


Figure 13: Response of NTL in Transacted Land on US MPs: Net Foreign and Domestic Bond Standings

Notes: MPs is aggregated to the weekly frequencies consistent with the dependent variable. The dashed ribbons are the 90 percent confidence intervals generated based on the Newey-West standard errors clustered to firm and week.

## 6.3 Cities with Worse Financial Conditions are More Affected

As we have shown in previous sections, the US tightening deteriorates China's financial market, which worsens firms' operations and then causes a decline in construction related activities. Consequently, cities with more fragile financial conditions should experience a larger adverse impact.

From the perspective of financial institutions, we look at the role of financial market

development, which is proxied by the number of bank subsidiaries per capita.[37] The identification strategy is the same as the urbanization rate regression (Equation 3), except for replacing the urbanization rate indicator with the financial market development indicator. The result is in the first panel of Figure 14. It is seen that the adverse effects are more pronounced for cities with less developed financial environments. This is plausible as in those places, the financial institutions are fragile and are more likely to be aggravated facing the US tightening, which then causes a larger decline in construction-related activity as is reflected in the NTL of non-built-up areas. The results using alternative indicators of financial market development, such as the ratio of loan and deposit to GDP, are in the second panel of Figure 14, which are qualitatively consistent with the baseline indicator.[38]

Consistently, we find that cities with more floor space waiting to sell experience larger drops in NTL because the real estate companies in these cities usually have worse liquidity and are more vulnerable to adverse shocks. See Figure E.9. Besides, for cities where the construction firms have higher average accounts-receivable-to-revenue ratio, the NTL declines more. See Figure E.8.

The impacts are also bigger for cities with more land transactions exposed to high-leverage firms. For each city, we define the "bad deal index" as the product of land transaction growth and the aggregated current liability ratio.[39] Using the above identification, we find that NTL in cities with a higher "bad deal index" declines more after a US tightening, as shown in Figure E.10.

[37] In advanced countries, people usually use the ratio of equity value over GDP to measure the financial development of a region. By comparison, in emerging markets, indirect financing like bank loans is more pervasive than direct financing such as equity and bond, thus using the intensity of bank subsidiaries is more suitable. This is especially relevant for the construction sector, where most of the firms are not listed.

[38] The map plot of bank subsidiaries per capita and floor space waiting to sell are in Figure E.6 and Figure E.7.

[39] For each city in each year, we identify the listed firm associated with each land transaction. Then, we obtain the financial condition of the corresponding listed firm for each land transaction. In this way, we obtain the associated financial condition for each land transaction. When aggregating the associated financial conditions to the city level, we weight each transaction by either revenue or area of the transaction. To incorporate lagged impact, we use the three-year moving average for both factors. The land transaction growth measurement is either area or revenue and should be the same as the aggregation weighting.

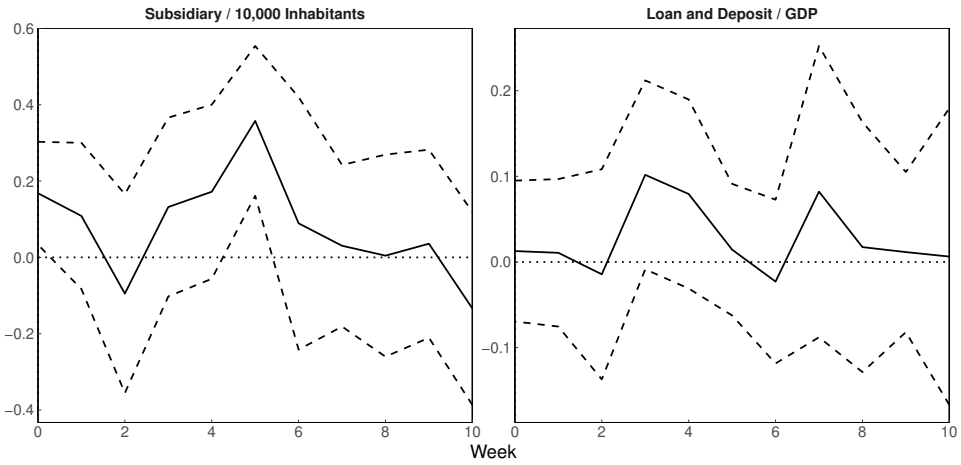


Figure 14: NTL Response to Interaction of US MPs and Financial Market Development, City level

Notes: The dashed ribbons are the 90 percent confidence intervals generated based on standard errors clustered to city and week.

# 7 Further Discussion

## 7.1 International Comparison

We extend our results to all economies in the world using monthly NTL data pre-processed by Earth Observation Group (Colorado School of Mines, 2024).[40] The results are in Figure 15. It is seen that the US tightening has almost negative effects throughout the world with a bigger impact on emerging economies than on advanced economies, which is in line with previous literature (e.g. Bräuning and Ivashina, 2020, Dedola et al., 2017). Moreover, among emerging markets, the effects are more prominent for those economies with rapid urbanization in Asia and Africa, which is consistent with our construction channel.[41]

[40]The VIIRS data covering all the world area starts from 2014. Therefore, we use the VIIRS instrument data since 2014. For months before 2014, we use the DMSP instrument data and match the trends with a conversion DMSP-to-VIIRS factor. The conversion factor is based on annual VIIRS and DMSP instrument data in 2012.

[41]Admittedly, the detailed reasons for country heterogeneity are mixed and the impacts depend on the receiving countries' characteristics such as trade and financial integration, exchange rate regime, financial market development, labor market rigidity, industry structure, and participation in global value chains (Georgiadis, 2016). This is beyond the scope of our paper and may be interesting for fu-

Apart from using monthly data for all the economies, we also selected several of mainland China's neighbors employing weekly NTL, which is more similar to our baseline analysis on China.[42] The results are in Figure F.1. The conclusion is consistent that emerging markets are usually more sensitive than advanced economies.[43]

ture study.

[42]The processing of weekly data is very time-consuming, so we only chose several economies for illustration. Emerging market economies include China, Mongolia, Vietnam, Thailand, Bangladesh, and India while advanced economies include Hong Kong (China), Macau (China), Taiwan (China), South Korea, Japan, and Australia.

[43]However, we should be cautious to interpret this difference between EM and AE as the real activities featured in these two types of economies are different. For example, urbanization and night shifts, two important sources of NTL in EM, are not pervasive in AE. By comparison, in advanced countries, NTL is more reflected in service activities at night, such as the operation of entertainment venues. Consequently, the transmission channel may differ from the one we proposed, which calls for future exploration.

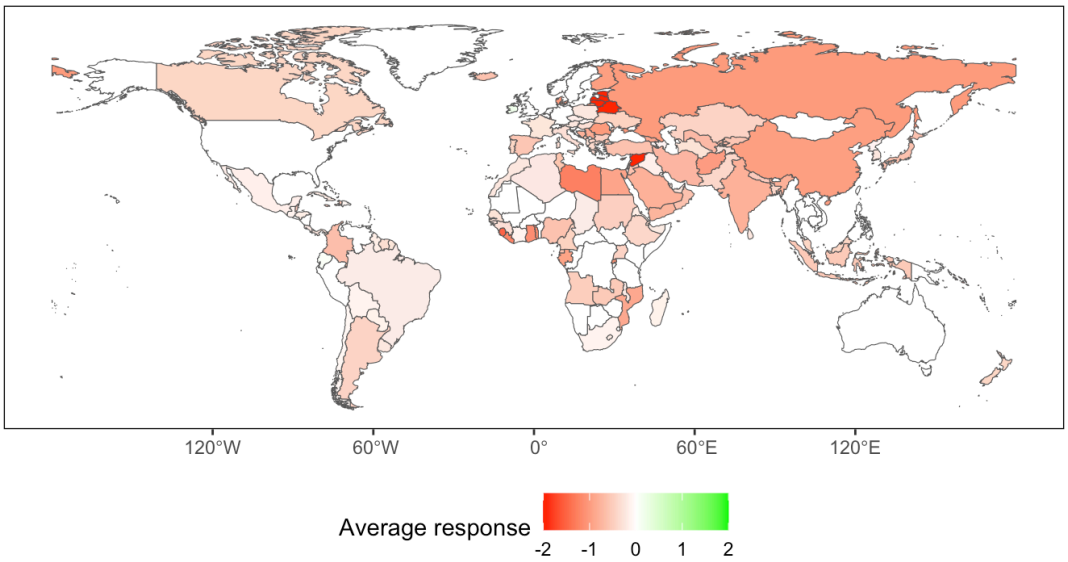


Figure 15: Average Response of NTL on US MPs by Economy

Notes: MPs is aggregated to the monthly frequencies consistent with the dependent variable. The number of lags of the dependent variable ($Q$) and the shock ($M$) are selected by the AIC criteria for up to 4 periods. When taking the average across the time horizon from the month the MPs is realized to 20 months later, insignificant values at a 90 percent confidence level are treated as zero. If the region has both significantly positive and significantly negative responses, the average response by the region is interpreted as zero. Extreme values with absolute values greater than 2 are winsorized on the map.

## 7.2 Conventional versus Unconventional Monetary Policy

To compare the effects of conventional monetary policy (CMP) and unconventional monetary policy (UMP), we test the impacts of target shock (close to the federal fund rate shock in the baseline) and path shock (i.e. forward guidance).[44] The US MPs we use other than our baseline are shown in Figure F.2. The comparison is displayed in Figure 16. It is found that only targeted FFR shock has a negative impact on NTL, but not

[44]These shocks were identified by R. Gürkaynak and Sack (2005) and then updated by Acosta (2022). This data is on the personal website of Miguel Acosta.

forward guidance, which suggests that the conventional monetary policy is more effective in affecting real output. The results using other UMP proxies by Jarociński (2024), including Large-scale asset purchase shock (LSAP), forward guidance (or called Odyssean forward guidance, close to the path shock in R. Gürkaynak and Sack, 2005), and information shock (or called Delphic forward guidance) are not significant either as shown in Figure F.3.

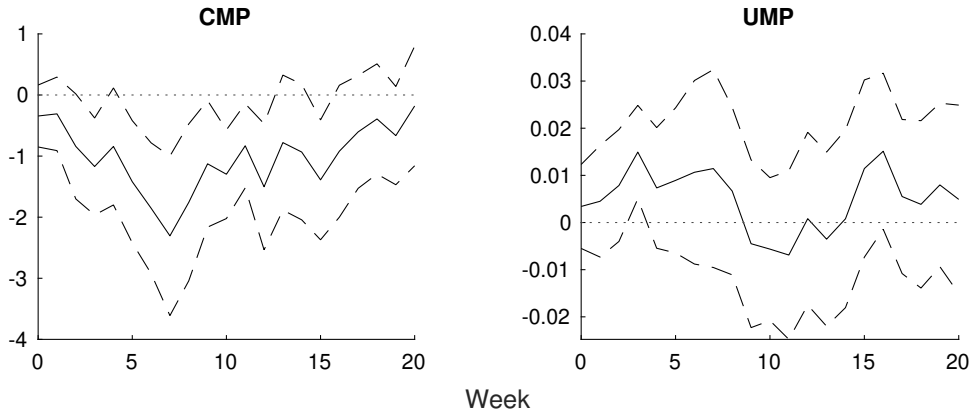


Figure 16: Local Projection of NTL on US MPs: CMP vs UMP

Notes: CMP and UMP denote the impact of target shock and path shock respectively. Shocks are aggregated to the weekly frequencies consistent with the dependent variable. The number of lags of the dependent variable ($Q$) and the shock ($M$) are selected by the AIC criteria for up to 4 periods. The dashed ribbons are the 90 percent confidence intervals generated based on the Newey-West standard errors.

## 7.3 MPs of China and Other Economies

Apart from MPs by the Fed, we also study the impact of MPs by other major central banks, such as the People's Bank of China (PBC), European Central Bank (ECB), and the Bank of Japan (BOJ) on the real economy in China, as shown in Figure F.4.[45] Specifically, we apply the baseline LP identification and replace US MPs with the shocks by PBC, ECB, and BOJ. The IRFs are in Figure 17.

[45]The PBC shock is obtained from Shieh (2024). The ECB shock is identified from Miranda-Agrippino and Nenova (2022). The BOJ shock is identified from Kubota and Shintani (2022).

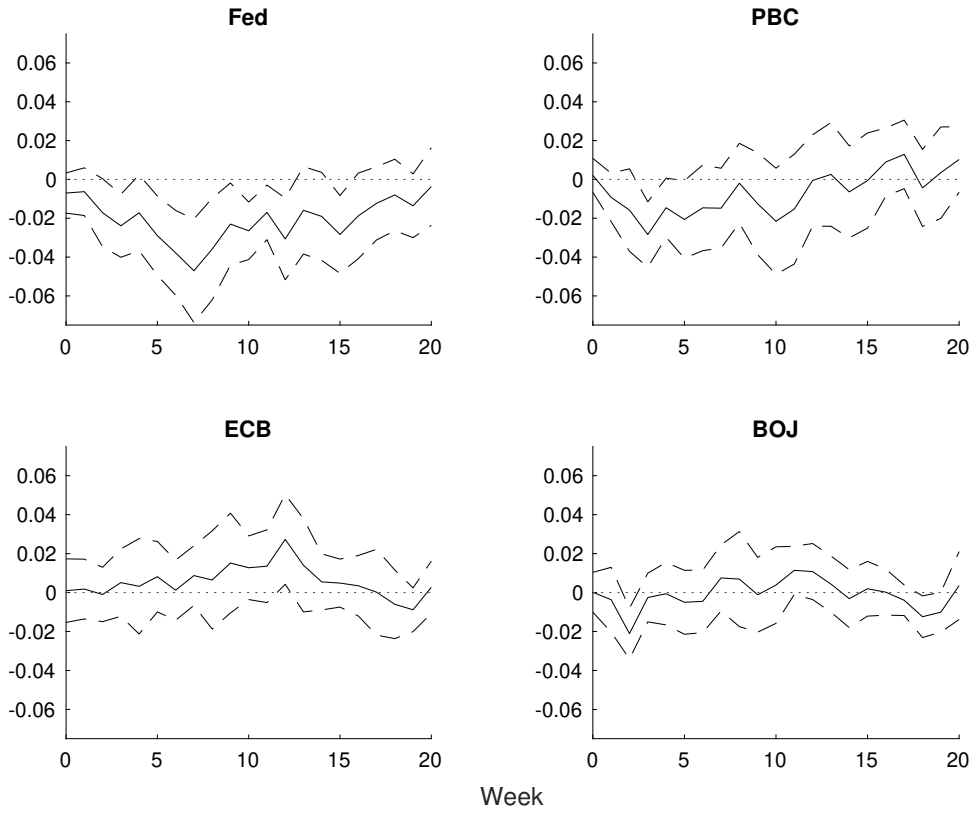


Figure 17: Local Projection of NTL on MPs by Different Central Banks

Notes: MPs is aggregated to the weekly frequencies consistent with the dependent variable. We normalize the standard deviation of all the shocks to be 1 for the full sample so that the impacts across the shocks are more comparable. The number of lags of the dependent variable ($Q$) and the shock ($M$) are selected by the AIC criteria for up to 4 periods. The dashed ribbons are the 90 percent confidence intervals generated based on the Newey-West standard errors.

As for China's own monetary policy shock, we find similar effects to those of the US shocks. This is plausible as China's tightening could also aggravate the financing conditions of Chinese firms and harm their real activities. Besides, compared with the Fed, the MPs by ECB and BOJ have less impact on the Chinese economy and the coefficients are overall insignificant. These results are consistent with previous literature such as Miranda-Agrippino and Nenova (2022) which documents that the US monetary policy is more effective in influencing other countries than ECB shocks. This makes sense as the US dollar constitutes a dominant role in international trade and financial transactions (Gopinath et al., 2020) and the US monetary policy is a key driver of the

global finance cycle (Miranda-Agrippino and Rey, 2020). Moreover, China's exchange rate is partially pegged to the US dollar, which may enhance the spillover effects from the US monetary policy.[46]

## 7.4 Trade Exposure

Although the overall negative responses are driven by construction investment, we find that trade exposure could mitigate these adverse impacts. This has already been verified in the previous low-frequency results where the net export of China increases after a tightening US shock. Consistently, we have also looked at the exchange rate responses (Chinese Yuan versus US Dollar) to the US MPs. Intuitively, a positive US MPs will depreciate the Chinese Yuan against the US Dollar (see Figure F.5), which will potentially boost the export.

Besides, we also provide some cross-sectional evidence.[47] We predict that cities with more trade exposure are less negatively impacted by a positive US MPs. The identification strategy is the same as the urbanization rate regression (Equation 3), except for replacing the urbanization rate indicator with the net export share. In the baseline, we use net export share in the last year as the proxy for net export share to preclude endogeneity issues. The key coefficient estimate is $\beta_2$. The IRF of $\beta_2$ obtained from varying $h$ from 0 to 10 is in Figure 18. Consistent with our prediction, the interaction term is overall positive, which suggests that cities with higher net export share have a smaller adverse impact from the US MPs. This conclusion is robust in subregions.[48]

[46] We also test the corresponding path shocks for each central bank, and don't find significant effects either.

[47] We show the ratio of net exports to GDP for each city with available data in 2019 (see Figure F.6). The trade balance is vastly uneven across China. The eastern coastal cities, notably cities in southern Guangdong, Zhejiang, and eastern Shandong, have a relatively high net export exposure. In contrast, cities in the West have a relatively lower and even negative exposure.

[48] As the trade exposure level substantially differs across regions, we look at the spatial heterogeneity for different subsamples of Chinese cities. We divide the cities into the East, the Middle, and the West and Northeast. The East contains the seven provinces defined as the East by NBSC plus Guangdong. The Middle contains NBSC's North excluding Inner Mongolia and Central and South excluding Guangdong. The West and Northeast contain Inner Mongolia and NBSC's Southwest and Northwest. The results shown in Figure F.7 suggest that the mitigation effect of trade is more prominent in the East, which is more trade-oriented.

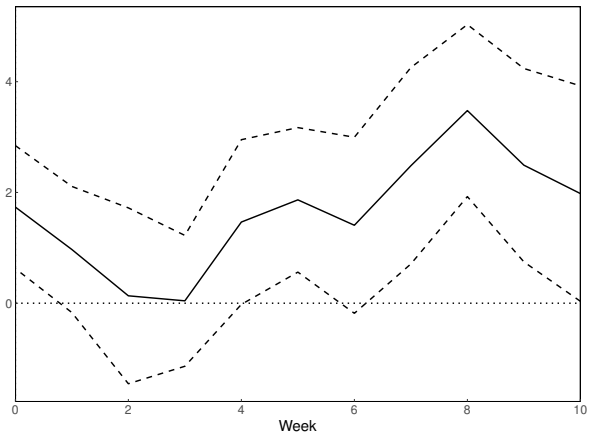


Figure 18: NTL Response to Interaction of US MPs and Trade Exposure, City level

Notes: The dashed ribbons are the 90 percent confidence intervals generated based on standard errors clustered to city and week.

# 8 Conclusion

This study leverages high-frequency nighttime light (NTL) data to examine the real economic effects of U.S. monetary policy shocks (MPs) on China. Using an event-study approach, we find that unexpected U.S. monetary tightening exerts an overall contractionary effect on China's real economy. This high-frequency NTL data allows for sharper identification of policy effects and finer dynamic responses compared to traditional low-frequency measures. Additionally, we exploit spatial heterogeneity to uncover differential impacts across city centers, suburbs, and non-built-up areas. Notably, we identify a new transmission channel: U.S. monetary tightening reduces economic activity in China by dampening construction-related output in non-built-up areas. In addition to the decomposition, this channel is also supported by firm/aggregate/city-level evidences. Consistent with this mechanism, we show that real estate firms' financing conditions play a key role in propagating U.S. shocks to China's real economy. Besides, our approach circumvents concerns about official data quality and cross-country statistical discrepancies, facilitating more comparable estimates of U.S. monetary spillovers globally.

Our paper is the first attempt to introduce high-frequency NTL data into the study

of monetary economics and revisit several classical questions in this area. We believe in the future this data could also be employed in other research where a high frequency of real economic activity measurement is needed, especially for emerging markets where the NTL is closely related to output. Admittedly, we only use NTL data to explore one of the mechanisms and some other channels like consumption are not well reflected in NTL data, which calls for future investigation.

# References


Aastveit, K. A., & Anundsen, A. K. (2022). Asymmetric Effects of Monetary Policy in Regional Housing Markets. *American Economic Journal: Macroeconomics*, *14*(4), 499–529. https://doi.org/10.1257/mac.20190011

Acosta, M. (2022). The perceived causes of monetary policy surprises. *Published manuscript*.

Akinci, Ö., & Queralto, A. (2024). Exchange Rate Dynamics and Monetary Spillovers with Imperfect Financial Markets (S. Giglio, Ed.). *The Review of Financial Studies*, *37*(2), 309–355. https://doi.org/10.1093/rfs/hhad078

Bhattarai, S., & Neely, C. J. (2022). An Analysis of the Literature on International Unconventional Monetary Policy. *Journal of Economic Literature*, *60*(2), 527–597. https://doi.org/10.1257/jel.20201493

Bickenbach, F., Bode, E., Nunnenkamp, P., & Söder, M. (2016). Night lights and regional GDP. *Review of World Economics*, *152*(2), 425–447. https://doi.org/10.1007/s10290-016-0246-0

Bluedorn, J. C., & Bowdler, C. (2011). The open economy consequences of U.S. monetary policy. *Journal of International Money and Finance*, *30*(2), 309–336. https://doi.org/10.1016/j.jimonfin.2010.11.001

Bluhm, R., & Krause, M. (2022). Top lights: Bright cities and their contribution to economic development. *Journal of Development Economics*, *157*, 102880. https://doi.org/10.1016/j.jdeveco.2022.102880

Bräuning, F., & Ivashina, V. (2020). U.S. monetary policy and emerging market credit cycles. *Journal of Monetary Economics*, *112*, 57–76. https://doi.org/10.1016/j.jmoneco.2019.02.005

Bustamante-Calabria, M., Sánchez De Miguel, A., Martín-Ruiz, S., Ortiz, J.-L., Vílchez, J. M., Pelegrina, A., García, A., Zamorano, J., Bennie, J., & Gaston, K. J. (2021). Effects of the COVID-19 Lockdown on Urban Light Emissions: Ground and Satellite Comparison. *Remote Sensing*, *13*(2), 258. https://doi.org/10.3390/rs13020258

Chari, A., Dilts Stedman, K., & Lundblad, C. (2021). Taper Tantrums: Quantitative Easing, Its Aftermath, and Emerging Market Capital Flows (A. Karolyi, Ed.). *The Review of Financial Studies*, *34*(3), 1445–1508. https://doi.org/10.1093/rfs/hhaa044

Chen, K., Higgins, P., & Zha, T. (2024). Constructing quarterly Chinese time series usable for macroeconomic analysis. *Journal of International Money and Finance*, *143*, 103052. https://doi.org/10.1016/j.jimonfin.2024.103052

Chen, X., & Nordhaus, W. D. (2011). Using luminosity data as a proxy for economic statistics. *Proceedings of the National Academy of Sciences*, *108*(21), 8589–8594. https://doi.org/10.1073/pnas.1017031108

Chor, D., & Li, B. (2024). Illuminating the effects of the US-China tariff war on China's economy. *Journal of International Economics*, *150*, 103926. https://doi.org/10.1016/j.jinteco.2024.103926

Clark, H., Pinkovskiy, M., & Sala-i-Martin, X. (2020). China's GDP growth may be understated. *China Economic Review*, *62*, 101243. https://doi.org/10.1016/j.chieco.2018.10.010

Cohen, F., & Gonzalez, F. (2024). Understanding the Link between Temperature and Crime. *American Economic Journal: Economic Policy*, *16*(2), 480–514. https://doi.org/10.1257/pol.20220118

Colorado School of Mines. (n.d.). Earth Observation Group - Payne Institute for Public Policy. https://payneinstitute.mines.edu/eog/

Colorado School of Mines. (2024). Earth Observation Group - Payne Institute for Public Policy. https://payneinstitute.mines.edu/eog/

Dedola, L., Karadi, P., & Lombardo, G. (2013). Global implications of national unconventional policies. *Journal of Monetary Economics*, *60*(1), 66–85. https://doi.org/10.1016/j.jmoneco.2012.12.001

Dedola, L., Rivolta, G., & Stracca, L. (2017). If the Fed sneezes, who catches a cold? *Journal of International Economics*, *108*, S23–S41. https://doi.org/10.1016/j.jinteco.2017.01.002

Di Giovanni, J., & Rogers, J. (2024). The Impact of U.S. Monetary Policy on Foreign Firms. *IMF Economic Review*, *72*(1), 58–115. https://doi.org/10.1057/s41308-023-00218-7

Drechsler, I., Savov, A., & Schnabl, P. (2022). How monetary policy shaped the housing boom. *Journal of Financial Economics*, *144*(3), 992–1021. https://doi.org/10.1016/j.jfineco.2021.06.039

Elvidge, C. D., Zhizhin, M., Ghosh, T., Hsu, F.-C., & Taneja, J. (2021). Annual Time Series of Global VIIRS Nighttime Lights Derived from Monthly Averages: 2012 to 2019. *Remote Sensing*, *13*(5), 922. https://doi.org/10.3390/rs13050922

Fratzscher, M., Lo Duca, M., & Straub, R. (2018). On the International Spillovers of US Quantitative Easing. *The Economic Journal*, *128*(608), 330–377. https://doi.org/10.1111/ecoj.12435

Georgiadis, G. (2016). Determinants of global spillovers from US monetary policy. *Journal of International Money and Finance*, *67*, 41–61. https://doi.org/10.1016/j.jimonfin.2015.06.010

Gibson, J., Olivia, S., Boe-Gibson, G., & Li, C. (2021). Which night lights data should we use in economics, and where? *Journal of Development Economics*, *149*, 102602. https://doi.org/10.1016/j.jdeveco.2020.102602

Gibson, J., Zhang, X., Park, A., Yi, J., & Xi, L. (2024). *Remotely measuring rural economic activity and poverty: Do we just need better sensors?* (CEI Working Paper Series No. 2023-08). Center for Economic Institutions, Institute of Economic Research, Hitotsubashi University. https://ideas.repec.org/p/hit/hitcei/2023-08.html

Gopinath, G., Boz, E., Casas, C., Díez, F. J., Gourinchas, P.-O., & Plagborg-Møller, M. (2020). Dominant Currency Paradigm. *American Economic Review*, *110*(3), 677–719. https://doi.org/10.1257/aer.20171201

Gürkaynak, R., Karasoy-Can, H. G., & Lee, S. S. (2022). Stock Market's Assessment of Monetary Policy Transmission: The Cash Flow Effect. *The Journal of Finance*, *77*(4), 2375–2421. https://doi.org/10.1111/jofi.13163

Gürkaynak, R., & Sack, B. (2005, November). *Do Actions Speak Louder Than Words? The Response of Asset Prices to Monetary Policy Actions and Statements* (Computing in Economics and Finance 2005 No. 323). Society for Computational Economics. Retrieved August 9, 2024, from https://econpapers.repec.org/paper/scescecf5/323.htm

Gürkaynak, R. S., & Wright, J. H. (2013). Identification and Inference Using Event Studies. *The Manchester School*, *81*(S1), 48–65. https://doi.org/10.1111/manc.12020

He, J., Jia, C. D., Li, K., & Wu, W. (2023). A High-Frequency Measure of Chinese Monetary Policy Shocks. *SSRN Electronic Journal*. https://doi.org/10.2139/ssrn.4599848

Henderson, J. V., Storeygard, A., & Weil, D. N. (2012). Measuring Economic Growth from Outer Space. *American Economic Review*, *102*(2), 994–1028. https://doi.org/10.1257/aer.102.2.994

Ho, S. W., Zhang, J., & Zhou, H. (2018). Hot Money and Quantitative Easing: The Spillover Effects of U.S. Monetary Policy on the Chinese Economy. *Journal of Money, Credit and Banking*, *50*(7), 1543–1569. https://doi.org/10.1111/jmcb.12501

Huang, Y., Panizza, U., & Portes, R. (2024). Corporate foreign bond issuance and interfirm loans in China. *Journal of International Economics*, *152*, 103975. https://doi.org/10.1016/j.jinteco.2024.103975

Iacoviello, M. (2005). House Prices, Borrowing Constraints, and Monetary Policy in the Business Cycle. *American Economic Review*, *95*(3), 739–764. https://doi.org/10.1257/0002828054201477

Jarociński, M. (2024). Estimating the Fed's unconventional policy shocks. *Journal of Monetary Economics*, *144*, 103548. https://doi.org/10.1016/j.jmoneco.2024.01.001

Jiang, H., Sun, Z., Guo, H., Xing, Q., Du, W., & Cai, G. (2022). A standardized dataset of built-up areas of China's cities with populations over 300,000 for the period 1990–2015. *Big Earth Data*, *6*(1), 103–126. https://doi.org/10.1080/20964471.2021.1950351

Jiang, L., & Liu, Y. (2023). China's Largest City-Wide Lockdown: How Extensively Did Shanghai COVID-19 Affect Intensity of Human Activities in the Yangtze River Delta? *Remote Sensing*, *15*(8), 1989. https://doi.org/10.3390/rs15081989

Jordà, Ò. (2005). Estimation and Inference of Impulse Responses by Local Projections. *American Economic Review*, *95*(1), 161–182. https://doi.org/10.1257/0002828053828518

Jordà, Ò., Schularick, M., & Taylor, A. M. (2015). Betting the house. *Journal of International Economics*, *96*, S2–S18. https://doi.org/10.1016/j.jinteco.2014.12.011

Kim, D. (2022). Assessing regional economy in North Korea using nighttime light. *Asia and the Global Economy*, *2*(3), 100046. https://doi.org/10.1016/j.aglobe.2022.100046

Kim, J., Kim, K., Park, S., & Sun, C. (2022). The Economic Costs of Trade Sanctions: Evidence from North Korea. *SSRN Electronic Journal*. https://doi.org/10.2139/ssrn.4032573

Kim, S. (2001). International transmission of U.S. monetary policy shocks: Evidence from VAR's. *Journal of Monetary Economics*, *48*(2), 339–372. https://doi.org/10.1016/S0304-3932(01)00080-0

Kolasa, M., & Wesołowski, G. (2020). International spillovers of quantitative easing. *Journal of International Economics*, *126*, 103330. https://doi.org/10.1016/j.jinteco.2020.103330

Kubota, H., & Shintani, M. (2022). High-frequency identification of monetary policy shocks in Japan. *The Japanese Economic Review*, *73*(3), 483–513. https://doi.org/10.1007/s42973-021-00110-x

Lakdawala, A., Moreland, T., & Schaffer, M. (2021). The international spillover effects of US monetary policy uncertainty. *Journal of International Economics*, *133*, 103525. https://doi.org/10.1016/j.jinteco.2021.103525

Lee, S., & Cao, C. (2016). Soumi NPP VIIRS Day/Night Band Stray Light Characterization and Correction Using Calibration View Data. *Remote Sensing*, *8*(2), 138. https://doi.org/10.3390/rs8020138

Li, X., Zhou, Y., Zhao, M., & Zhao, X. (2020). A harmonized global nighttime light dataset 1992–2018. *Scientific Data*, *7*(1), 168. https://doi.org/10.1038/s41597-020-0510-y

Maćkowiak, B. (2007). External shocks, U.S. monetary policy and macroeconomic fluctuations in emerging markets. *Journal of Monetary Economics*, *54*(8), 2512–2520. https://doi.org/10.1016/j.jmoneco.2007.06.021

Martínez, L. R. (2022). How Much Should We Trust the Dictator's GDP Growth Estimates? *Journal of Political Economy*, *130*(10), 2731–2769. https://doi.org/10.1086/720458

Michalopoulos, S., & Papaioannou, E. (2018). Spatial Patterns of Development: A Meso Approach. *Annual Review of Economics*, *10*(1), 383–410. https://doi.org/10.1146/annurev-economics-080217-053355

Miranda-Agrippino, S., & Nenova, T. (2022). A tale of two global monetary policies. *Journal of International Economics*, *136*, 103606. https://doi.org/10.1016/j.jinteco.2022.103606

Miranda-Agrippino, S., & Rey, H. (2020). U.S. Monetary Policy and the Global Financial Cycle. *The Review of Economic Studies*, *87*(6), 2754–2776. https://doi.org/10.1093/restud/rdaa019

Miranda-Agrippino, S., & Ricco, G. (2021). The Transmission of Monetary Policy Shocks. *American Economic Journal: Macroeconomics*, *13*(3), 74–107. https://doi.org/10.1257/mac.20180124

Nakamura, E., & Steinsson, J. (2018). High-Frequency Identification of Monetary Non-Neutrality: The Information Effect*. *The Quarterly Journal of Economics*, *133*(3), 1283–1330. https://doi.org/10.1093/qje/qjy004

NASA. (2020, July). NASA's Black Marble. https://blackmarble.gsfc.nasa.gov

National Institute for Environmental Studies. (2023). ODIAC Fossil Fuel Emission Dataset. Retrieved December 29, 2023, from https://db.cger.nies.go.jp/dataset/ODIAC/

NewHorizon. (2022). NewHorizon. http://horizon2021.xyz

NOAA National Centers of Environmental Information. (1999). Global Surface Summary of the Day - GSOD. 1.0. https://www.ncei.noaa.gov/metadata/geoportal/rest/metadata/item/gov.noaa.ncdc:C00516/html

Pinkovskiy, M., & Sala-i-Martin, X. (2016). Lights, Camera … Income! Illuminating the National Accounts-Household Surveys Debate. *Quarterly Journal of Economics*, *131*(2), 579–631. https://doi.org/10.1093/qje/qjw003

Rogers, J. H., Sun, B., & Sun, T. (2024). U.S.-China Tension. *SSRN Electronic Journal*. https://doi.org/10.2139/ssrn.4815838

Rudebusch, G. D. (1998). Do Measures of Monetary Policy in a Var Make Sense? *International Economic Review*, *39*(4), 907. https://doi.org/10.2307/2527344

Sherman, L., Proctor, J., Druckenmiller, H., Tapia, H., & Hsiang, S. (2023, March). *Global High-Resolution Estimates of the United Nations Human Development Index Using Satellite Imagery and Machine-learning* (tech. rep. No. w31044). National Bureau of Economic Research. Cambridge, MA. https://doi.org/10.3386/w31044

Shieh, H. (2024). Can you hear me now? Identifying the effect of Chinese monetary policy announcements. *Journal of International Money and Finance*, *144*, 103078. https://doi.org/10.1016/j.jimonfin.2024.103078

Swanson, E. T. (2021). Measuring the effects of federal reserve forward guidance and asset purchases on financial markets. *Journal of Monetary Economics*, *118*, 32–53. https://doi.org/10.1016/j.jmoneco.2020.09.003

Team, S. D. C. (2020). Metadata record for: A harmonized global nighttime light dataset 1992-2018 [Artwork Size: 4268 Bytes Pages: 4268 Bytes]. https://doi.org/10.6084/M9.FIGSHARE.12312125

Uribe, M., & Yue, V. Z. (2006). Country spreads and emerging countries: Who drives whom? *Journal of International Economics*, *69*(1), 6–36. https://doi.org/10.1016/j.jinteco.2005.04.003

Wang, X. (n.d.). Historical data of air quality and weather in China. https://quotsoft.net/air/

Xu, G., Xiu, T., Li, X., Liang, X., & Jiao, L. (2021). Lockdown induced night-time light dynamics during the COVID-19 epidemic in global megacities. *International Journal of Applied Earth Observation and Geoinformation*, *102*, 102421. https://doi.org/10.1016/j.jag.2021.102421

Yang, J., & Huang, X. (2024, August). The 30 m annual land cover datasets and its dynamics in China from 1985 to 2023. https://doi.org/10.5281/ZENODO.4417809

Yang, P., & Pan, J. (2022). Estimating Housing Vacancy Rate Using Nightlight and POI: A Case Study of Main Urban Area of Xi'an City, China. *Applied Sciences*, *12*(23), 12328. https://doi.org/10.3390/app122312328

# Appendix A Data Appendix

## A.1 Monetary policy shock

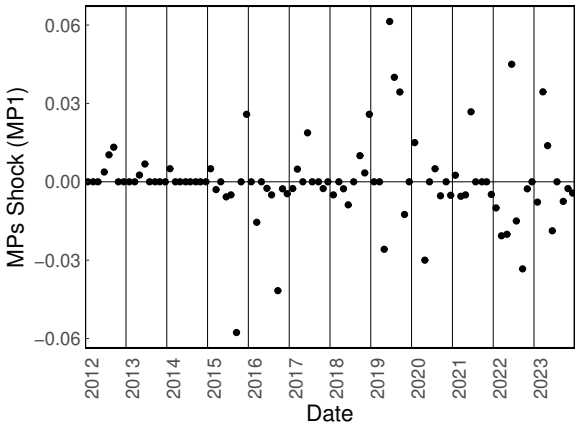


Figure A.1: Proxies of Monetary Policy Shock: Baseline

Notes: For each MPs event, the corresponding date is the day when the FOMC is held.

## A.2 Baseline Panel Summary Statistics

Table A.1: Summary Statistics: Weekly NTL and Shocks

| | N | Mean | SD | Min | Max |
|---|---|---|---|---|---|
| Year | 624 | 2017.51 | 3.45 | 2012.00 | 2024.00 |
| Log NTL | 624 | 0.00 | 0.17 | -0.46 | 0.50 |
| MPs: MP1 | 624 | 0.00 | 0.01 | -0.06 | 0.06 |
| MPs: Acosta | 562 | -0.00 | 0.01 | -0.06 | 0.06 |
| MPs: Target | 562 | 0.01 | 0.15 | -1.48 | 1.22 |
| MPs: Path | 562 | 0.01 | 0.31 | -2.61 | 3.39 |
| MPs: Forward Guidance | 624 | -0.01 | 0.40 | -3.04 | 3.35 |
| MPs: LSAP | 624 | -0.01 | 0.28 | -4.13 | 1.74 |
| MPs: Information | 624 | 0.02 | 0.24 | -1.84 | 1.92 |

Notes: Date ranges from 2012-01-16 to 2024-01-01. The last week with non-zero baseline MPs: MP1 is on 2023-12-11. MPs shocks are aggregated to week level. For MPs, a week includes at most one shock, so the value for the week is either zero or the shock in that week.

## A.3 Details of NTL Data

### A.3.1 Data Availability

Partially-corrected raw daily data (Black Marble) are available on the official website of NASA at: https://ladsweb.modaps.eosdis.nasa.gov/missions-and-measurements/products/VNP46A2, and Google Earth Engine (GEE) at: https://developers.google.com/earth-engine/datasets/catalog/NOAA_VIIRS_001_VNP46A2.

As an illustration, the map of NTL in the East Asia and Pacific region released by NASA in 2016 is as follows.[49]

Figure A.2: Nighttime Luminosity Captured by NASA Satellite in 2016

Apart from NASA, the monthly VIIRS series has also been available on EOG (Earth Observation Group) since April 2012, and the annual VIIRS series has been available since 2012 (Elvidge et al., 2021).[50] While the annual VIIRS series is available to all areas with a latitude lower than 65 degrees, the monthly series without stray-light correction is unavailable in summer in places with higher latitudes due to long daytime and even longer astronomical light in summer. Therefore, we use the stray-light corrected version for the monthly NTL series. We use the cleaned NTL series from the source to associate NTL with economic indicators, including GDP, for its broader coverage. We also use the series when studying the country-level NTL response to US MPs, as it is available globally without the necessity for post-processing.[51] The processed annual and monthly datasets are publicly available on the Earth Observation Group (EOG) website hosted by the Colorado School of Mines at: https://payneinstitute.mines.edu/eog/. EOG processes original satellite images to filter out ephemeral lights such as fire.

The shape files used to crop the GeoTiff files of NTL are from NewHorizon, most recently updated in 2022: http://horizon2021.xyz. Using the official shape files published by the National Bureau of Statistics of China (NBSC) in 2020 does not substantially change the results of the study.

### A.3.2 Daily NTL Data Processing

**Data Source** The daily NTL data is derived from NASA's Black Marble product using the VIIRS instrument (NASA 2020). The product code of the stray light-corrected daily

[49]The original file is publicly available at:
https://www.nasa.gov/specials/blackmarble/media/BlackMarble20161km.jpg.

[50]The annual VIIRS data in 2012 is derived from April to December, while the annual VIIRS data in forwarding years are all derived from corresponding monthly VIIRS series from January to December in the same year. The derivation is based on the stray light-corrected monthly series since 2014.

[51]The Black Marble series and the EOG series are indistinguishable at the city-year level.

NTL series is VNP46A2. It corrects for stray light, such as wildfire and moonlight. It also adjusts for the satellite angle that varies each day when the satellite captures the image of the same place. The public access is available from NASA and GEE.

To smooth the cloud computing process on the Google Cloud Platform (GCP), we use the GEE repository to capture the daily NTL geospatial data. Firstly, we extract the map using a rectangle with longitudes from 75 to 135 degrees and latitudes from 18 to 53 degrees. The rectangle contains the whole land area of mainland China.[52] For each day's map, we save four layers to the corresponding TIFF file: daily NTL (DNB_BRDF_Corrected_NTL), NASA-filled daily NTL (Gap_Filled_DNB_BRDF_ Corrected_NTL), quality flag (Mandatory_Quality_Flag), and snow flag (Snow_Flag). We do this for each day from 1 January 2018 to 31 December 2023 with 2,174 files.[53]

**Panel Construction** For each city, we use the GIS shape file as introduced in the data section. We crop from the daily rectangles using the shape file and only include cells where the center falls within the shape file. For the cropped dataset, we filter out observations without NASA-filled daily NTL, as the value is supposed to be available for every legible cell in the map. The cropped dataset includes longitude, latitude, and the values of the four layers for each cell. For computational efficiency, we exclude cities with more than 500,000 cells.

We filter out cells with contaminated daily NTL and fill them with previous values. For each cell (defined by longitude and latitude), we keep the daily NTL value only if both the quality flag and the snow flag are zero, indicating no quality (e.g., cloud coverage) issue or snow-coverage issue in the cell. Then, we concatenate the dataset to a cell-level daily panel. For each cell, we obtain a time series with several missing values for the daily NTL. We fill the NA values with the latest valid value from the beginning to the end. Then, we fill the starting NA values using the earliest valid value, so the time series cell is fully filled as long as one valid value exists. We call the filled daily NTL series the manually-filled NTL series. Then, we aggregate the panel into a daily NTL series. For each day, we record the number of valid cells. In the aggregated daily NTL series, we drop the dates where the valid cell numbers are less than 90 percent of the maximum cell number for either the NASA-filled NTL or the manually-filled NTL. Finally, we concatenate the time series for each city, and the merged dataset is a city-level daily panel. The key variables in the panel include the city code and the date.

**Built-up Area and Other Economies** We also apply the GIS shape file for the built-up area to crop from the daily rectangles. Different from the process above for cities, we include a cell as long as it touches the shape file. We implement the adjustment as the built-up areas can be discretionary, and excluding potential light sources adds to the measurement error. Similar to the city-level daily panel of NTL, we generate a city-level daily panel of NTL for each definition of built-up area. The key variables in the panel

[52]For Hainan province, we use another rectangle with longitudes from 108 to 112 degrees and latitudes from 17 to 21 degrees. We omit Sansha, a remote city with a small area far from the main body of Hainan Island.

[53]The maps are unavailable for late July 2022 due to the satellite issue. However, the missing data in the period do not interfere with the study.

include the city code, the definition year of the built-up area (each five years from 1990 to 2015), and the date.

We apply the same method to crop regions in other economies, including Hong Kong (China), Macau (China), Taiwan (China), Mongolia, North Korea, South Korea, Japan, Vietnam, Thailand, Bangladesh, India, Mexico, United States, Australia, and New Zealand. Like the balance we keep for computation power-saving and population coverage, we exclude some regions with relatively large area and small population. For Mongolia, we select 10 out of 21 regions, which represents over 70 percent of the national population. For Japan, we exclude Hokkaido. For Vietnam, we only include the 25 out of 63 regions, which are in the northern part and represent about 40 percent of the national population. For India, we include 498 out of 676 secondary regions, excluding the southern, western, and Jammu and Kashmir regions. For Mexico, we include the states of Baja California, Sonora, Chihuahua, Coahuila, Nuevo Leon, Tamaulipas, Chiapas, Quintana Roo, covering about 60 percent of the national population. For the United States, we include the states of Texas and Louisiana. For Australia, we include Australian Capital Territory, Victoria, New South Wales (coastal), Queensland (greater Brisbane area), and South Australia (Adelaide metropolitan area), which cover more than 80 percent of the national population.

**Mountain Areas** To remove mountain areas and other inhabitable areas in China, we use the land cover map from CLCD.[54] The geospatial map is derived from the Landsat satellite images on the Google Earth Engine. We use the version with 30 meter resolution identified for the year 2022. For each original cell, we identify it as inhabitable if it is not cropland or impervious, which consequently includes all forest, shrub, grassland, water, snow and ice, barren, and wetland cells. The cells are converted to 500-meter cells used in the NTL geospatial data. For each converted cell, we identify it as inhabitable if all associated original cells are inhabitable.

## A.4 Land Transaction Data of China

China's land transaction data are processed from Land China (www.landchina.com).[55] Each land transaction is identified by an Electronic Identification number (EID). The sample period ranges from 2000 to 2020. For each land transaction, the dataset records the city, the address, the source of the land, the area, the financial amount of the transaction, the upper and lower bounds of the contracted floor-area ratio, the signing date of the contract, and the transacted party (usually a person or a firm).

To match each land transaction with a listed firm, we identify the best match from the name of the transacted party, searching for the name of the potential parent firm of the transacted party. Additionally, we expand the scope to subsidiaries of each listed firm, including those not directly identified from their names. If the name of a transacted party matches a subsidiary firm, we match the transaction with the parent firm corresponding to the subsidiary firm. Currently, matches are available for all transactions from 2007 to 2015 and from 2017 to 2019.

[54]The tif file is publicly available at: https://zenodo.org/records/8176941.

[55]We thank Xiaoyu Zhang for sharing the processed data, including matching transactions to list firms and aggregating them to city level.

To aggregate the data to city level, we add the total area or revenue of all the transactions occurred within each city. We also aggregate the transactions by category of land transaction purpose. For both area and revenue, we classify all transactions into four categories: commercial, industrial, residential, and public.

## A.5 Bond issuance data

The confidential bond issuance data of Chinese firms are from Huang et al. (2024).[56] Each bond issuance is identified by an unique identification number. The sample period ranges from 2000 to 2015. For each bond issuance, the dataset records the issuer's name, the issuer's parent firm's name (if diffrent from the issuer), the matched listed firm (through stock market code), the firm's industry, the pricing date, the maturity date, the currency of the bond, and the value of the bond. It also provides information such as bond rating at issuance, current bond rating, whether the bond is of investment grade, yield to maturity, and the interest rate of the US and China on the bond pricing date.

We identify whether the issuance is domestic or foreign based on the currency of the bond. If the currency of the bond is Chinese Yuan (CNY), we classify the record as domestic. Otherwise, we classify it as foreign. In this study, we focus on the records matched to a listed real estate firm. For such records, 94.14 percent of the classified foreign issuance are denominated in US dollars (USD). Therefore, the US interest rate can be used as a good measure of the reference bond issuance rate.

## A.6 Other Data

### A.6.1 Firm Data of China

The operation information of listed firms in China is from China Stock Market Accounting Research (CSMAR). It contains the quarterly financial reporting information of all listed firms in China's equity market from 2007 to 2023. Each listed firm is identified by the stock quote code. Key information we use includes the industry of the firm as classified by CSRC, balance sheet indicators (assts, liabilities, bill and accounts receivable, bill and accounts payable), earning indicators (revenue, cost, profit, net profit, total comprehensive income) and cashflow indicators (total cashflow, and cashflow from operation, investment, and financing activities).

### A.6.2 National Accounts

To associate variations in NTL with changes in economic activities, we need to obtain GDP and other national account indicators and adjust the NTL data to the same frequency. Two datasets are used for this purpose. The first is the city-level annual panel in China, which corresponds to our baseline spatial heterogeneity analysis at city level. The second is the country-level annual panel, which supports our cross-country comparison. We obtain the city-level national accounts of China from statistical yearbooks, which are published annually by the NBSC, and use data from 2012 to 2023. Indicators we use include total GDP, GDP in the primary, secondary, and tertiary sectors, import, and export.[57] The summary statistics of the city-level national accounts are in Table A.2. Then,

[56] We thank Yi Huang for sharing the data.

[57] Import and export are available until 2021.

we get country-level national accounts from the World Development Indicator (WDI) of the World Bank and associate them with country-level NTL series from the Light pollution statistics. [58] We use data from 2012 to 2023 in line with the main panel. The summary statistics of the country-level national accounts are in Table A.3.

Table A.2: Summary Statistics: National Accounts, Annual series, City

| | N | Mean | SD | Min | Max |
|---|---|---|---|---|---|
| Year | 8788 | 2010.50 | 7.50 | 1998.00 | 2023.00 |
| GDP | 8253 | 1677.65 | 3171.75 | 4.55 | 51404.47 |
| Primary sector GDP share | 7291 | 14.76 | 9.63 | 0.03 | 54.73 |
| Secondary sector GDP share | 7292 | 44.68 | 11.55 | 9.21 | 90.97 |
| Tertiary sector GDP share | 7291 | 40.73 | 10.17 | 8.55 | 89.34 |
| Import | 1447 | 425.31 | 1944.38 | 0.00 | 24891.68 |
| Export | 1454 | 513.57 | 1669.25 | 0.00 | 19263.41 |
| Population | 6436 | 430.85 | 308.08 | 0.00 | 3416.00 |
| Nonrural population | 3205 | 134.64 | 134.38 | 6.00 | 1693.00 |
| Urban area | 6637 | 114.41 | 164.75 | 5.00 | 3371.00 |
| Administration area | 6117 | 2619.91 | 25746.77 | 13.00 | 2000013.00 |
| Urban constructed rate | 4763 | 8.28 | 9.45 | 0.00 | 97.18 |
| Number of bank subsidiaries | 4359 | 840.46 | 733.57 | 1.00 | 7518.00 |
| Loan | 5473 | 2462.33 | 6167.42 | 0.06 | 88260.13 |
| Deposit | 5477 | 3390.92 | 9620.24 | 1.60 | 192104.31 |

Notes: The unit of GDP, import, export, loan, and deposit is 100 million Yuan. The unit of GDP share and urban constructed rate is percent. The unit of population is 10,000. The unit of area is squared km.

Table A.3: Summary Statistics: National Accounts, Annual series, Country

| | N | Mean | SD | Min | Max |
|---|---|---|---|---|---|
| Year | 2321 | 2017.00 | 3.16 | 2012.00 | 2022.00 |
| GDP | 2209 | 393083.69 | 1688939.02 | 31.95 | 20926835.05 |
| Import share in GDP | 1908 | 48.93 | 29.10 | 1.13 | 221.01 |
| Export share in GDP | 1908 | 43.30 | 32.77 | 1.57 | 221.61 |
| Population | 2321 | 35815141.62 | 138030915.26 | 10444.00 | 1417173173.00 |
| Urban population | 2288 | 19798987.35 | 69580700.43 | 5245.00 | 897578430.00 |
| NTL | 2321 | 860425.20 | 2874406.73 | 0.00 | 34976796.00 |

Notes: The unit of GDP is one million constant 2015 US Dollar (World Bank API indicator code: NY.GDP.MKTP.KD). The unit of GDP share is percent. The unit of NTL is the sum of nW/cm2/sr across cells.

### A.6.3 Financial Data of China

We use China's financial market data, including interest rates, stock market indices, and exchange rates. They are at daily frequency, and we use full sample starting from

[58] The country-level NTL data here are from the Light pollution map, but they are derived from the same source as our main NTL series.

1990s. Interest rates we use include R007 (7-day interbank repo rate with collaterals) and SHIBOR (Shanghai Interbank Offering Rate). Stock market indices we use include SSE (Shanghai Stock Exchange) indices (Composite, Industrial, Real Estate, Infrastructure, Financial, SSE 180). Exchange rates we use include the exchange rate of USD to CNY.

### A.6.4 Time Series Data of China at Different Regional Levels

Most of the time series data we use are from CEIC, a comprehensive database for aggregated economic indicators, including the China Premium Database. We use national, province-level, and city-level indicators at annual, quarterly, and monthly frequencies. We use the full sample starting from as early as 1990s. We also use some data from NBSC.

**National Data** For quarterly series, we use real GDP growth (YoY) (overall, consumption, investment, and net export). We use both official data provided by CEIC and revised data by K. Chen et al. (2024). For monthly series, we use real estate related investment growth (YoY, YTD) (overall, residential building, construction, land purchase), number of projects under construction, building sold growth (YoY, YTD), industrial production growth (YoY, YTD), and land transaction data from CREI (China Real Estate Information) (number of cases, land area, land sold, all in YoY, YTD). We also use foreign reserve, export (FOB), import (CIF), and FDI data. They are provided by CEIC. For daily series, we use China Yicai High Frequency Economic Activity Index from CEIC.

**Province-level Data** Annual series we use include construction firm data (number of enterprises, total asset, project payment receivable, total liability, revenue, financial expense) and real estate firm data (total asset, total liability, financial expense, sales revenue). Monthly series we use include fixed asset investment (number of projects under construction).

**City-level Data** Annual series we use include urbanization indicators (population urbanization percentage, urban area percentage, percent of construction field across area), and financial development indicators (number of bank subsidiaries, loan and deposit in financial institutions) from NBSC. From CEIC, we use investment-related indicators (such as floor space sold and waiting for sale, fixed asset investment in real estate).

### A.6.5 Time Series Data of the US

Data of the US economy are from the FRED database provided by the Federal Reserve Bank (Fed) of St. Louis. We use GDP data at quarterly frequency (GDPC1), Industrial Production data at monthly frequency (INDPRO), and S&P 500 index at daily frequency.

Corresponding to the US MPs series, we also adopt the US news shocks (including shocks on GDP, CPI, PPI, employment). A shock is the difference of realized and ex-ante expected values. The consensus expectations are available from the widely used survey by Action Economics, the successor to Money Market Services. We use the "advance" GDP release, headline CPI and PPI inflation, and non-farm payrolls from the employment report. This data is obtained from Lakdawala et al. (2021).

### A.6.6 Weather

Like the NTL data, weather data are also available daily. Weather potentially impacts NTL through channels irrelevant to productivity. Therefore, we control for daily weather conditions as a robustness check. The weather series can also be used as a placebo test, as their changes are supposed to be relatively irrelevant to the MPs. The data source is the Global Surface Summary of the Day (GSOD) from the National Oceanic and Atmospheric Administration (NOAA).[59] We use the average daily temperature, precipitation, visibility, and wind speed data since 2014 in the study. The summary statistics of the weather data are in Table A.4.

Table A.4: Summary Statistics: Weather Data, Daily Series, City

| | N | Mean | SD | Min | Max |
|---|---|---|---|---|---|
| Year | 881043 | 2018.47 | 2.86 | 2014.00 | 2023.00 |
| Average temperature | 881043 | 14.15 | 11.63 | -45.39 | 42.67 |
| Visibility | 867629 | 1.65 | 0.84 | 0.00 | 7.00 |
| Wind speed | 877511 | 0.91 | 0.48 | 0.00 | 14.63 |

Notes: Date ranges from 2014-01-01 to 2023-12-31. Each observation is a city (average across weather stations) in a day. Temperature is in degrees Celsius. Precipitation is in millimeter. Visibility is in kilometer. Wind speed is in kilometer per hour.

[59]The data are publicly accessible at: https://www.ncei.noaa.gov/access/metadata/landing-page/bin/iso?id=gov.noaa.ncdc:C00516.

# Appendix B More Results on NTL and Output

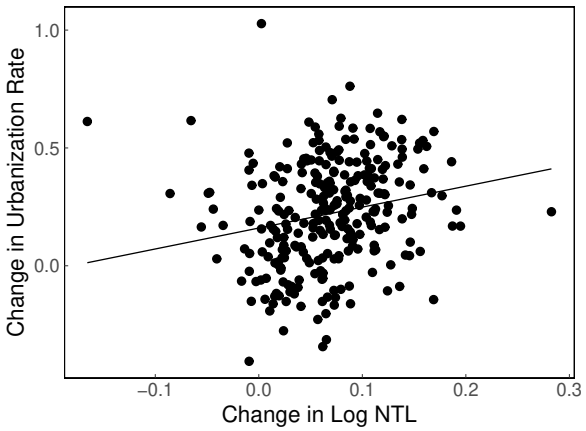


Figure B.1: NTL and Urbanization Rate by City

Notes: Log NTL is converted to the corresponding frequency of the national account indicator. Log NTL shown is the logged value of the average NTL across every day in the converted periods. For each day, NTL is the average value of all cells in each city. The graph shows the changes from 2012 to 2019.

Table B.1: Regression of GDP on NTL: Sector

| Dependent Variable: | Log GDP | | | |
|---|---|---|---|---|
| Sector: | All | Primary | Secondary | Tertiary |
| Model: | (1) | (2) | (3) | (4) |
| *Variables (Second stage)* | | | | |
| Log NTL | 0.4900*** | 0.1053 | 0.8280*** | 0.4938*** |
| | (0.0793) | (0.0708) | (0.1254) | (0.0866) |
| *Fixed-effects* | | | | |
| City | Yes | Yes | Yes | Yes |
| Year | Yes | Yes | Yes | Yes |
| *Fit statistics* | | | | |
| N | 2,527 | 2,293 | 2,293 | 2,293 |
| $R^2$ | 0.9873 | 0.9834 | 0.9676 | 0.9878 |
| F-test | 3,161.7 | 2,128.7 | 1,115.1 | 3,021.7 |

Notes: The COVID period from years 2020 to 2022 (both included) are excluded. The instrumental variable of the log nighttime light is the same indicator in the previous period. The first-stage regression coefficient is 0.6867 (s.e.: 0.0220). Significance levels are based on Clustered (Region) standard-errors. Significance Codes: ***: 0.01, **: 0.05, *: 0.1.

Table B.2: Regression of GDP on NTL: Periods

| Dependent Variable: | Log GDP | | | |
|---|---|---|---|---|
| Period: | All | Exclude COVID | 2012-2016 | 2017-2023 |
| Model: | (1) | (2) | (3) | (4) |
| *Variables (Second stage)* | | | | |
| Log NTL | 0.2559*** | 0.4900*** | 0.9435*** | 0.2802*** |
| | (0.0583) | (0.0793) | (0.1124) | (0.0844) |
| *Variables (First stage)* | | | | |
| Log NTL (Lag 1) | 0.7234*** | 0.6867*** | 0.5188*** | 0.5060*** |
| | (0.0135) | (0.0220) | (0.0317) | (0.0627) |
| *Fixed-effects* | | | | |
| City | Yes | Yes | Yes | Yes |
| Year | Yes | Yes | Yes | Yes |
| *Fit statistics* | | | | |
| N | 3,475 | 2,527 | 1,580 | 947 |
| $R^2$ | 0.9861 | 0.9873 | 0.9936 | 0.9953 |
| F-test | 2,041.7 | 3,161.7 | 10,708.6 | 21,922.0 |

Notes: The COVID period includes years 2020 to 2022 (both included). The subperiod 2017 to 2023 also excludes the COVID period. Significance levels are based on Clustered (Region) standard-errors. Significance Codes: ***: 0.01, **: 0.05, *: 0.1.

Table B.3: Regression of GDP on NTL: Trade and Construction Indicators

| Dependent Variables: | Urbanization rate | Net export | Export | Import |
|---|---|---|---|---|
| Model: | (1) | (2) | (3) | (4) |
| *Variables (Second stage)* | | | | |
| Log NTL | 0.0433*** | 7.0013*** | 14.0010*** | 7.0535*** |
| | (0.0121) | (1.3456) | (2.4384) | (2.0025) |
| *Variables (First stage)* | | | | |
| Log NTL (Lag 1) | 0.8419*** | 0.6942*** | 0.6927*** | 0.6959*** |
| | (0.0141) | (0.0197) | (0.0193) | (0.0199) |
| *Fixed-effects* | | | | |
| City | Yes | Yes | Yes | Yes |
| Year | Yes | Yes | Yes | Yes |
| *Fit statistics* | | | | |
| N | 2,484 | 1,414 | 1,421 | 1,415 |
| $R^2$ | 0.9876 | 0.8246 | 0.8472 | 0.8443 |
| F-test | 2,441.4 | 270.2 | 317.0 | 309.6 |

Notes: Significance levels are based on Clustered (Region) standard-errors. Significance Codes: ***: 0.01, **: 0.05, *: 0.1.

Table B.4: Regression of GDP on NTL: Countries by Income Group

| Dependent Variable: | Log GDP | | |
|---|---|---|---|
| Group: | All | Higher income | Lower income |
| Model: | (1) | (2) | (3) |
| *Variables (Second stage)* | | | |
| Log NTL | 0.1420*** | 0.0403 | 0.1277** |
| | (0.0444) | (0.0717) | (0.0511) |
| *Variables (First stage)* | | | |
| Log NTL (Lag 1) | 0.7791*** | 0.6812*** | 0.7687*** |
| | (0.0407) | (0.0460) | (0.0588) |
| *Fixed-effects* | | | |
| Country | Yes | Yes | Yes |
| Year | Yes | Yes | Yes |
| *Fit statistics* | | | |
| N | 1,997 | 984 | 1,003 |
| $R^2$ | 0.9990 | 0.9992 | 0.9986 |
| F-test | 19,166.4 | 11,904.7 | 7,313.8 |

Notes: The economies are classified into higher income and lower income economics by comparing their GDP per capita in 2012 with the median of all the economies in the sample. GDP value used is the constant GDP in 2015 US dollars (World Bank API indicator code: NY.GDP.MKTP.KD). Significance levels are based on Clustered (Region) standard-errors. Significance Codes: ***: 0.01, **: 0.05, *: 0.1.

# Appendix C More Results on Spillover Effects

## C.1 High-frequency Effects Robustness

***Low-frequency factors***. To exclude the noises from low-frequency factors, we add year-quarter fixed effects (FE) to our baseline specification. Note that the horizon of our baseline IRF is 20 weeks, which is less than two quarters. Therefore, adding such a FE does not substantially alter the short-term variation we intend to capture. The results are in Figure C.1, which are, as expected, qualitatively identical to our baseline.

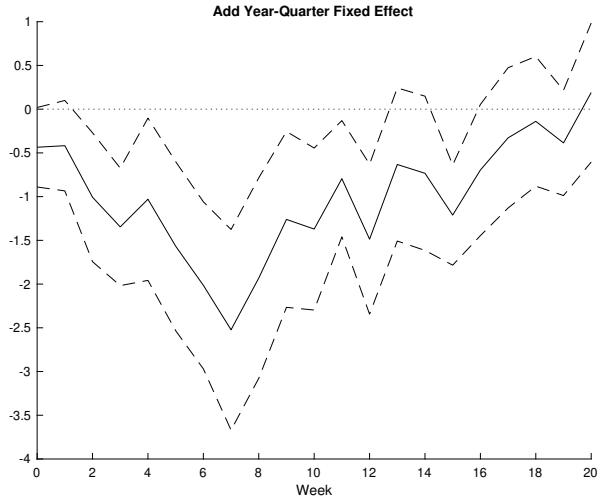


Figure C.1: Response of China's NTL on US MPs: With Year-Quarter Fixed Effect

Notes: MPs is aggregated to the weekly frequencies consistent with the dependent variable. The number of lags of the dependent variable ($Q$) and the shock ($M$) are selected by the AIC criteria for up to 4 periods. The dashed ribbons are the 90 percent confidence intervals generated based on the Newey-West standard errors.

***Subsample results***. A natural question is whether our findings are robust in subsamples. There has been a trade war between the US and China since January 2018, which potentially changed the transmission of the US shock to China. To verify this conjecture, we conduct the baseline analysis across two periods: Before the trade war (2012-2017) and Since the trade war (2018-2023). The results are in Figure C.2, which shows that the US tightening could weak China's NTL in both periods with magnitudes before the trade war slightly bigger and more significant. This is plausible as the two economies are more connected before the intensification of trade conflicts.

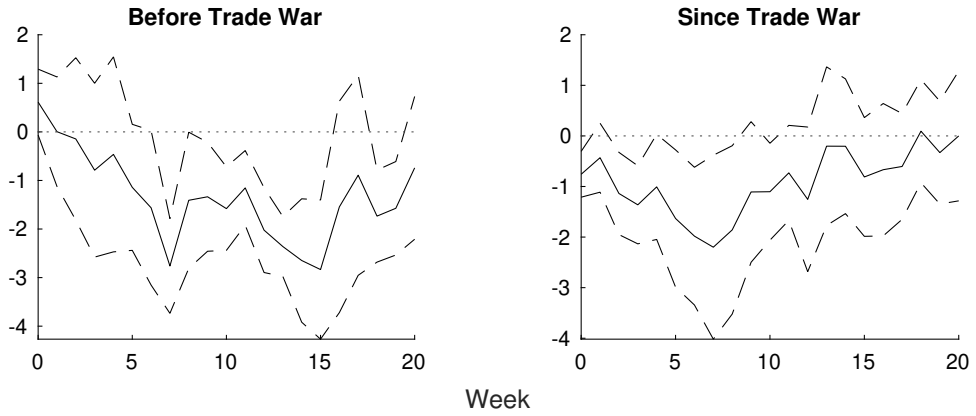


Figure C.2: Local Projection of NTL on US MPs: Before and Since the US-China Trade War

Notes: The Before Trade War period is from early 2012 to late 2017. Correspondingly, the Since Trade War period is from early 2018 to late 2023. MPs is aggregated to the weekly frequencies consistent with the dependent variable. The number of lags of the dependent variable ($Q$) and the shock ($M$) are selected by the AIC criteria for up to 4 periods. The dashed ribbons are the 90 percent confidence intervals generated based on the Newey-West standard errors.

***Alternative Measurements and Specifications***. (1) The response remains almost the same by replacing our baseline shock with the conventional MPs identified by Acosta (2022), as shown in Figure C.3. (2) Using another high-frequency economic activity index also produces negative outcomes after US tightening, see Figure C.4.[60] (3) The confidence band is qualitatively the same by bootstrapping the standard error instead of using the Newey-West in the baseline, as shown in Figure C.5. (4) We restrict the identification to exclude the lags of the shocks and use only one period lag of NTL change as a control. The results are in Figure C.6, which remain qualitatively unchanged, though the peaks of the negative responses are in the eighth week. (5) By changing the frequency of the series from weekly to daily, the results are consistent as in Figure C.7. The peaks of the negative responses are at about the 50th day, close to the 7-week peaks in the weekly identification. (6) Concerning the measurement error induced by recorded light in the human-less areas, we remove the mountain and other inhabitable areas, and the overall NTL responses are in Figure C.8.

[60]Here we use the "Yicai High Frequency Economic Activity Index". It is a daily index of China's economic activities available since 2020. It is derived from a range of mobility, transport, and consumption indicators.

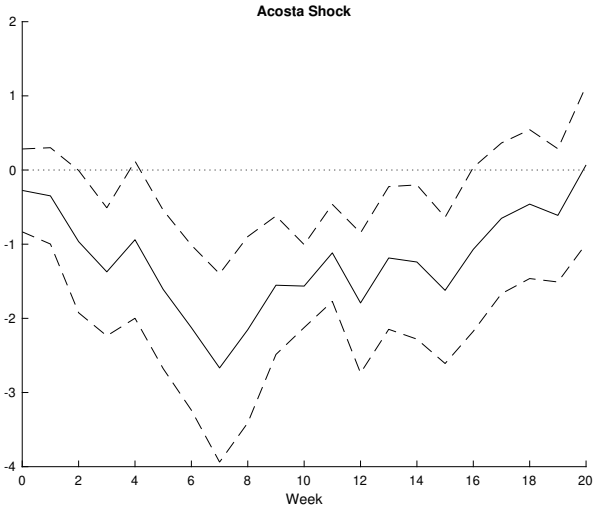


Figure C.3: Local Projection of NTL on US MPs: Acosta Shock

Notes: MPs is aggregated to the weekly frequencies consistent with the dependent variable. The number of lags of the dependent variable ($Q$) and the shock ($M$) are selected by the AIC criteria for up to 4 periods. The dashed ribbons are the 90 percent confidence intervals generated based on the Newey-West standard errors.

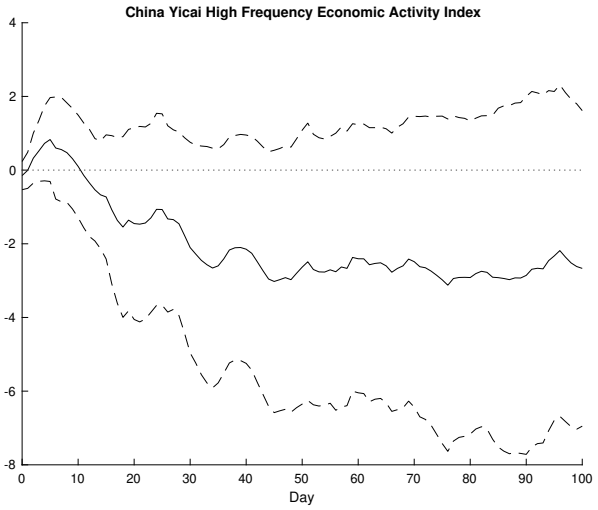


Figure C.4: Local Projection of China Yicai High Frequency Economic Activity Index on US MPs

Notes: The number of lags of the dependent variable ($Q$) and the shock ($M$) are selected by the AIC criteria for up to 4 periods. The dashed ribbons are the 90 percent confidence intervals generated based on the Newey-West standard errors.

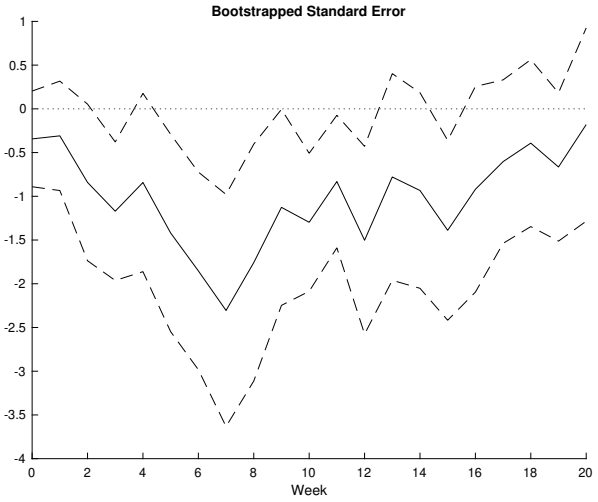


Figure C.5: Local Projection of NTL on US MPs: Baseline, Bootstrapped Standard Error

Notes: MPs is aggregated to the weekly frequencies consistent with the dependent variable. The number of lags of the dependent variable ($Q$) and the shock ($M$) are selected by the AIC criteria for up to 4 periods. The dashed ribbons are the 90 percent confidence intervals generated by bootstrapping with 1,000 draws.

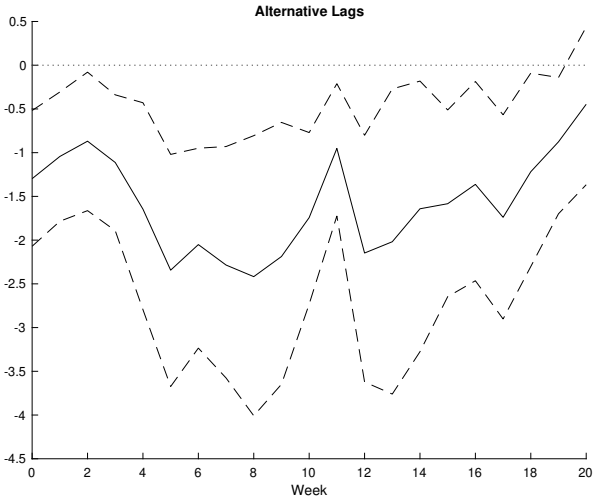


Figure C.6: Local Projection of NTL on US MPs: Alternative Lags (M = 0, Q = 1)

Notes: MPs is aggregated to the weekly frequencies consistent with the dependent variable. The dashed ribbons are the 90 percent confidence intervals generated based on the Newey-West standard errors.

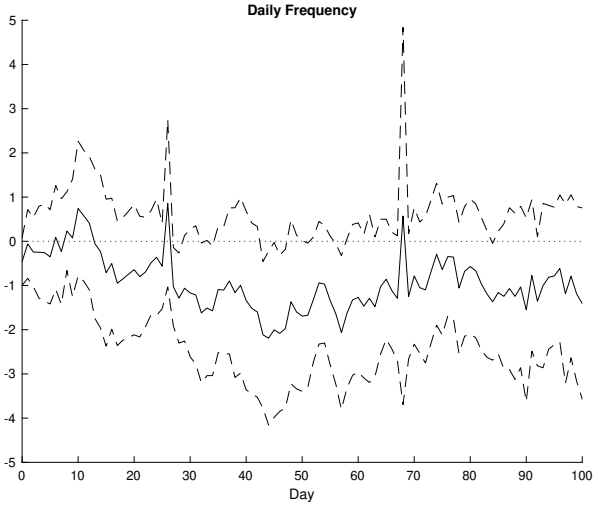


Figure C.7: Local Projection of NTL on US MPs: Daily

Notes: The number of lags of the dependent variable ($Q$) and the shock ($M$) are selected by the AIC criteria for up to 4 periods. The dashed ribbons are the 90 percent confidence intervals generated based on the Newey-West standard errors.

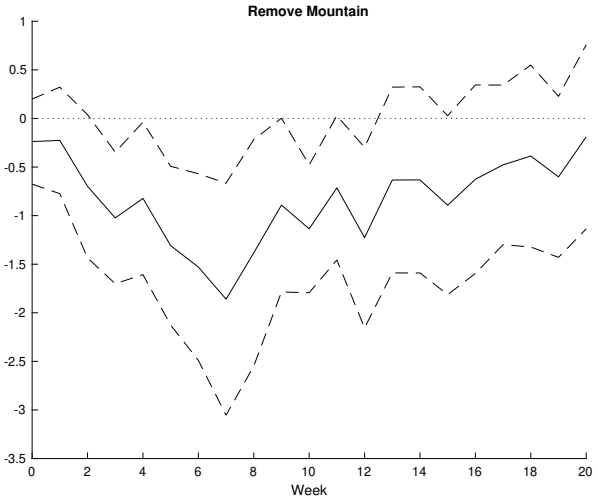


Figure C.8: Local Projection of NTL on US MPs: Remove Mountain Areas

Notes: MPs is aggregated to the weekly frequencies consistent with the dependent variable. The number of lags of the dependent variable ($Q$) and the shock ($M$) are selected by the AIC criteria for up to 4 periods. The dashed ribbons are the 90 percent confidence intervals generated based on the Newey-West standard errors.

***Other confounding factors***. There might be some confounding factors other than MPs that affect the NTL in China. (1) The NTL may also be affected by the US news shock that happened in the same week as the monetary announcement. So, we add some concurrent macro news shocks (such as GDP, CPI, PPI, and Employment) or $S\&P$ 500 return to the identification and find robust results, as shown in Figure C.9.[61] As another way to control the US macro or financial news effect, we also add past cumulative news

[61]The regression specification is the same as our baseline, and we control one news shock or equity return each time. The macro news shocks are the differences between the data release and the previ-

shocks or equity return to the baseline LP regression, and the result is qualitatively similar, see Figure C.10.[62] Moreover, controlling US GDP or Industrial Production also yields a consistent conclusion, see Figure C.11. (2) The NTL possibly changes with the weather conditions irrelevant to economic performance. To address this concern, we add weather controls to the baseline, and the results are robust and are displayed in Figure C.12. We also perform a falsification test by replacing the baseline's NTL with weather indicators. The results are in Figure C.13. As expected, we do not find any significant responses by these indicators. (3) The trade relationship between China and the US may determine China's real activities as we have illustrated above, thus we also try to control the US-China tension constructed by Rogers et al. (2024) in the baseline, and the results are almost unchanged. Refer to Figure C.14.

---

ous consensus expectations, which are obtained from the widely used survey by Action Economics, the successor to Money Market Services. We use the "advance" GDP release, headline CPI and PPI inflation, and non-farm payrolls from the employment report. The data are from Lakdawala et al. (2021). Equity return is the $S\&P$ 500 equity index change in the same week.

[62]The regression specification is the same as our baseline, and we add past news as control variables. We use cumulative values for each macro news shock or equity return with a 60-day window before the FOMC meetings. Adjusting the window length does not qualitatively change the results.

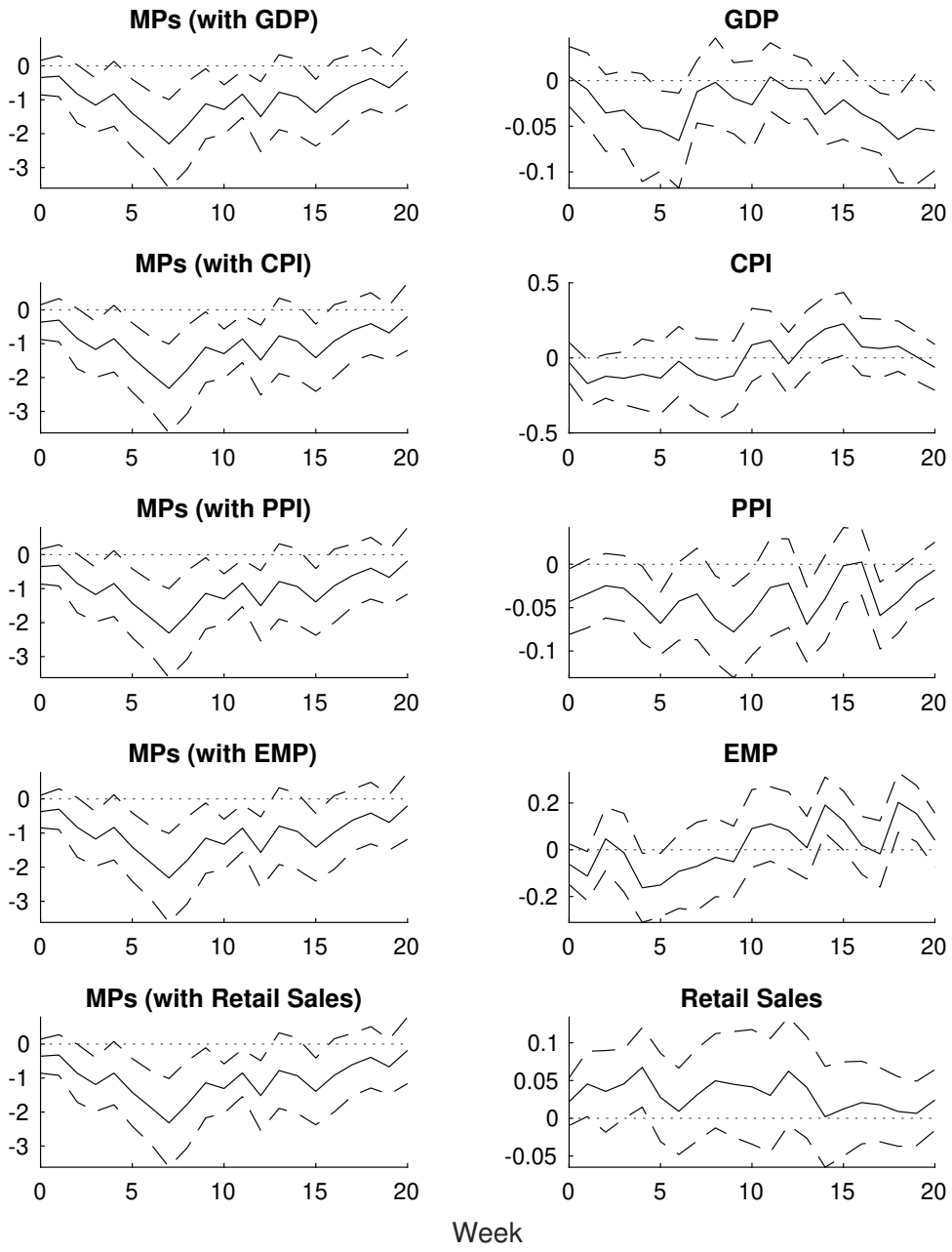


Figure C.9: Local Projection of NTL on US MPs and News Shock: News

Notes: Each row represents a LP regression, with the left column showing the NTL response to MPs, and the right column showing the NTL response to news shock or equity return. MPs is aggregated to the weekly frequencies consistent with the dependent variable. The number of lags of the dependent variable ($Q$) and the shocks ($M_1$ and $M_2$) are selected by the AIC criteria for up to 4 periods. The dashed ribbons are the 90 percent confidence intervals generated based on the Newey-West standard errors.

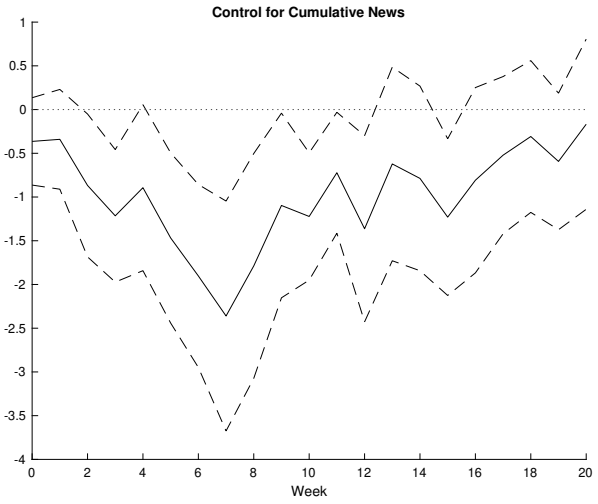


Figure C.10: Local Projection of NTL on US MPs and News Shock: Cumulative News

Notes: The control variables include cumulative GDP, CPI, PPI, employment news shocks, and past equity return. Each news shock is cumulative with a 60-day window. Equity return is the $S\&P$ 500 equity index change in the past 60 days. MPs is aggregated to the weekly frequencies consistent with the dependent variable. The number of lags of the dependent variable ($Q$) and the shocks ($M_1$ and $M_2$) are selected by the AIC criteria for up to 4 periods. The dashed ribbons are the 90 percent confidence intervals generated based on the Newey-West standard errors.

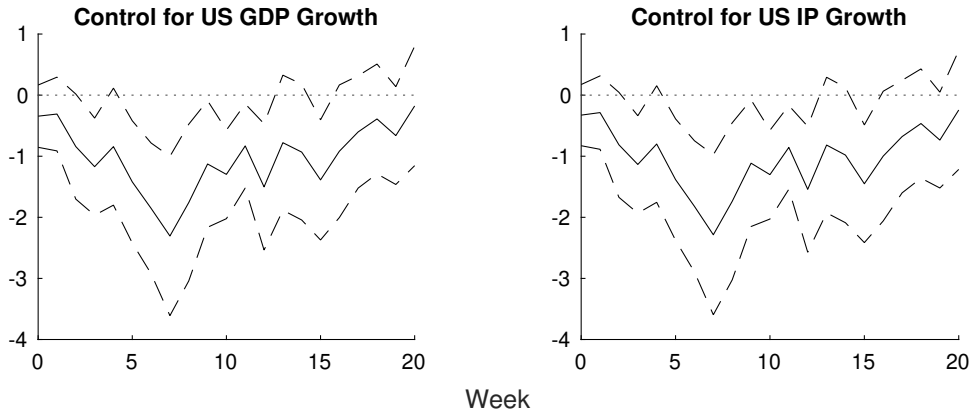


Figure C.11: Local Projection of NTL on US MPs: With US GDP or Industrial Production as Control

Notes: GDP is from quarterly series, and Industrial Production is from monthly series. Their values attached to each week are the period-to-period changes in the last period corresponding to the quarter or month of the week. MPs is aggregated to the weekly frequencies consistent with the dependent variable. The number of lags of the dependent variable ($Q$) and the shock ($M$) are selected by the AIC criteria for up to 4 periods. The dashed ribbons are the 90 percent confidence intervals generated based on the Newey-West standard errors.

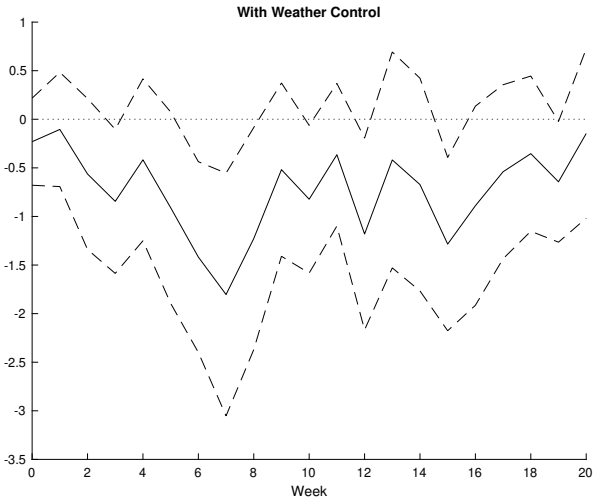


Figure C.12: Local Projection of NTL on US MPs: With Weather Control

Notes: Weather control variables include average temperature, precipitation, visibility, and wind speed. MPs is aggregated to the weekly frequencies consistent with the dependent variable. The number of lags of the dependent variable ($Q$) and the shock ($M$) are selected by the AIC criteria for up to 4 periods. The dashed ribbons are the 90 percent confidence intervals generated based on the Newey-West standard errors.

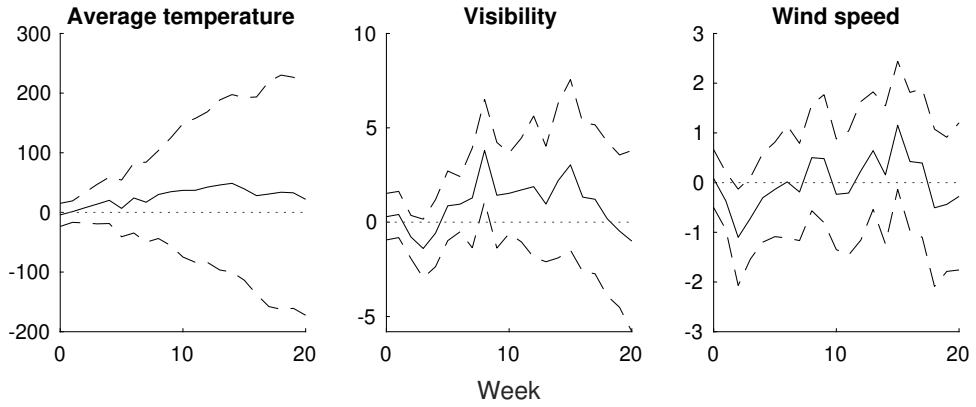


Figure C.13: Local Projection of Weather on US MPs

Notes: Weather indicators and MPs are aggregated to the weekly frequencies. The number of lags of the dependent variable ($Q$) and the shock ($M$) are selected by the AIC criteria for up to 4 periods. The dashed ribbons are the 90 percent confidence intervals generated based on the Newey-West standard errors.


Figure C.14: Local Projection of NTL on US MPs: With US-China Tension Index as Control

Notes: MPs is aggregated to the weekly frequencies consistent with the dependent variable. The number of lags of the dependent variable ($Q$) and the shock ($M$) are selected by the AIC criteria for up to 4 periods. The dashed ribbons are the 90 percent confidence intervals generated based on the Newey-West standard errors.

## C.2 Low-frequency Results

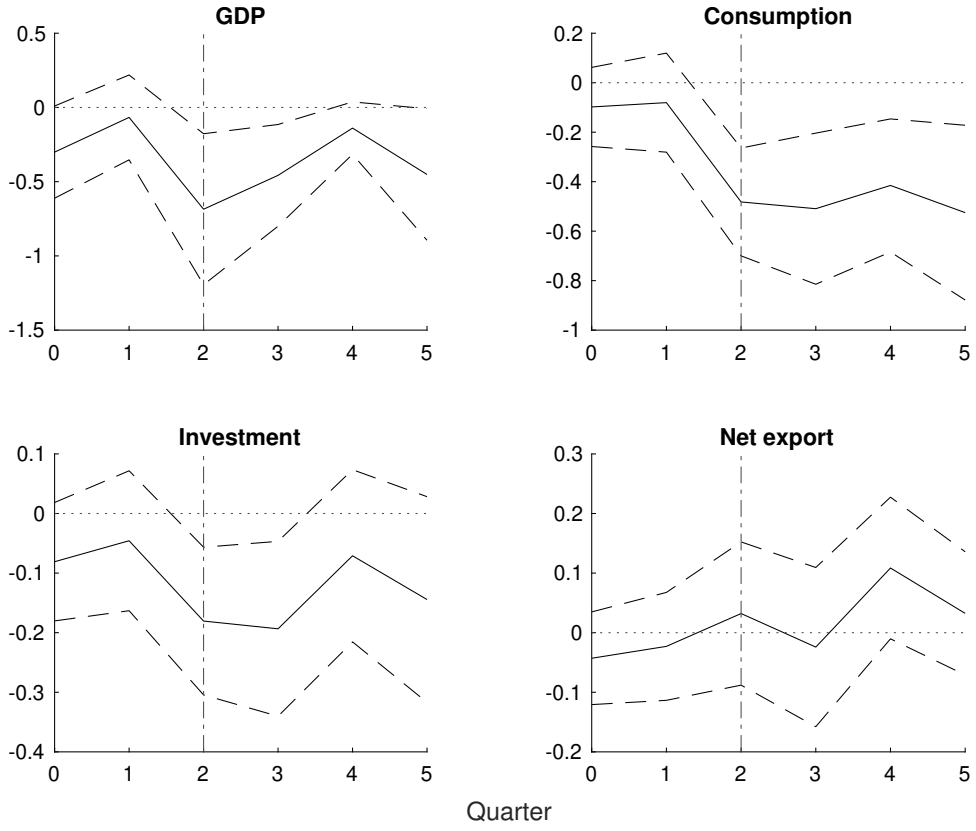


Figure C.15: IRF of China's Quarterly Consumption, Investment, and Net Export on US MPs

Notes: MPs is aggregated to the quarterly frequencies consistent with the dependent variable. The number of lags of the dependent variable ($Q$) and the shock ($M$) are selected by the AIC criteria for up to 4 periods. The dashed ribbons are the 90 percent confidence intervals generated based on the Newey-West standard errors.

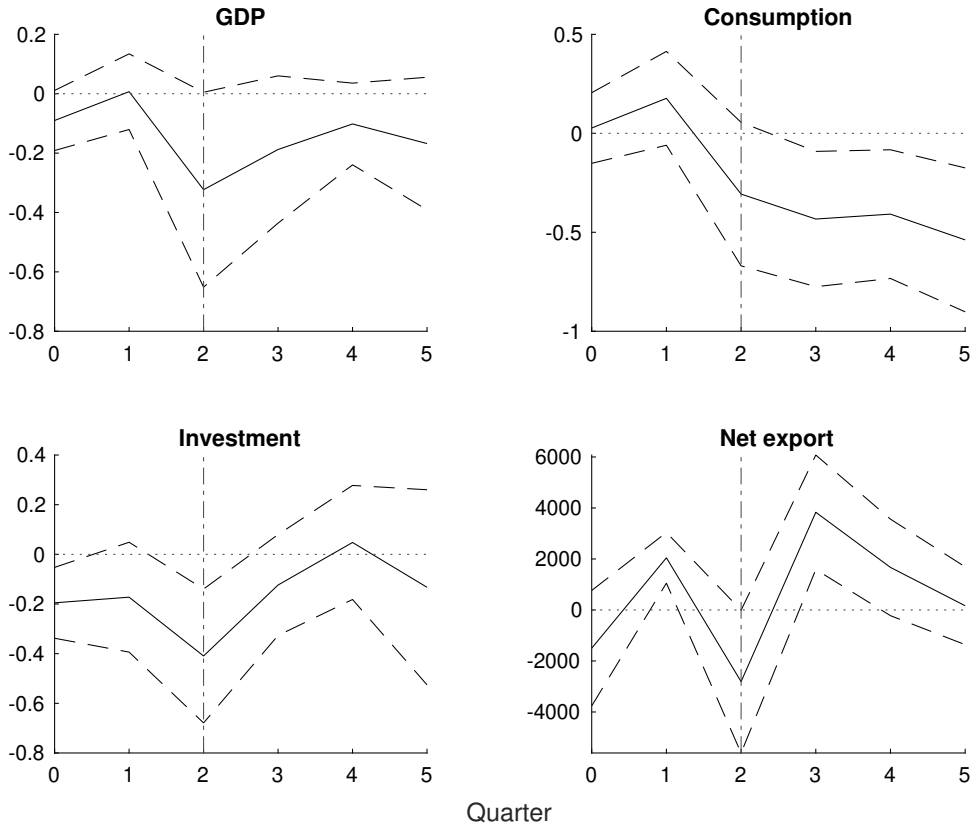


Figure C.16: IRF of China's Quarterly Alternative Economic Indicators on US MPs

Notes: MPs is aggregated to the quarterly frequencies consistent with the dependent variable. The data of economic indicators is from K. Chen et al. (2024). The number of lags of the dependent variable ($Q$) and the shock ($M$) are selected by the AIC criteria for up to 4 periods. The dashed ribbons are the 90 percent confidence intervals generated based on the Newey-West standard errors.

## C.3 Heterogeneous Effects Robustness

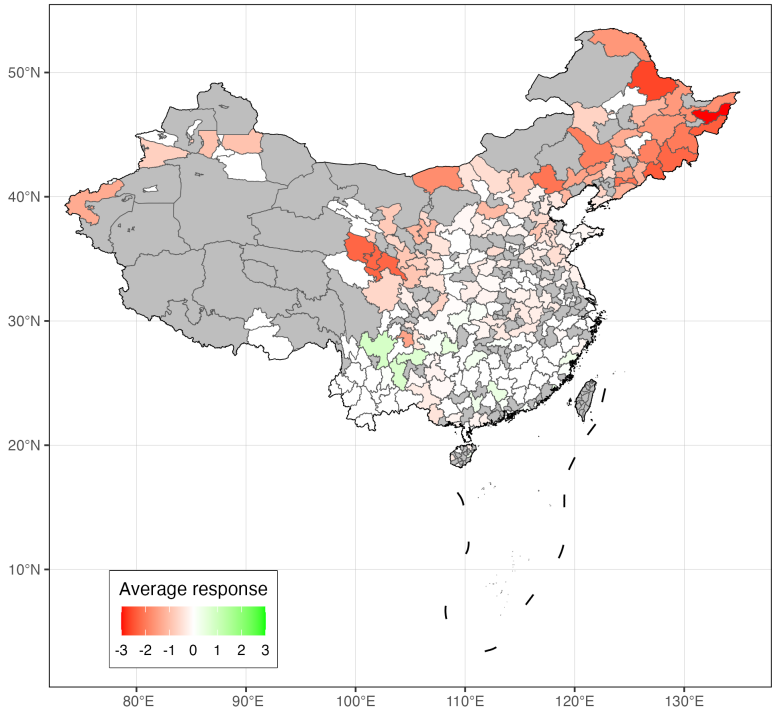


Figure C.17: Average Response of NTL on US MPs by City, With Weather Control

Notes: MPs is aggregated to the weekly frequencies consistent with the dependent variable. The number of lags of the dependent variable ($Q$) and the shock ($M$) are selected by the AIC criteria for up to 4 periods. Weather control variables include average temperature, precipitation, visibility, and wind speed.

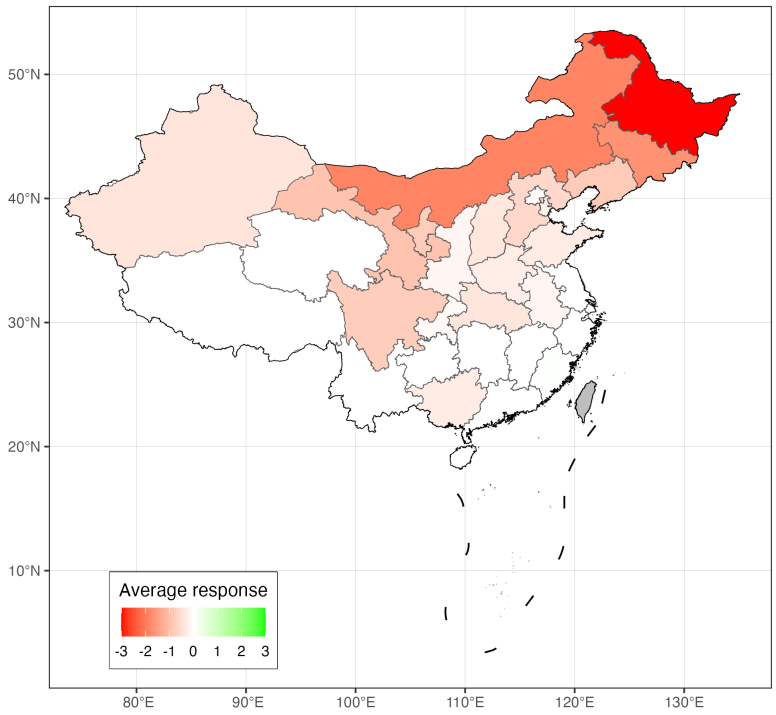


Figure C.18: Average Response of NTL on US MPs by Province

Notes: MPs is aggregated to the weekly frequencies consistent with the dependent variable. The number of lags of the dependent variable ($Q$) and the shock ($M$) are selected by the AIC criteria for up to 4 periods.

# Appendix D More Results on Channel

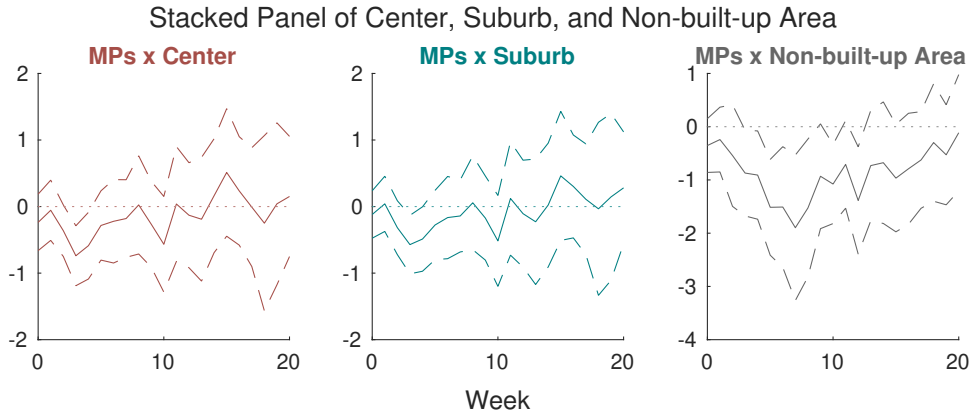


Figure D.1: Local Projection of NTL on US MPs: City Areas, Stacked Panel

Notes: MPs is aggregated to the weekly frequencies consistent with the dependent variable. The dashed ribbons are the 90 percent confidence intervals generated based on the Newey-West standard errors.

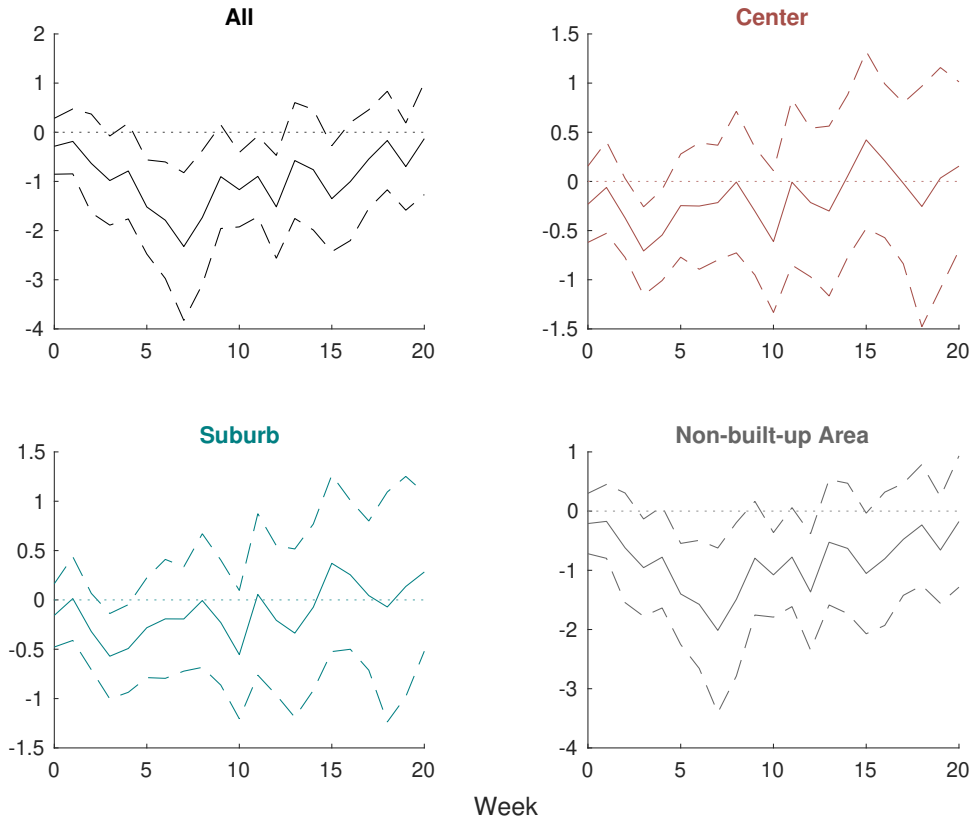


Figure D.2: Local Projection of NTL on US MPs: City Areas, Identified Built-up Area in 2015

Notes: MPs is aggregated to the weekly frequencies consistent with the dependent variable. The dashed ribbons are the 90 percent confidence intervals generated based on the Newey-West standard errors.

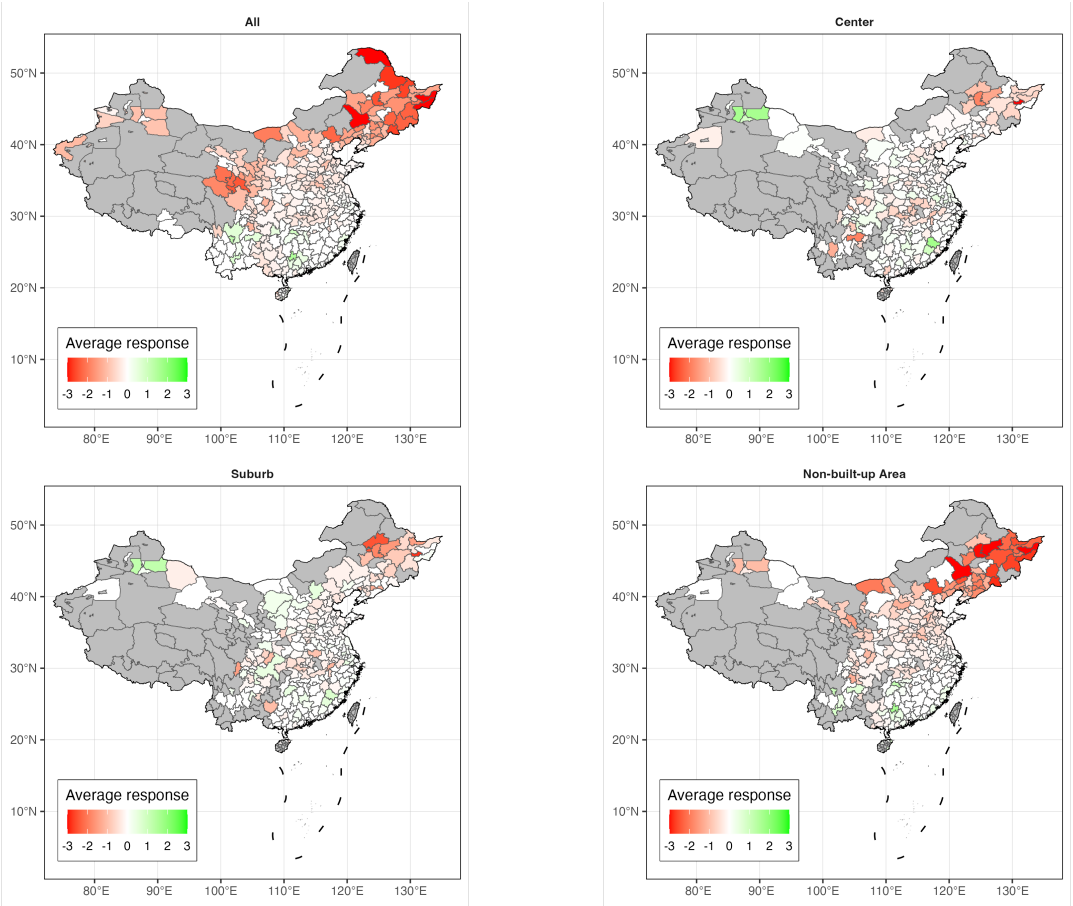


Figure D.3: Average Response of NTL on US MPs by City: City Areas

Notes: MPs is aggregated to the weekly frequencies consistent with the dependent variable. The number of lags of the dependent variable ($Q$) and the shock ($M$) are selected by the AIC criteria for up to 4 periods. When taking the average across the time horizon from the week the MPs is realized to 20 weeks later, insignificant values at a 90 percent confidence level are treated as zero. If the city has both significantly positive and significantly negative responses, the average response by the city is interpreted as zero. Extreme values with absolute values greater than 3 are winsorized on the map.

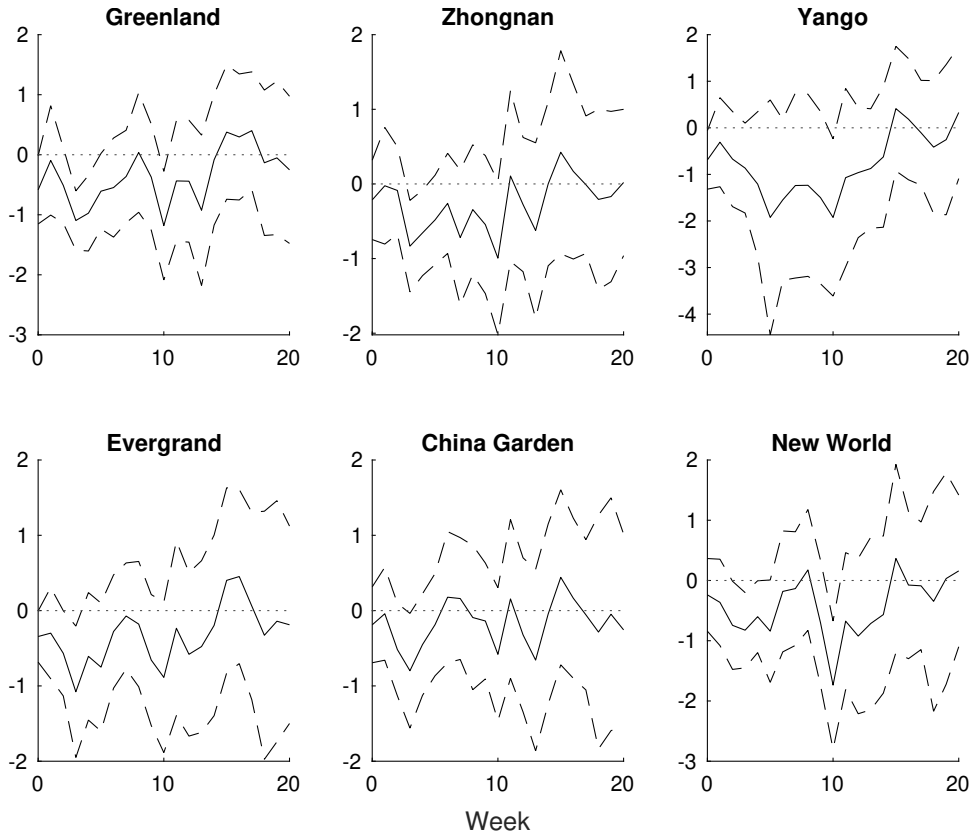


Figure D.4: Response of NTL in Transacted Land on US MPs: Transacted Lands by Selected Real Estate Firms

Notes: MPs is aggregated to the weekly frequencies consistent with the dependent variable. The number of lags of the dependent variable ($Q$) and the shock ($M$) are selected by the AIC criteria for up to 4 periods. The dashed ribbons are the 90 percent confidence intervals generated based on the Newey-West standard errors.

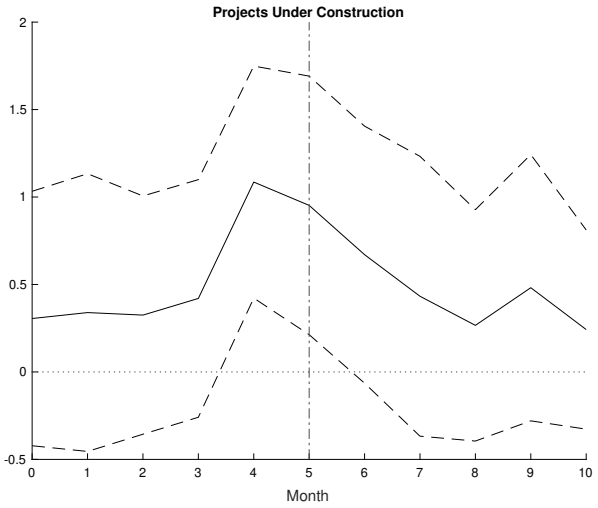


Figure D.5: IRF of NTL on China's Monthly Land Projects Under Construction (IV: US MPs)

Notes: MPs is aggregated to the monthly frequencies consistent with the dependent variable. In the first stage, the number of lags of the endogenous variable is selected by the AIC criteria for up to 4 periods. The number of lags of the shock is the IRF horizon (10 months). In the second stage, the number of lags of the dependent variable ($Q$) and the endogenous variable ($M$) are selected by the AIC criteria for up to 4 periods. The dashed ribbons are the 90 percent confidence intervals generated by bootstrapping with 1,000 draws.

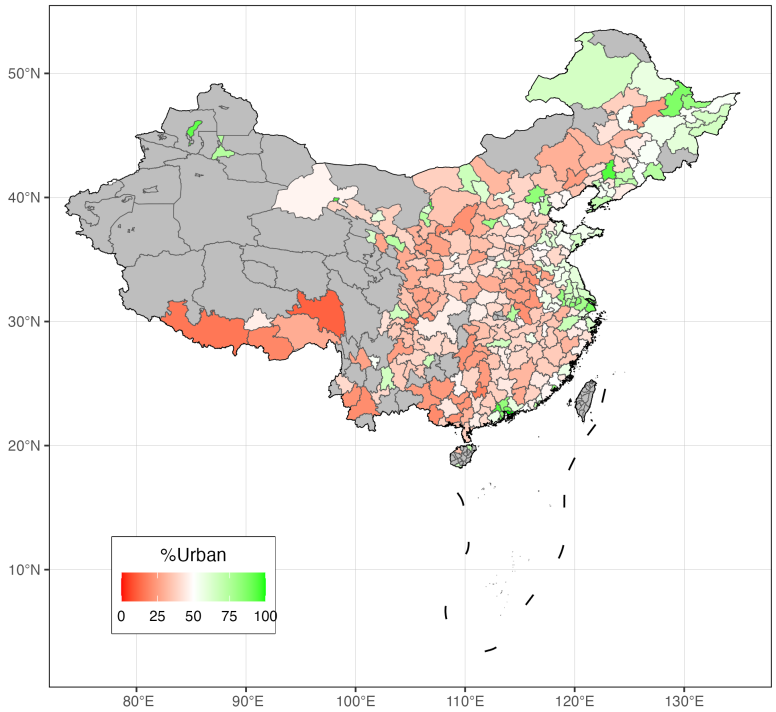


Figure D.6: Urbanization Rate in 2019 by City, Linearly Interpolated

Notes: The data are from the statistical yearbooks of each city published by NBSC.

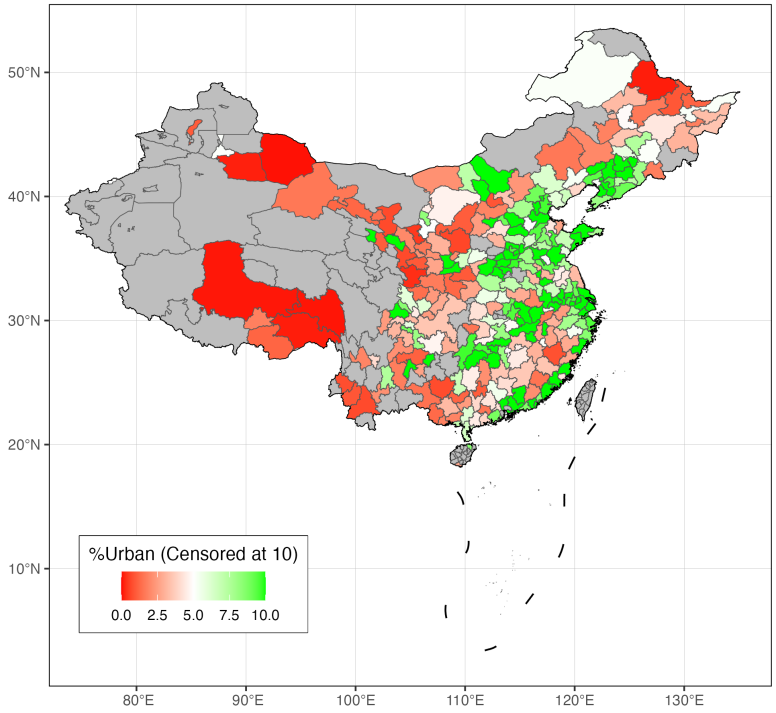


Figure D.7: Urbanization Area Rate in 2019 by City

Notes: The data are from the statistical yearbooks of each city published by NBSC. Extreme values greater than 10 are winsorized on the map.

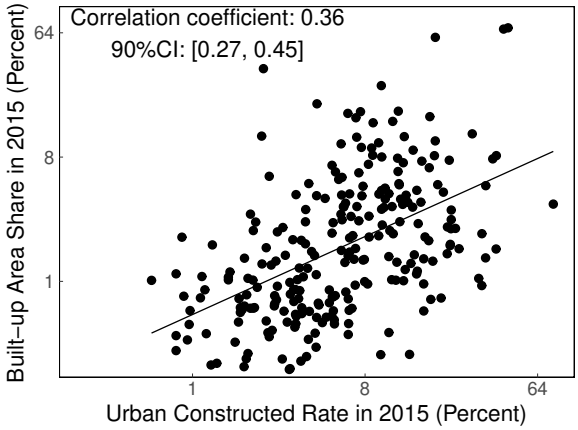


Figure D.8: Built-up Area Share and Urbanization Rate by City

Notes: For each city, the built-up area share is calculated as the ratio of the total number of NTL cells of the built-up area of the city over the total number of NTL cells of the city.

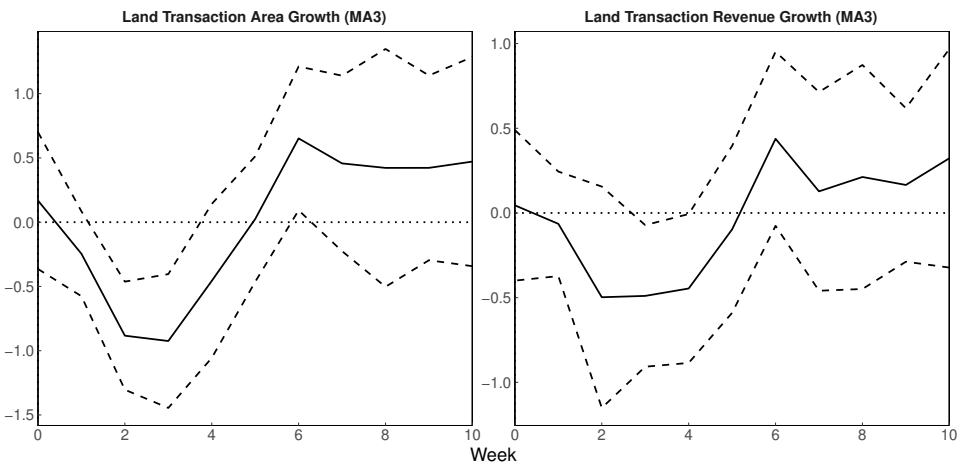


Figure D.9: NTL Response to Interaction of US MPs and Land Transaction or Related Investment and Projects, City level

Notes: For each city, the growth rate is calculated as the moving average of the annualized growth rates of aggregated values in the last three years (inclusive). The dashed ribbons are the 90 percent confidence intervals generated based on standard errors clustered to city and week.

# Appendix E More Results on Financing Conditions

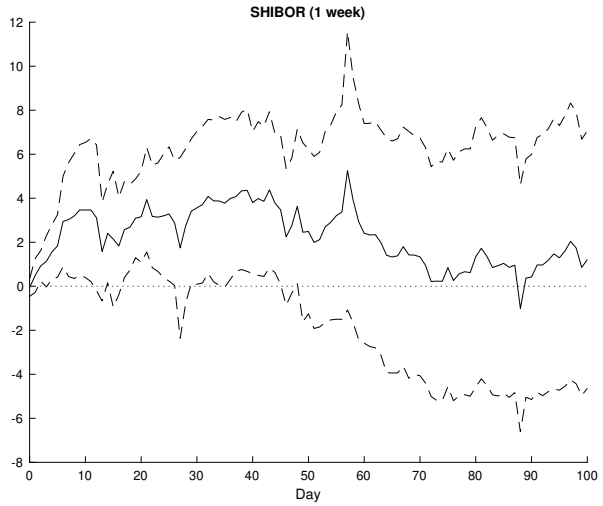


Figure E.1: IRF of SHIBOR on US MPs

Notes: The number of lags of the dependent variable ($Q$) and the shock ($M$) are selected by the AIC criteria for up to 4 periods. The dashed ribbons are the 90 percent confidence intervals generated based on the Newey-West standard errors.

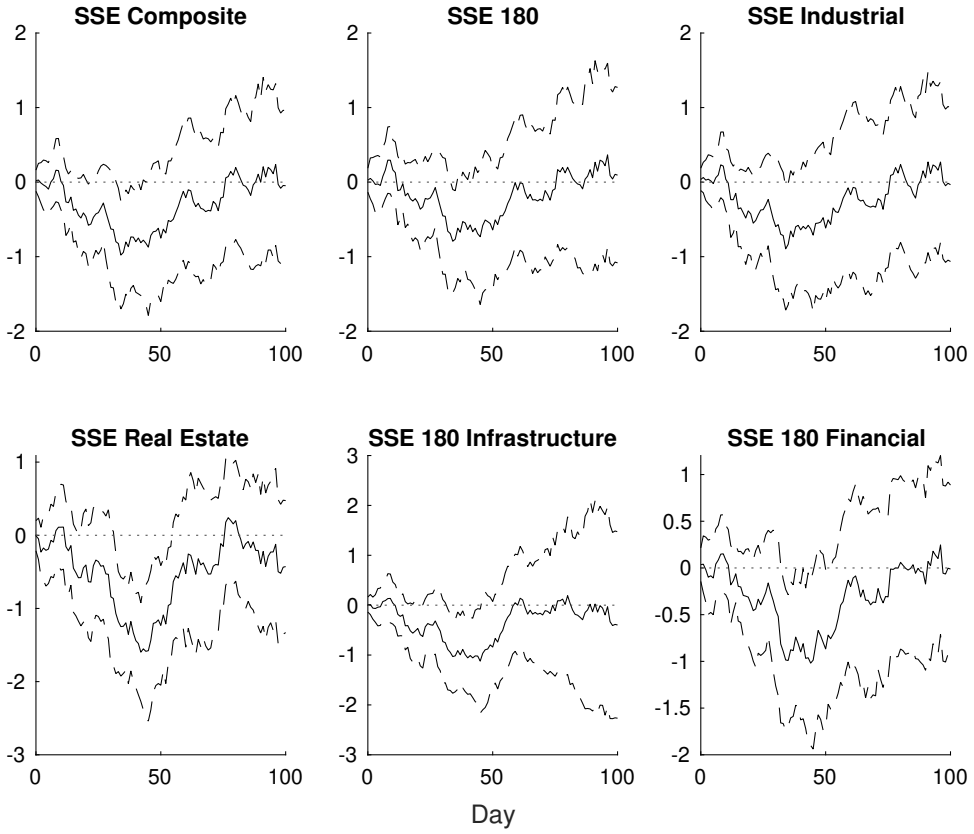


Figure E.2: IRF of Shanghai Stock Index on US MPs by Maturity

Notes: The number of lags of the dependent variable ($Q$) and the shock ($M$) are selected by the AIC criteria for up to 4 periods. The dashed ribbons are the 90 percent confidence intervals generated based on the Newey-West standard errors.

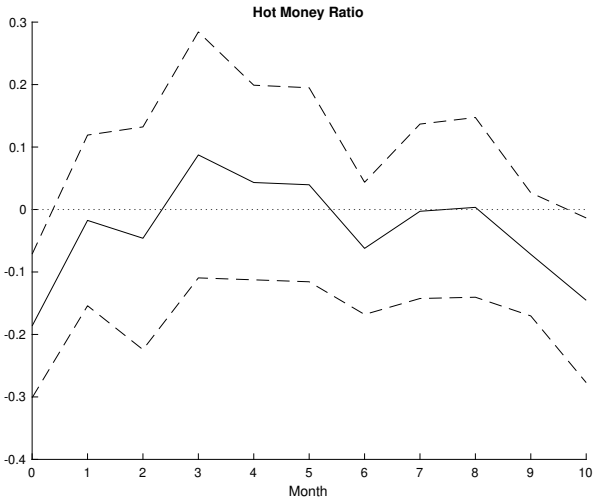


Figure E.3: Local Projection of Hot Money Ratio on US MPs

Notes: Hot money ratio is defined as the ratio of (Period-by-ceriod change in Foreign Reserve - Net Export - FDI) over Foreign Reserve, all in USD. MPs is aggregated to the monthly frequencies consistent with the dependent variable. The number of lags of the dependent variable ($Q$) and the shock ($M$) are selected by the AIC criteria for up to 4 periods. The dashed ribbons are the 90 percent confidence intervals generated based on the Newey-West standard errors.

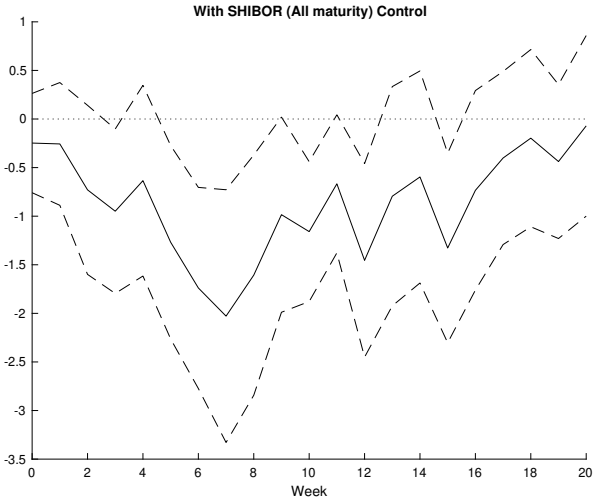


Figure E.4: Local Projection of NTL on US MPs: With SHIBOR (All maturity) Control

Notes: SHIBOR maturities include overnight, 1 week, 1 month, 3 months, 6 months, and 1 year. MPs is aggregated to the weekly frequencies consistent with the dependent variable. The number of lags of the dependent variable ($Q$) and the shock ($M$) are selected by the AIC criteria for up to 4 periods. Weather control variables include average temperature, precipitation, visibility, and wind speed. The dashed ribbons are the 90 percent confidence intervals generated based on the Newey-West standard errors.

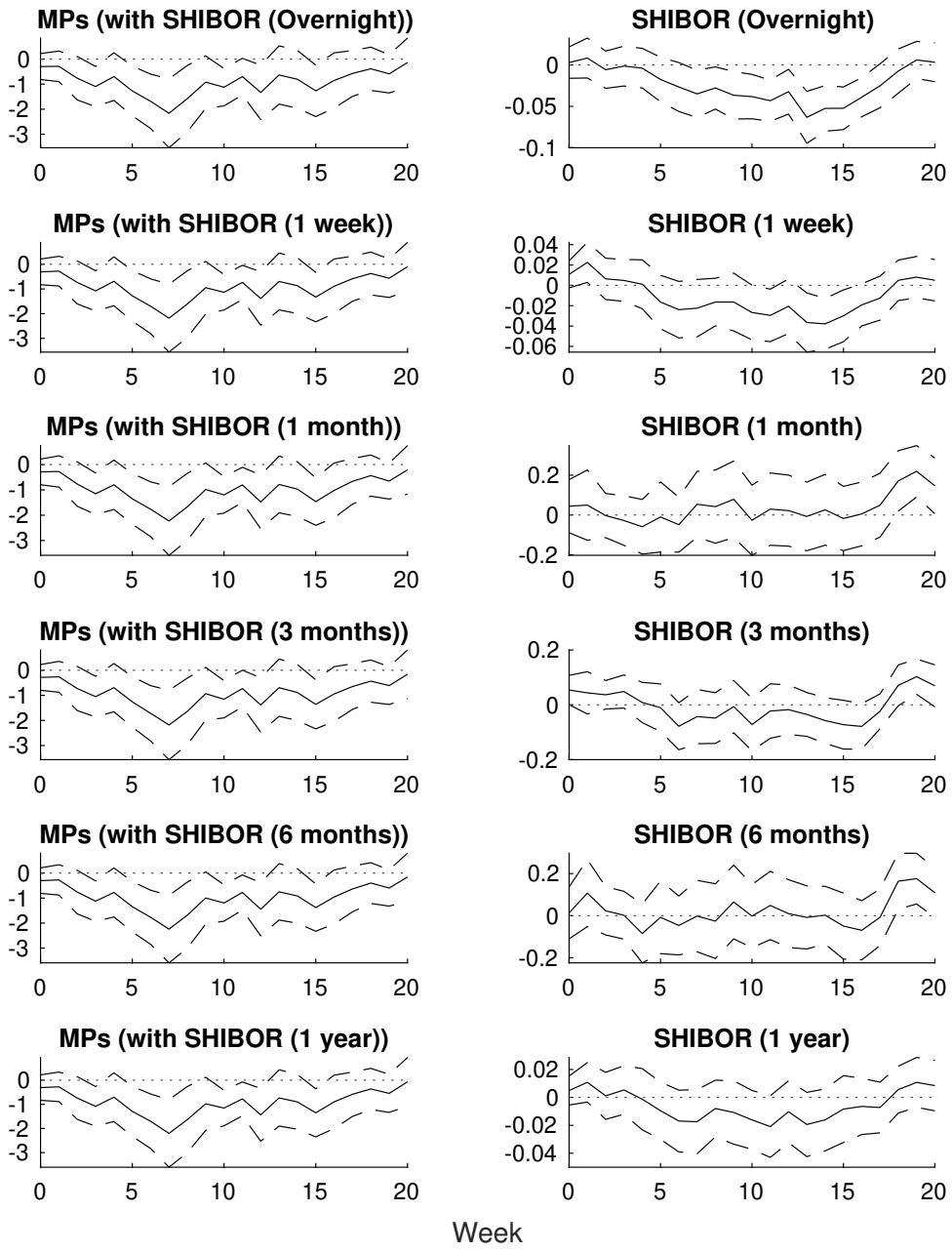


Figure E.5: Local Projection of NTL on US MPs and SHIBOR

Notes: MPs is aggregated to the weekly frequencies consistent with the dependent variable. The number of lags of the dependent variable ($Q$) and the shocks ($M_1$ and $M_2$) are selected by the AIC criteria for up to 4 periods. The dashed ribbons are the 90 percent confidence intervals generated based on the Newey-West standard errors.

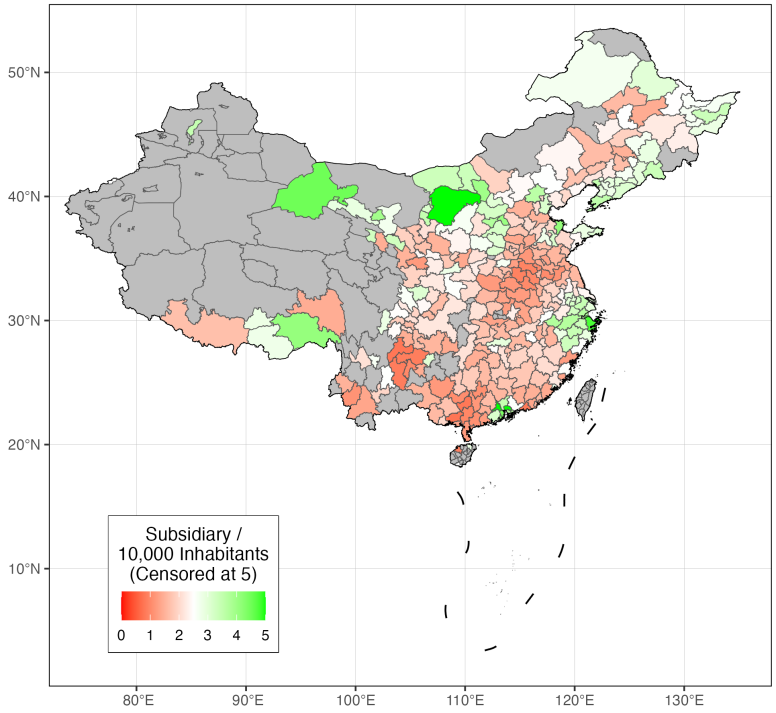


Figure E.6: Number of Bank Subsidiaries Per 10,000 Inhabitants in 2020 by City

Notes: The data are from the statistical yearbooks of each city published by NBSC. The population of each city is based on the household residency (hukou) status. Extreme values greater than 5 are winsorized on the map.

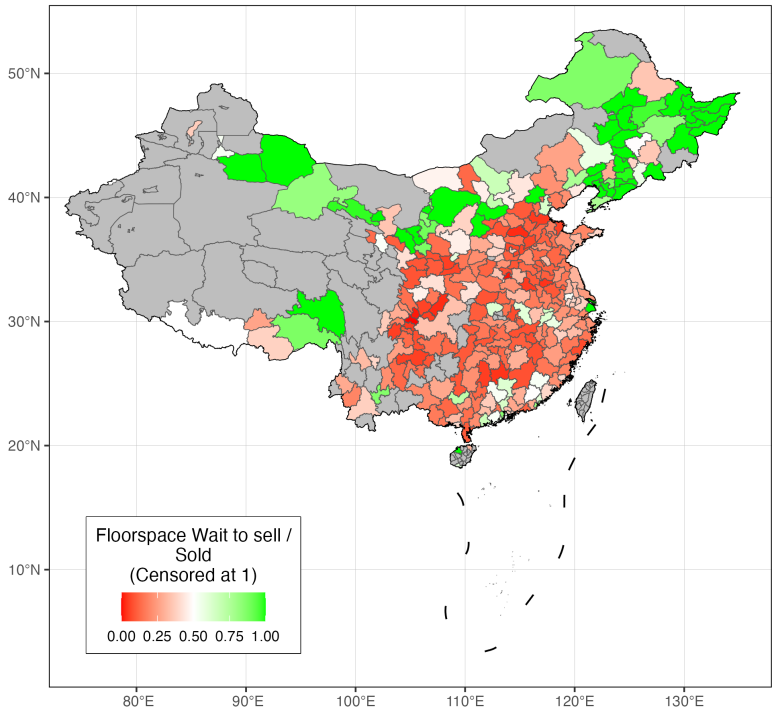


Figure E.7: Ratio of Floor Space Wait to Sell over Floor Space Sold in 2020 by City

Notes: The data are from CEIC China Premium Database. Extreme values greater than 1 are winsorized on the map.

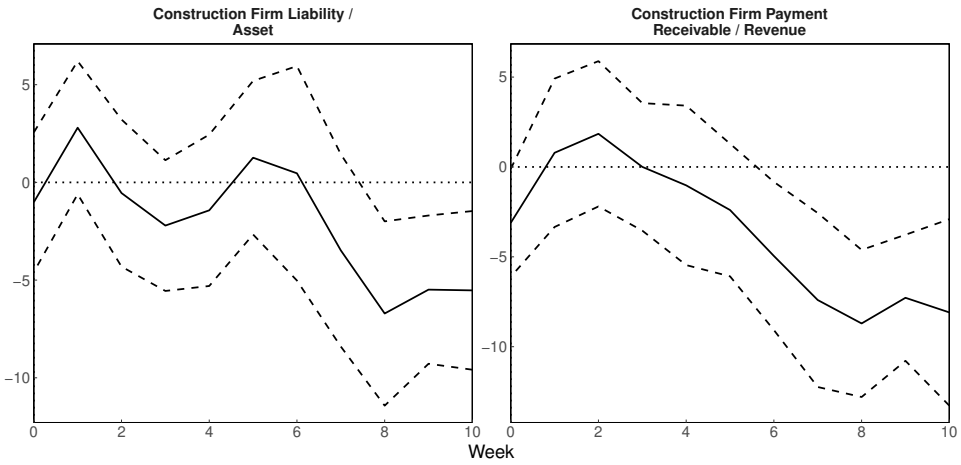


Figure E.8: NTL Response to Interaction of US MPs and Construction Firms' Financial Condition, City level

Notes: The aggregated firm data are at the province level. For each city in each year, I assign the corresponding indicators of the province to which the city belongs. The dashed ribbons are the 90 percent confidence intervals generated based on standard errors clustered to city and week.

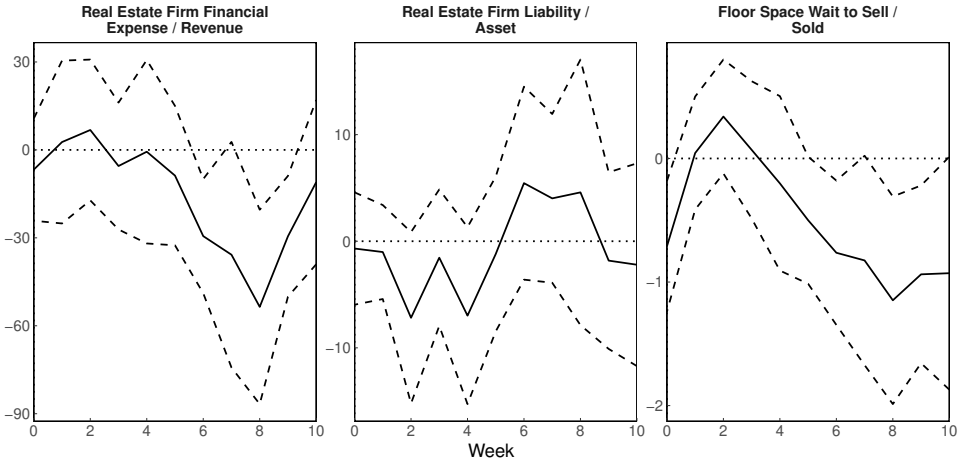


Figure E.9: NTL Response to Interaction of US MPs and Real Estate Firms' Financial Condition, City level

Notes: The aggregated firm data are at the province level. For each city in each year, I assign the corresponding indicators of the province the city belongs to. The dashed ribbons are the 90 percent confidence intervals generated based on standard errors clustered to city and week.

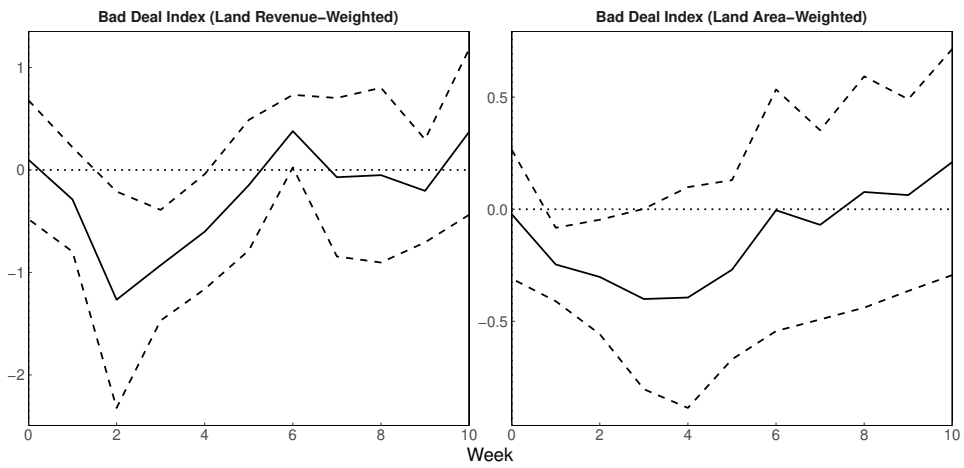


Figure E.10: NTL Response to Interaction of US MPs and Bad Deal Index, City level

Notes: The dashed ribbons are the 90 percent confidence intervals generated based on standard errors clustered to city and week.

Table E.1: Firm Operation Condition Responses to MPs, by Firm Operation Indicator

| | Revenue | Account Receivable | Account Payable | Profit |
|---|---|---|---|---|
| Real Estate | -0.0129 | -0.0123 | -0.0022 | -0.3389$^{+}$ |
| | (0.0307) | (0.0172) | (0.0123) | (0.2262) |
| MPs × Real Estate | -2.0428$^{+}$ | -0.9730$^{*}$ | -1.0129$^{**}$ | -23.8807$^{**}$ |
| | (1.3265) | (0.4499) | (0.3583) | (9.8719) |
| Firm FE | Yes | Yes | Yes | Yes |
| Year-Quarter FE | Yes | Yes | Yes | Yes |
| N | 144,281 | 142,633 | 129,147 | 145,252 |
| $R^2$ | 0.1333 | 0.0362 | 0.0339 | 0.0240 |

Notes: Significance levels are based on Clustered (Year, Firm) standard-errors. Significance Codes: ***: 0.01, **: 0.05, *: 0.1, +: 0.2.

Table E.2: Real Estate Firm Operation Condition Responses to MPs, by Firm Operation Indicator

| | Revenue | Account Receivable | Account Payable | Profit |
|---|---|---|---|---|
| MPs | -2.2486$^{+}$ | -0.5504$^{*}$ | -1.0476$^{**}$ | -16.4012$^{**}$ |
| | (1.5346) | (0.2558) | (0.3611) | (5.9230) |
| Firm FE | Yes | Yes | Yes | Yes |
| N | 6,365 | 6,013 | 5,932 | 6,475 |
| $R^2$ | 0.0070 | 0.0146 | 0.0163 | 0.0029 |

Notes: Significance levels are based on Clustered (Year, Firm) standard-errors. Significance Codes: ***: 0.01, **: 0.05, *: 0.1, +: 0.2.

Table E.3: Land Transaction Impact on Real Estate Firm Operation Condition Responses to MPs, by Firm Operation Indicator

| | Revenue | Account Receivable | Account Payable |
|---|---|---|---|
| Land transaction | 0.0296 | 0.0182 | 0.0265 |
| | (0.0249) | (0.0429) | (0.0199) |
| MPs × Land transaction | -0.8812$^{+}$ | -0.2758 | -0.5088$^{*}$ |
| | (0.5793) | (0.9244) | (0.2954) |
| Firm FE | Yes | Yes | Yes |
| Year-Quarter FE | Yes | Yes | Yes |
| N | 5,361 | 5,043 | 4,927 |
| $R^2$ | 0.2548 | 0.0305 | 0.1174 |

Notes: Significance levels are based on Clustered (Year, Firm) standard-errors. Significance Codes: ***: 0.01, **: 0.05, *: 0.1, +: 0.2.

Table E.4: Real Estate Firm Foreign Bond Issue Net Standing Value (Scaled by Operation Indicator) Responses to MPs

| | / Asset | / Liability | / Current Liability | / Long-term Liability |
|---|---|---|---|---|
| MPs | -0.0598$^{***}$ | -0.0801$^{***}$ | -0.1298$^{***}$ | -0.6261$^{+}$ |
| | (0.0140) | (0.0199) | (0.0362) | (0.3868) |
| Firm FE | Yes | Yes | Yes | Yes |
| N | 2,238 | 2,238 | 2,238 | 2,226 |
| $R^2$ | 0.3390 | 0.3371 | 0.3616 | 0.1860 |

Notes: Significance levels are based on Clustered (Firm) standard-errors. Significance Codes: ***: 0.01, **: 0.05, *: 0.1, +: 0.2.

Table E.5: Real Estate Firm Domestic Bond Issue Net Standing Value (Scaled by Operation Indicator) Responses to MPs

| | Asset | Liability | Current Liability | Long-term Liability |
|---|---|---|---|---|
| MPs | -0.0143 | 0.0891 | 0.0238 | -1.9571 |
| | (0.0819) | (0.2804) | (0.2952) | (1.6913) |
| Firm FE | Yes | Yes | Yes | Yes |
| N | 3,955 | 3,955 | 3,955 | 3,862 |
| $R^2$ | 0.4900 | 0.5744 | 0.5388 | 0.2400 |

Notes: Significance levels are based on Clustered (Firm) standard-errors. Significance Codes: ***: 0.01, **: 0.05, *: 0.1, +: 0.2.

# Appendix F More Results on Further Discussion

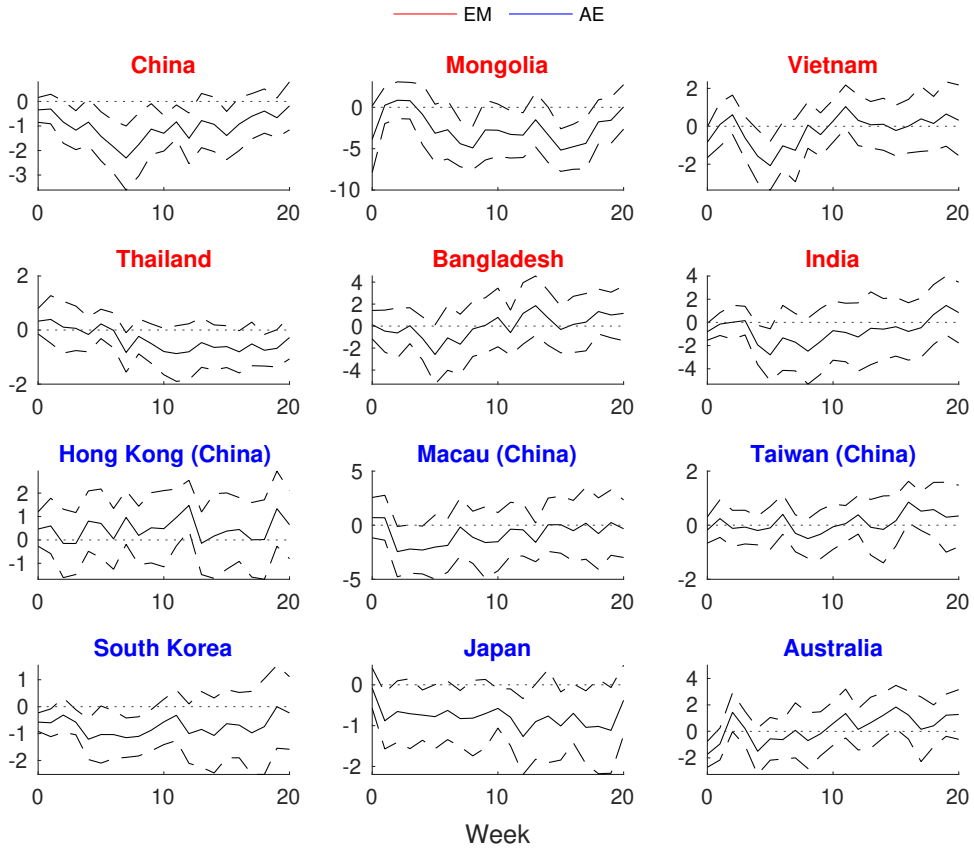


Figure F.1: Local Projection of NTL on US MPs: Other Economies

Notes: We apply the baseline specification on different economies respectively. MPs is aggregated to the weekly frequencies consistent with the dependent variable. The number of lags of the dependent variable ($Q$) and the shock ($M$) are selected by the AIC criteria for up to 4 periods. The dashed ribbons are the 90 percent confidence intervals generated based on the Newey-West standard errors.

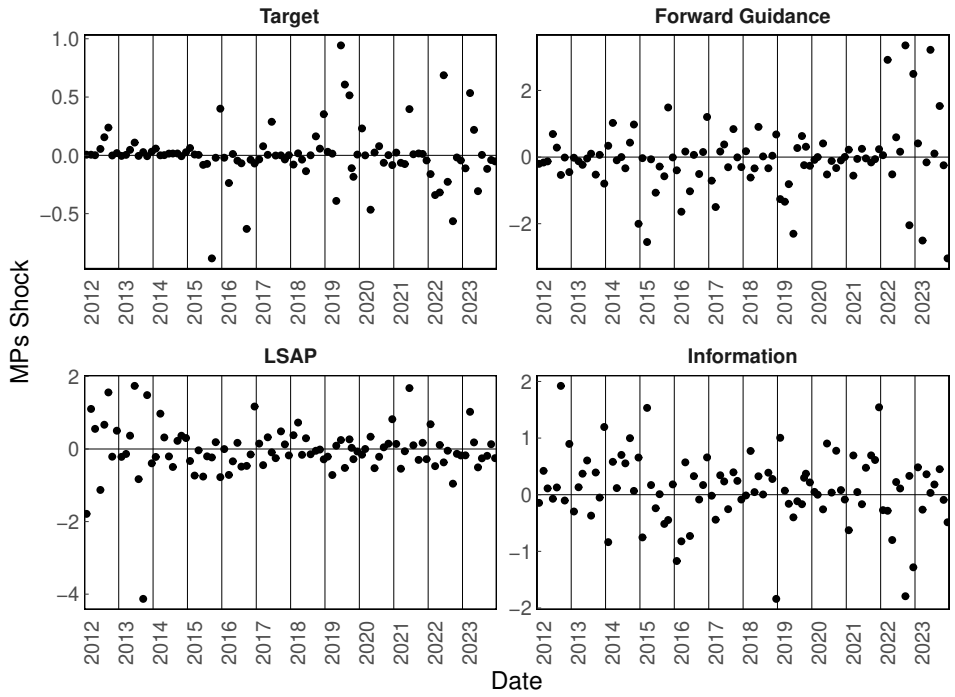


Figure F.2: Proxies of Monetary Policy Shock

Notes: For each MPs event, the corresponding date is the day when the FOMC is held.

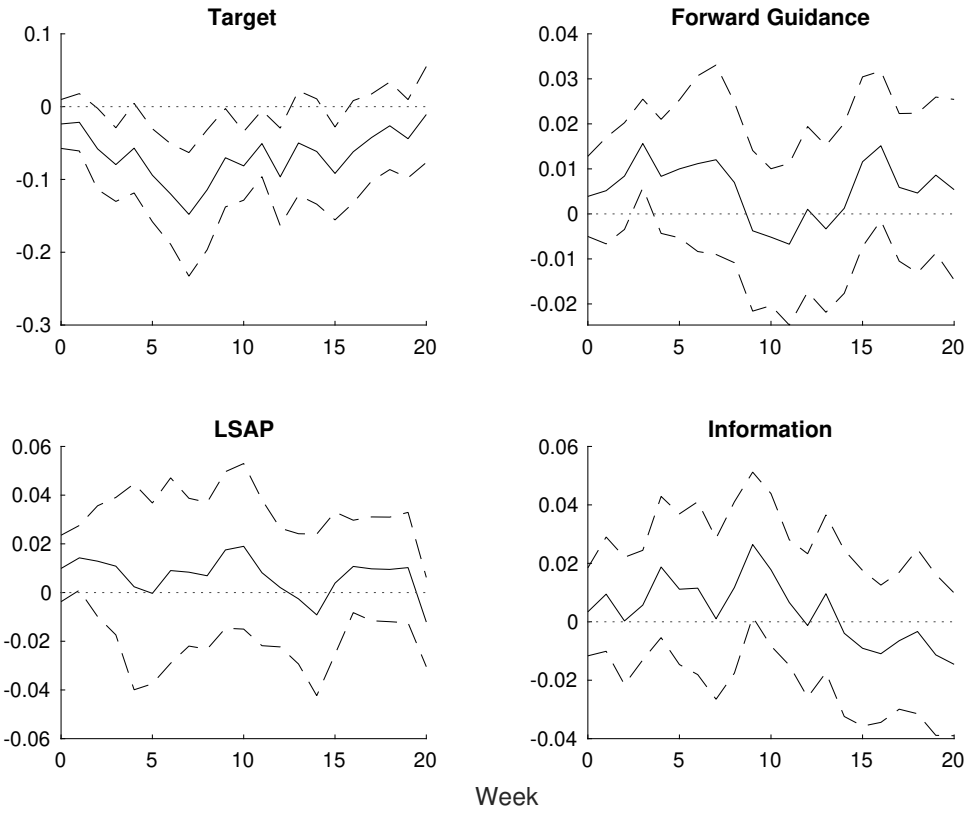


Figure F.3: Local Projection of NTL on US MPs: Alternative Unconventional MPs

Notes: MPs is aggregated to the weekly frequencies consistent with the dependent variable. The number of lags of the dependent variable ($Q$) and the shock ($M$) are selected by the AIC criteria for up to 4 periods. The dashed ribbons are the 90 percent confidence intervals generated based on the Newey-West standard errors.

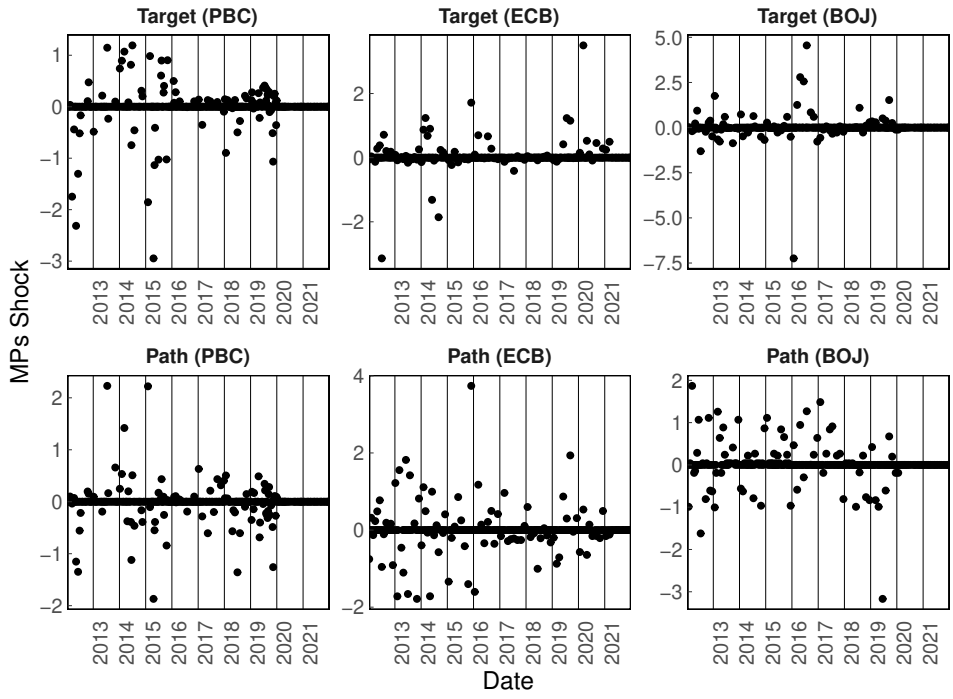


Figure F.4: Proxies of Monetary Policy Shock: Other Central Banks

Notes: For each MPs event, the corresponding date is the day when the FOMC is held.

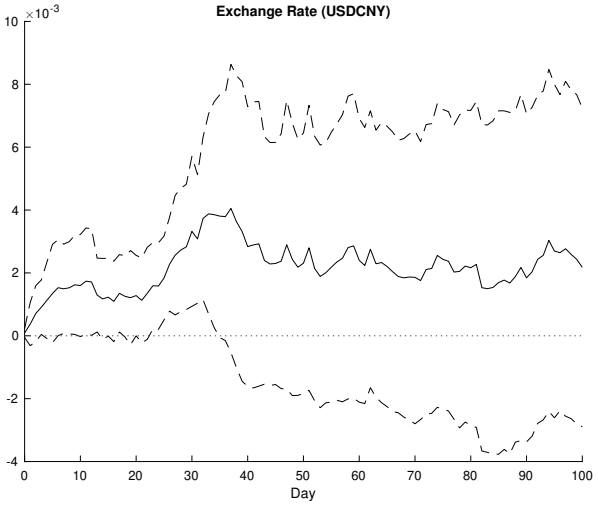


Figure F.5: IRF of Exchange Rate of USD/CNY on US MPs, by MPs Specification

Notes: The number of lags of the dependent variable ($Q$) and the shock ($M$) are selected by the AIC criteria for up to 4 periods. The dashed ribbons are the 90 percent confidence intervals generated based on the Newey-West standard errors.

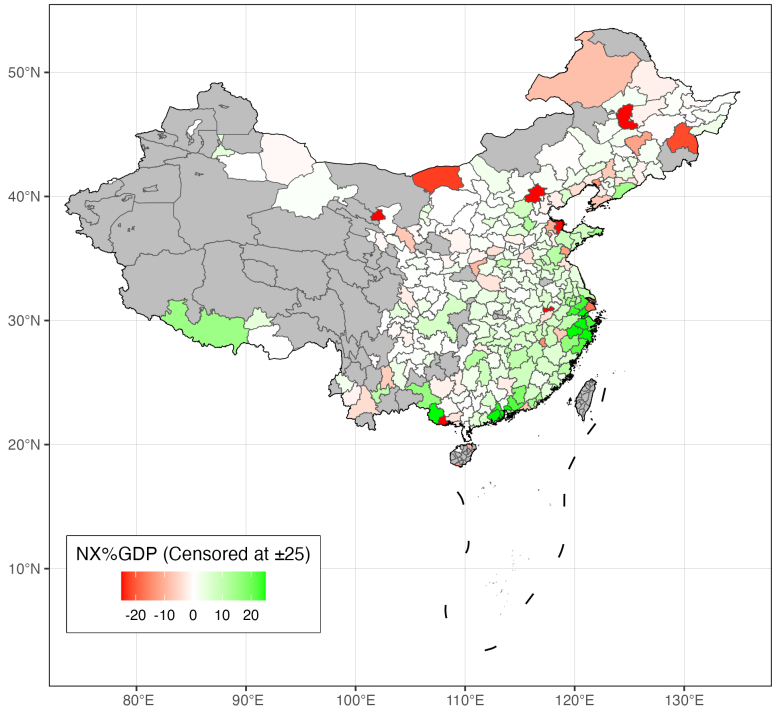


Figure F.6: Trade Exposure in 2019 by City

Notes: The data are from the statistical yearbooks of each city published by NBSC. Trade exposure is calculated as export value minus import value, then divided by GDP, all in current Chinese Yuan units. By comparison, the national overall ratio in 2019 was about 2.5 percent. Extreme values with absolute values greater than 25 are winsorized on the map.

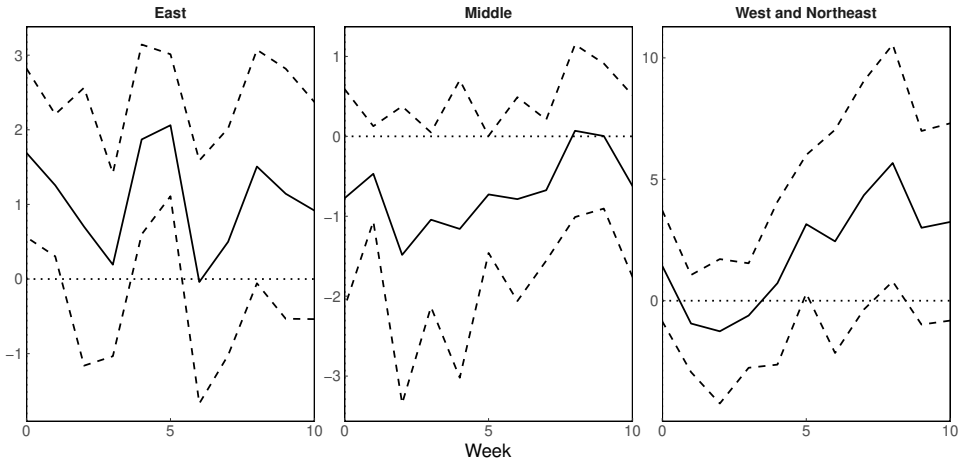


Figure F.7: NTL Response to Interaction of US MPs and Trade Exposure, City level, by Region

Notes: The dashed ribbons are the 90 percent confidence intervals generated based on standard errors clustered to city and week.